

UCSF

UC San Francisco Electronic Theses and Dissertations

Title

Decoding DNA signals that instruct glucocorticoid receptor structure and function

Permalink

<https://escholarship.org/uc/item/6jr4h313>

Author

Watson, Lisa Christine

Publication Date

2012

Peer reviewed|Thesis/dissertation

Decoding DNA signals that instruct glucocorticoid receptor
structure and function

by

Lisa C. Watson

DISSERTATION

Submitted in partial satisfaction of the requirements for the degree of

DOCTOR OF PHILOSOPHY

in

Biochemistry and Molecular Biology

in the

GRADUATE DIVISION

of the

UNIVERSITY OF CALIFORNIA, SAN FRANCISCO

Copyright 2012

by

Lisa C. Watson

Acknowledgements

All of the work I did at UCSF would not be possible without the support and collaborative efforts of others, so I have many people to thank.

Keith Yamamoto has been a fantastic mentor—he is an infinite source of support and encouragement and his advice is always focused on the bigger picture. He has taught by example how to be a good scientist and a great leader. I also want to thank Keith for inspiring me to become a serious SF bike commuter, as the transition to freedom from bus schedules, traffic, and parking was a turning point for me to truly enjoy being in San Francisco.

I am very grateful to Jenny Banaszek for her ability to interface between the lab, between Keith's many roles, and between the many programs she is coordinating—always with apparent effortlessness and a great sense of humor. Aside from that, she also has provided amazing support and advice throughout my time in the lab.

I am extremely thankful for the expertise and encouragement of the entire Yamamoto Lab. I owe a huge acknowledgement to Miles Pufall, who contributed significantly to this project by providing exceptional knowledge, ideas and expertise throughout the entire time he was in the lab. Miles not only gave me lots of encouragement but he also pushed me to challenge myself and get the most out of my graduate experience. It was not until he left to start his own lab that I fully realized how invaluable it was to have his joint interest in my experiments and results. Miles continues to be a role model as a Biochemist, a Scientist and a team-player.

When I joined the Yamamoto lab, I was inspired by the scientific enthusiasm and camaraderie. Alex So played a major role in this, as his positive attitude is contagious. He immediately welcomed me to the lab and he has an amazing ability to bring people together. He also set the standard for hard work and gave me lots of grad school survival advice. Jason Huff helped my project with numerous scientific discussions and by asking tough but important questions. I also want to thank him for being extremely giving of his time in helping me with Macro class and especially in Bioreg. Carlos Pantoja provided good advice, music, friendship, and extensive knowledge of biology and San Francisco hipster hotspots. Abby Kroch and I sat back-to-back and for several years and she was an infinite source of creativity, ideas, hilarity and advice. I really appreciated all of her scientific and non-scientific insight and encouragement. Sebastiaan Meijning provided many creative scientific ideas and

technical expertise and I was lucky to work with him on a collaborative project as he moved on to start his own lab.

From the next generation of Yamamotos, I want to especially thank Marlisa Pillsbury for providing me with infinite encouragement. I have learned a lot from her strength, scientific curiosity and perseverance. I am thankful to Jordan Ward for his advice regarding both science and career development as well as his mutual passion for good beer. I had a great experience working with Ben Schiller and I admire his fearlessness towards learning new techniques and taking leadership of a collaborative project, which really expanded the scope of my thesis work. Samantha Cooper pioneered ChIP-seq in the lab and I am thankful for all her great protocols and advice and her tremendous effort in making all her work accessible and available. I am truly thankful to everyone in the lab, especially Stefan Taubert, Eric Bolton, Karin Engel, Linet Mera, Lindsey Pack, Sheng-Hong Chen and Matthew Knuesel for great discussions and advice.

My thesis committee provided me with lots of great ideas and critique. I am grateful to Sandy Johnson, Geeta Narlikar and John Gross for thinking deeply about my project and for their guidance throughout my graduate career.

The collaboration with the John Gross' lab was integral to the success of my project. John Gross was phenomenal to work with because of his genuine enthusiasm for science and for teaching NMR. He was extremely giving of his time in teaching me how to set up NMR experiments and directing my project. I am indebted to Stephen Floor for his help in running NMR experiments and

especially for scripts for chemical shift difference analysis. He was always happy to answer questions and help in thinking about my data. I also want to thank Mark Borja, David Stanley and Greg Lee for their NMR advice. I appreciate Mark Kelly's guidance in setting up NMR experiments and his hard work in keeping the NMR facility running.

Kris Kuchenbecker was the driving force for SPR experiments and contributed lots of hard work and well as great insight with discussions on structural biology, biophysics and NHRs. I appreciated his encouragement and enthusiasm, and his patience as I fumbled through Matlab. I hope I will have another opportunity to compete with him at serial dilutions—this time I will win.

I am very lucky to have met so many fantastic friends at UCSF who have made graduate school a great experience. Han Li has been a partner in crime for countless SF shenanigans and amazing adventures. She has been extremely supportive and has also pushed me to push myself. Han is the most energetic, giving and driven person I know and she will continue to be a role model as well as a best friend.

I am also thankful to Mari Nishino, Tina Shahian Sarah Goodwin, Manisha Ray and Alana Lerner for all the fun memories and adventures throughout grad school and for their friendship. I have learned so much from each of them.

I am thankful to my parents, Gary and Linda Watson, for their unconditional love and support. They have taught me to work hard, to believe in

myself and not to give up. I admire them both and am forever grateful for their encouragement throughout this entire experience.

Lastly, I am forever grateful to my husband, Justin Cheney, for his patience, his positive attitude and support. He has been by my side throughout all the ups and downs of grad school. I cannot express how much I appreciate the infinite times he commuted between San Diego and San Francisco without complaint, so that we could be together. I could not have gotten this thesis finished without his help and encouragement (and Matlab scripts and cooking). I am so glad to have completed this milestone so that we can start our next adventures together.

Abstract

The glucocorticoid receptor (GR) binds to genomic response elements and regulates gene transcription with exquisite cell- and gene-specificity. Within a response element, the precise sequence to which GR binds has been implicated in directing receptor structure and activity. Here, we use NMR to show that different binding sequences affect the conformation of distinct regions of the GR DNA binding domain. Chemical shift difference mapping and analysis of a GR mutant suggest that an allosteric pathway links the DNA-binding surface, the dimerization interface and the associated dimer partner. We show that disrupting this pathway alters sequence-specific conformations, DNA-binding kinetics and gene-specific transcriptional activity. Our study provides insight into mechanisms by which binding sequences may impart multiple activities to a single factor through gene-specific structural changes.

Contents

Acknowledgements	iii
Abstract	viii
Chapter 1 Overview	1
1.1 Introduction	1
1.2 Methods	11
Chapter 2 An allosteric pathway transmits sequence-specific DNA signals to modulate glucocorticoid receptor conformation and activity	19
2.1 Introduction	19
2.2 Results	21
2.3 Discussion	48
2.4 Supplemental Figures	52
Chapter 3 The role of the GR dimer interface in gene-specific transcriptional activation and DNA occupancy	64
3.1 Introduction	64
3.2 Results	67
3.3 Discussion	83
Chapter 4 A naturally occurring insertion of a single amino acid rewires the transcriptional program induced by the glucocorticoid receptor	89
4.1 Introduction	89

4.2 Results	92
4.3 Discussion	100
References	107

List of Figures

Figure 1.1 DNA recognition by GR-DBD.....	4
Figure 1.2 Cellular signals that influence GR activity.....	8
Figure 1.3 GBS-dependent alternate conformations in lever arm.	10
Figure 2.1 Non-contacted GBS bases modulate GR structure and activity	24
Figure 2.2 Comparison of ¹⁵ N-HSQC spectra of three GR-DBD:GBS complexes.....	29
Figure 2.3 GBS affects GR-DBD conformation at distinct surfaces.	30
Figure 2.4: Disrupting the dimerization interface alters GR-DBD conformation at the lever arm and DNA recognition helix.	34
Figure 2.5 A477T impairs dimerization but not monomer DNA-binding.	39
Figure 2.6 GR A477T disrupts cooperativity and GBS-specific dissociation.	41
Figure 2.7 GR A477T disrupts cooperativity and GBS-specific dissociation.	43
Figure 2.8 Sequence-specific lever-arm conformation is dependent on intact dimerization interface.....	46
Figure 2.9 NMR assignment of DNA-bound GR-DBD.....	52

Figure 2.10 Heatmap of chemical shifts differences between GR-DBD WT complexes.....	53
Figure 2.11 Heatmap of chemical shift differences between WT and A477T complexes.....	54
Figure 2.12 ¹⁵N-HSQC comparison of the DNA-bound GR WT and GR A477T versus apo GR-DBD	55
Figure 2.13 Effect of GBS Spacer on cooperativity and dissociation.	57
Figure 2.14 Comparison of affinity and dissociation of GR WT and A477T.	58
Figure 2.15 SPR comparison of GR WT and A477T across seven binding sites at 8°C.....	59
Figure 2.16 Assignment of ¹⁵N-HSQC of GR-DBD at 25°C.....	60
Figure 2.17 Comparison of apo and DNA-bound GR-DBD.....	61
Figure 2.18 Analysis of GR-DBD conformational exchange.....	62
Figure 2.19 The effects of each GBS nucleotide position on the conformation of the lever-arm residue G470.....	63
Figure 3.1 GR-DBD:DNA highlighting the inter-subunit contact between A477 and I483	66
Figure 3.2 Effect of GR A477T mutation on GR gene transcription.....	69

Figure 3.3: GR occupancy of WT- and A477T-specific genes detected by ChIP-sequencing.	74
Figure 3.4 GR occupancy at WT and A477T non-differentially regulated genes by ChIP-sequencing.....	75
Figure 3.5 GR occupancy at WT and A477T occupied regions at A477T- specifically regulated genes.	76
Figure 3.6 GR occupancy at WT and A477T non-differentially regulated regions with GBS half sites.	77
Figure 3.7 Comparison of WT and A477T binding motifs in U20S cells.....	78
Figure 3.8 Genomic response elements recapitulate WT and A477T- specific patterns of transcriptional regulation.	81
Figure 3.9 Model for mechanisms of regulation by WT and A477T.....	88
Figure 4.1 Model for mechanisms of regulation by WT and A477T.....	91
Figure 4.2 Isoform specific binding and regulation by GRγ	95
Figure 4.3 GRγ compensates for A477T mutation at SPINK5L3 gene.....	97
Figure 4.4 GRγ lever arm insertion results in widespread conformational shifts in the GR-DBD.....	102
Figure 4.5 Comparison of conformation changes induced by GBS or arginine insertion in the lever arm.....	104

**Figure 4.6 Comparison of ^1H - ^{15}N HSQC for GR α -DBD and GR γ -DBD bound
to FKBP5 and ITPRIP.106**

List of Tables

Table 1.1 Binding sequences used in NMR studies.....	18
Table 2.1 Summary of DNA-binding parameters of GR-DBD across seven binding sites.....	56
Table 3.1 Identification of distinct classes of activated genes.....	73

Chapter 1 Overview

1.1 Introduction

The genome encodes all the necessary instructions for living organisms to develop and function. It consists of genes that are translated into proteins, but also contains the information required to regulate the expression of each gene. While the code for translating DNA sequences into strings of amino acids is known, the rules by which genomic regulatory elements specify transcriptional programs are not as well defined. These regulatory elements interact specifically with DNA binding factors that can modulate transcriptional activity.

One such factor, the glucocorticoid receptor (GR), modulates the transcription of hundreds of genes involved in diverse processes including cell differentiation, glucose metabolism and immune response. GR is universally expressed throughout all tissues in the human body, and like other steroid receptors, its activity and availability within the nucleus is highly regulated by hormone binding. In the absence of hormone, GR is sequestered in the cytoplasm, but in the presence of glucocorticoids such as dexamethasone (dex),

GR is translocated into the nucleus where it interacts with DNA at GR response elements (GREs) that are associated with target genes.

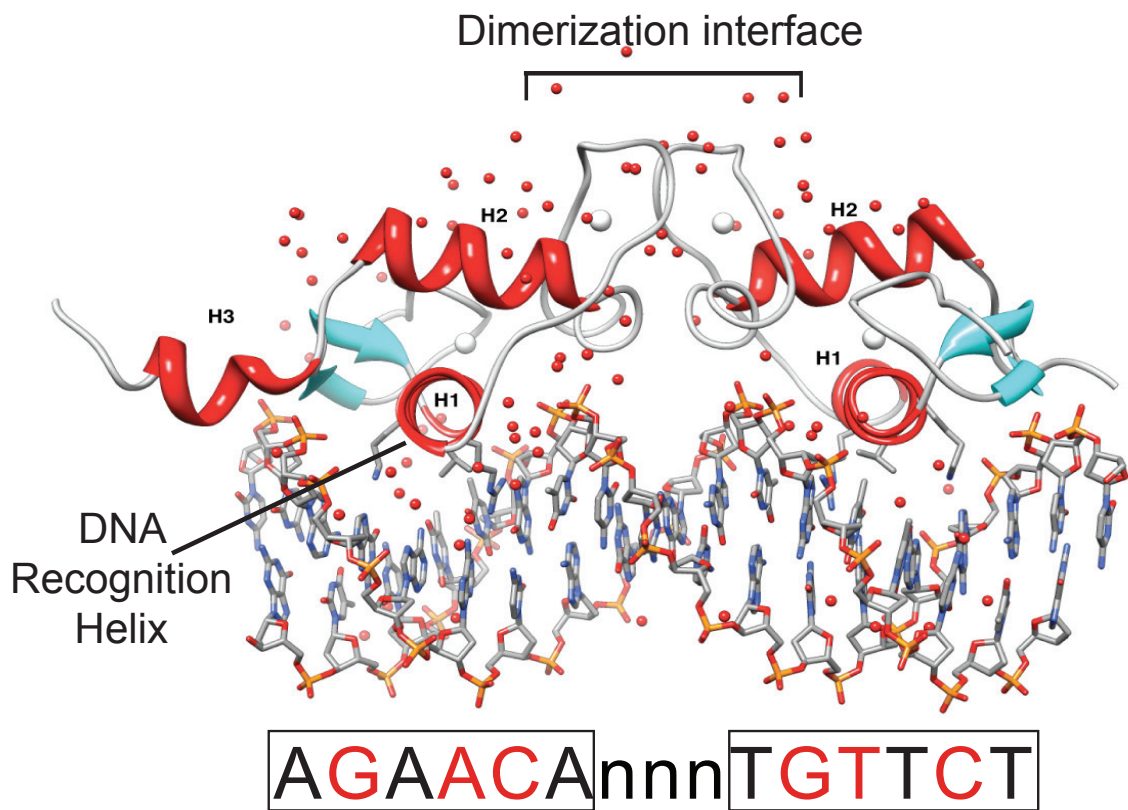
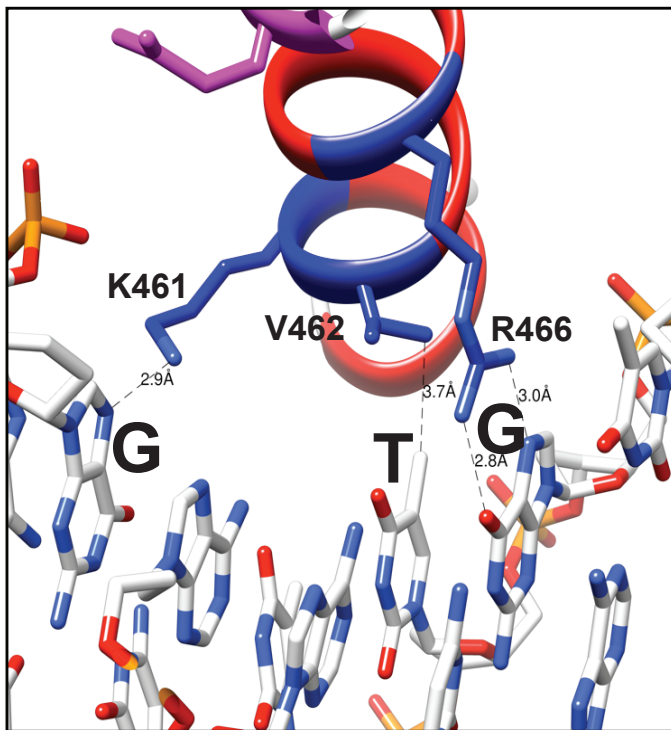
Glucocorticoid hormone binding to the GR ligand-binding domain (LBD), results in a conformational change in the receptor exposing a hydrophobic surface, termed activation function 2 (AF2), that binds coregulator proteins that contain an LXXLL interaction motif[1]. While a subset of coregulators contain binding motifs that interact with the AF2 surface, other cofactors instead bind at different surfaces of GR, including the activation function 1 domain (AF1)[2] and the DNA-binding domain (DBD)[3]. Once bound to GREs, GR coregulators mediate specific functions that impact gene transcriptional, such as chromatin remodeling, protein-modification, or recruitment of general transcription machinery [4]. Thus, GR serves as a scaffold for building transcriptional complexes that are precisely targeted to GR-bound GREs.

The transcriptional activity of GR is multifaceted; such the GR mediates either activation or repression of transcription depending on the cellular and genomic context. Within these two classes of activity, the effect among different genes can vary by several orders of magnitude. The precise determinants that define the gene-specific activity of GR at individual genes are not clear. The combinatorial assembly of regulators and coregulators at response elements, termed combinatorial control, provide a mechanism for gene-specific transcriptional regulation based on two principles: (1) the response element for each gene has a specific set of regulatory factors that govern its transcription and (2) the availability and accessibility of these factors for their response elements

are further regulated according to cellular programs and environmental cues. Thus, a single regulator can employ gene-specific control by assembling distinct multifactor complexes at different genes. The incorporation or omission of any individual factor in a regulatory complex could result in differential gene-expression.

GR is targeted to GREs through direct interaction with GR binding sequences (GBS), consisting of two loosely palindromic, hexameric half sites separated by a three-base pair spacer. Crystallographic studies of the rat GR-DBD (residues 440-525) show that GR binds to the GBS as a dimer. Each dimer partner directly contacts three nucleotide bases from each half site through specific side-chain interactions with the recognition helix residues K461, V462, R466. [5][6] (**Figure1.1**) Each GR dimer partner consist of two zinc-finger motifs, where the first zinc finger orients the DNA recognition helix for binding in the GBS major groove, and the second zinc finger forms the dimerization surface.

Figure 1.1 DNA recognition by GR-DBD



Comparison of the apo GR-DBD solution structure to the DNA-bound crystal structure provides information about the changes mediated by DNA-binding. The most significant changes between the apo and DNA-bound GR-DBD are within the second zinc finger at regions that form the dimerization interface in the DNA-bound complex. The orientation of residues C476-C482 consisting of the dimerization loop (A477-D481) is rotated about 90° between the two structures, suggesting that DNA-binding induces a conformation change in this region that contributes to the formation of the dimerization interface.[7] While this region is less defined compared to other parts of the receptor in the apo GR-DBD, the DNA-bound conformation is not detected within the ensemble of apo NMR structures. Additional dimerization contact residues K486-N491 in the second zinc finger appear disordered in the apo GR-DBD structure reported by van Tilborg, *et al.* and Hard, *et al.*[8][9], but become structured into a distorted helix in the GR-DBD:GBS complex. Thus, DNA-binding mediated by the recognition helix (in zinc finger 1), imparts structural changes in the dimerization surface (in zinc finger 2) providing an explanation for the cooperative association of the GR-DBD dimer to DNA.[10]

The dimer interface of the receptor is formed by symmetrical intersubunit interactions within the second zinc finger: (1) between both N491 side chains, (2) between dimerization loop residues R479 and D481 and (3) between A477 and I483. There is also a hydrophobic contact between I487 and L475[5]. The apo GR-DBD does not dimerize in solution[9], but in the presence of DNA, GR binds cooperatively at GBS recognition sites [11]. Mutations across all five of the

dimerization loop residues result in reduced cooperativity of dimerization[12].

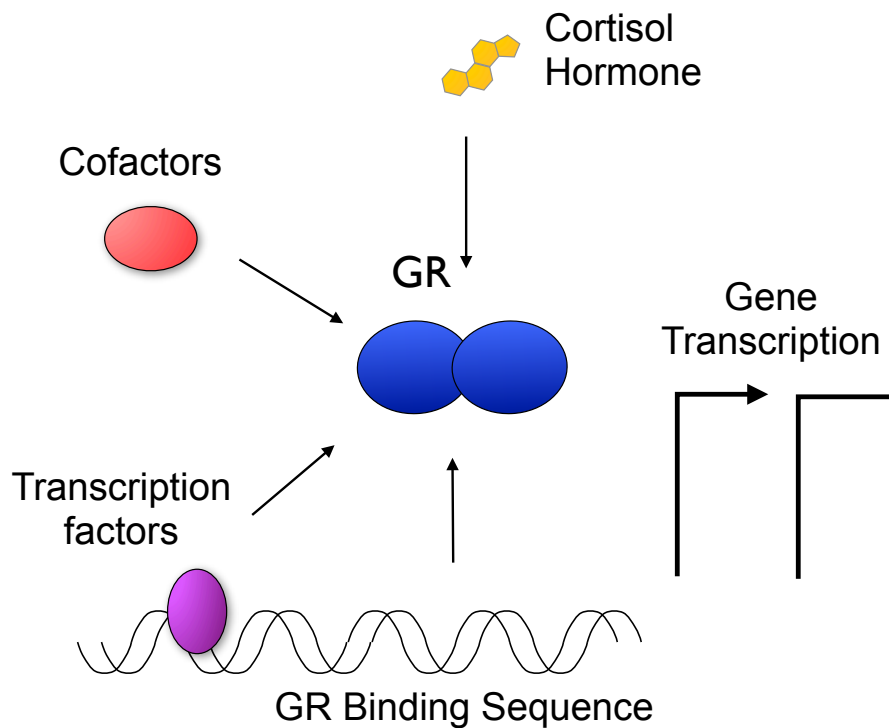
Interestingly, some structural and functional studies have provided hints that the dimer interface may be functionally coupled with DNA sequence recognition. Three GR recognition helix mutations (GR_{EGA}) that affect the sequence specificity of DNA binding also induce structural changes at dimerization contact residues, as measured by NMR chemical shift [13]. These mutations also result in reduced DNA cooperativity, suggesting that sequence recognition may dimerization surface function[14]. This raises the question as to how recognition of different DNA sequences might impact GR dimerization and cooperativity.

Structural and biochemical studies of GR and other nuclear hormone receptors have provided numerous examples of how DNA- or ligand-binding at mediates structural changes at distinct surfaces that ultimately enhance interactions with dimer partners or coregulators, respectively. This ability of one site to structurally modulate a second site, termed allostery, appears to be an important mechanism in nuclear hormone receptor signaling, allowing information to be transmitted across a single domain and also between distinct receptor domains. For example, DNA binding at the DBD affects the structure of the receptor's coregulator interaction surfaces[15], induces selective interaction with coregulator peptides[16], and initiates structure in the N-terminal AF1 domain [17]. Similarly, binding of different ligands to the LBD can modulate coregulator peptide interactions[18], increase the structural flexibility of the DBD[19], and modulate selective ligand-binding of the adjacent dimer partner[20]. Therefore, it

is likely that GR activity in a given cellular or genomic context is defined by multiple interactions with signaling factors at different surfaces of the receptor.

We hypothesize that GR integrates cellular signals including hormones, coregulators, and DNA binding sites through structural changes, and that the combination of distinct signals determines GR activity at a given gene (**Figure 1.2**). Given the diversity and complexity of potential GR signals within the cell, this work aims to take a reductionist approach to understand how the interaction between a single domain of GR (DBD) and a single 15 bp GR binding site (GBS) can affect GR activity by modulating other interaction surfaces of the receptor. By perturbing this simple system with precise changes in GBS sequence or single mutations in GR functional surfaces across multiple *in vitro* and cell-based assays, this thesis aims to define rules by which input signals determine GR gene-specific function.

Figure 1.2 Cellular signals that influence GR activity.



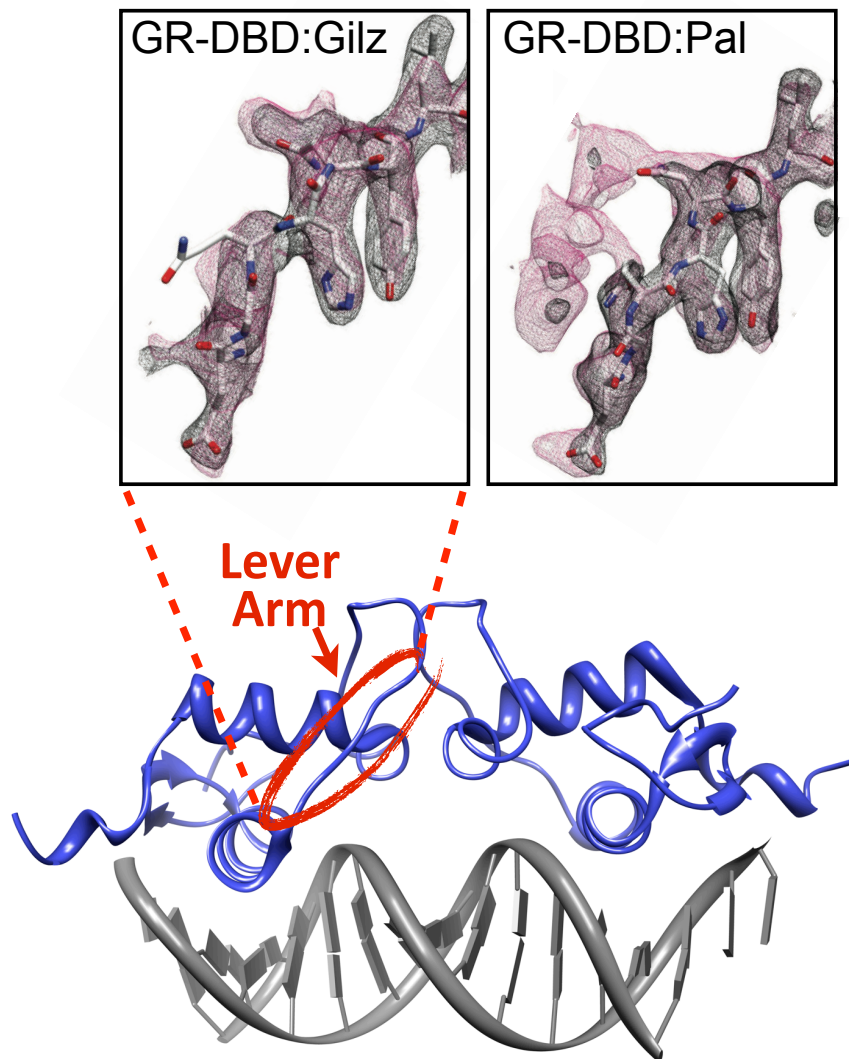
Chapter 2 of this thesis focuses on how signals encoded in the DNA binding sequence impact GR structure and activity and is motivated by the findings of Meijnsing et al., which show that 15 bp GBS sequences are sufficient to generate different magnitudes and mechanisms of transcriptional activation[6] Crystallographic analysis of GR-DBD bound to different GBSs showed that the base-specific contacts made between the GBS and the GR recognition helix are invariant among the binding sites tested. However, differences in the GBS at base positions that are not contacted by GR induce alternate conformations within a loop region between the recognition helix and the dimer interface of the

GR-DBD, termed the lever arm (**Fig. 1.3**). Thus, the conformation of the lever arm is dependent on the GBS sequence, though it does not make any contacts with DNA. This result raised several exciting questions: (1) how does GR “read” non-directly contacted bases, (2) how do alternate conformations in the GR lever arm result in gene-specific GR signaling, and (3) are additional conformations detectable by solution methods?

In attempting to answer these questions, we identified the dimer interface of the DBD as responsive to GBS sequence, and also important for GR gene-specific activity. We took advantage of a GR dimer interface mutant with potential therapeutic interest, to test how perturbation of the dimerization surface impacts GR structure and function. In Chapter 3 of this thesis, the relationship between DNA-binding and transcriptional activity is compared for the dimerization mutant and the wild-type GR at endogenous genes. Lastly, Chapter 4 investigates the functional and structural interplay between the lever arm and other GR surfaces and the mechanisms by which the lever arm influences gene-specific regulation.

Figure 1.3 GBS-dependent alternate conformations in lever arm.

The electron density map of the GR lever arm region of the GR-DBD:Gilz and GR-DBD:Pal crystal structures is shown. Modeled electron density ($2F_o - F_c$) is shown in black, and the density of alternate conformations is outlined in red. An alternate lever arm conformation is indicated for the Pal but not the Gilz complex. The location of the lever arm within the GR-DBD:GBS complex is circled in red.



1.2 Methods

Protein expression and purification:

Expression vector pET28a containing rat GR DNA-binding domain, residues 440-525, (rGR-DBD) has been described previously[6]. Vector for rGR-DBD A477T was derived from the rGR-DBD plasmid by PCR site-directed mutagenesis. BL21 Gold E. coli cells were grown in 50mL LB media to optical density of ~0.4-1.0, then pelleted and resuspended in 1L labeling media (minimal media containing 2 g/L $^{15}\text{NHCl}_4$ as the only Nitrogen source). Cultures were grown to an optical density of ~0.7 and rGR-DBD WT or rGR-DBD A477T expression was induced with 0.5mM IPTG for ~16 hours at 18°C or 8 hours at 30°C (both produced equivalent spectra). Cells were pelleted and resuspended at 40mL/L culture in lysis buffer containing 50mM Tris pH 7.5, 500mM NaCl and 15mM Imidazole, then frozen in liquid nitrogen, and stored at -80°C. Thawed cells were lysed using an EmulsiFlex C5 homogenizer, and lysate was centrifuged for 45 min at 40,000 rpm at 4°C and run over a Ni Sepharose (GE Healthcare) column equilibrated with lysis buffer and eluted with a linear gradient reaching 350mM Imidazole. Pooled fractions were dialyzed into 20mM Tris pH 7.5, 50mM NaCl, 2.5mM CaCl_2 , and 0.5mM β -mercaptoethanol and cleaved at 4°C overnight with 50-100 units Thrombin. Protein was centrifuged for 45 min at 40,000 rpm at 4°C to remove precipitate and further purified over a Resource S ion exchange column with a linear gradient of 50mM-300mM NaCl, 20mM Tris

pH 7.5, and 0.5mM β -mercaptoethanol. Pooled samples were concentrated using Amicon Ultra 5K MWCO (Millipore) and run over a 16/60 Superdex75 gel filtration column in NMR Buffer (20mM Sodium Phosphate pH 6.7, 100mM NaCl, 1mM DTT).

Protein-DNA Complex Formation:

Single-stranded GBS oligos were ordered from Integrated DNA Technology (IDT) and purified by MonoQ Column (GE Healthcare) equilibrated with 10mM NaOH, 100mM NaCl and eluted by linear gradient reaching approximately 600mM NaCl. Purified oligos were dialyzed into H₂O, lyophilized, and resuspended at ~2mM in H₂O. Complimentary oligos were annealed in 20mM Sodium Phosphate, 100mM NaCl, 5mM MgCl₂ in a boiling waterbath and cooled slowly to room temperature. To prevent protein crashing upon addition of concentrated DNA, DNA duplexes were diluted in 10x volume cold NMR buffer and then combined with rGR-DBD at a ~40% excess DNA to GR-DBD dimer, to ensure that all protein was bound. Dilute GR-DBD:DNA complexes were concentrated slowly at 4°C using a 3K MWCO Centrifugal Filter (Amicon) to 150-300 μ M dimer complex. Concentrated complexes were filtered to remove any precipitate using Ultrafree PVDF 0.22 μ m columns (Millipore).

Protein NMR assignment:

For preparation of triple-labeled rGR-DBD, BL21 Gold cells were grown in 50mL LB to optical density of ~0.6, pelleted and resuspended in 1L unlabeled minimal media and grown to optical density of 0.2. Then cells were pelleted and resuspended in 1L of triple-label media (minimal media containing 2g of $^{15}\text{NHCl}_4$ (or ammonium sulfate), 2g ^{13}C -glucose in 90-100%-pure D_2O). At optical density of ~0.6, expression was induced at 30°C under 0.5mM IPTG for 8 hours. Protein was purified as described above. For unbound rGR-DBD, protein was dialyzed into NMR buffer containing 20 mM sodium phosphate, pH 6.7, 100 mM NaCl, 5 mM MgCl_2 , and 1 mM DTT, and concentrated to 1.7mM for NMR. The following experiments were run at 25°C on a Bruker 500MHz spectrometer: reference ^{15}N -HSQC, HNCOCACB, HNCO, HNCACO, HNCA, HNCOCA, and CC(CO)NH-TOCSY. A ^{15}N -edited NOESY was run on a Bruker 800MHz spectrometer.

For assignment of DNA-bound rGR-DBD, complexes with the Gha GBS were prepared as described above and concentrated to 500 μM dimer complex. NMR assignments were generated from standard 3D experiments that were conducted on 500, 600, or 900 MHz spectrometers at two temperatures (25°C and 35°C), because a subset of peaks gave more signal at the higher temperature. Experiments included: ^{15}N -edited NOESY, TROSY-HNCO, TROSY-HNCA, TROSY-HN(CO)CA, TROSY-HNCACB, TROSY HN(CA)CO. Assignments were aided by ^{15}N -HSQC of ^{15}N -single amino acid labeling of Ile,

Leu, Val, Phe, Tyr, Lys, Arg. Data were processed in NMRPipe (National Institute of Health), and assignments were generated using Sparky (UCSF).

Chemical Shift Perturbation Analysis:

^1H - ^{15}N -HSQC spectra were acquired on a Bruker 800MHz spectrometer at 35°C. Data were processed in NMRPipe (National Institute of Health), and analyzed in Sparky (UCSF). Peak assignments were transferred from the GR-DBD:Gha complex to additional GBS complexes. In most cases peaks could be transferred by measuring the minimal distance from each assigned GR:Gha peak to the nearest peak in the GR-DBD:GBS complexes. Chemical shift differences between GR WT and GR mutant complexes were determined by measuring the minimal distance from each assigned GR WT peak to the nearest peak in the GR mutant spectrum using the formula: combined chemical shift $\Delta\delta = [(\Delta\text{H ppm})^2 + (\Delta\text{N ppm}/5)^2]^{1/2}$ [21].

Transcriptional Reporter Assays:

For GBS reporters: Plasmids were constructed with 15 bp binding sites flanked by overhangs for cloning into the Kpn1 and Xho1 sites of pGL3-Promoter (Promega) as described previously[6]. U2OS cells (ATCC) were seeded in DMEM supplemented with 5% FBS in 24-well plates at roughly 20,000 cells/well one day prior to transfection. Cells were transfected with 20ng/well GR plasmid,

20ng/well GBS-luciferase plasmid, 200 pg/well pRL Renilla, 120ng/well empty p6R plasmid, 1 uL PLUS Reagent and 0.7 uL/well Lipofectamine Reagent (Invitrogen) for 4 hours in no-serum DMEM media. Cells were washed and recovered in DMEM + 5% FBS for 3 hours. Cells were then treated with 100nM dexamethasone or ethanol for 12 hours. Luciferase induction was measured using Promega Dual-Luciferase Reporter kit (Promega) in 96-well format using a Tecan plate reader. Each dex-treated luciferase sample was normalized to Renilla signal and then normalized to ethanol control samples. Normalized dex-induced luciferase induction for each GBS was then normalized against empty pGL3 vector.

For GRBR Reporters: Luciferase reporters were generated from approximately 500 bp regions corresponding to peaks identified in Table 3.1 cloned into pGL4 modified with an E4TATA promoter. U2OS cells with stable over-expression of GR WT or GR A477T were transfected as described above, except that GR expression plasmids were omitted and cells were harvested after ~12 hours of 100nM dex treatment.

Surface Plasmon Resonance:

A Biacore T100 instrument was used in the SPR analysis of GR-DBD (WT and A477T) interaction with the seven different GBS oligos. All surface preparation was conducted at 25°C in 20mM HEPES (pH 7.2), 150mM NaCl before introducing assay buffer and changing the analysis

temperature to 35°C or 8°C. In brief, matrix-free surfaces were prepared by injection of Neutravidin (Invitrogen) across a planar saccharide monolayer with covalently coupled biotin (BP chips, Xantec Bioanalytics). Double-stranded GBS oligos with a single 5' biotin-TEG label (IDT) were subsequently captured at immobilization levels ranging from 20 to 65 RU. To minimize bulk shift during sample injection, the purified WT and A477T GR-DBDs were dialyzed overnight in SPR assay buffer (20mM Sodium Phosphate, pH 6.7, 100mM NaCl, 1mM DTT). Following dialysis, protein concentration was determined by UV absorbance at 280nm and BSA (Sigma) was added to both the assay buffer and the protein samples (BSA concentration = 0.1 mg / mL). Fifteen point concentration series of the protein samples were prepared by two 0.5-fold serial dilutions followed by twelve 0.7-fold serial dilutions, generating titration curves spanning ~700pM to 200nM for the WT GR-DBD and ~1.4nM to 400nM for the A477T GR-DBD. Association and dissociation times for the WT and A477T were selected to ensure equilibrium and complete dissociation. All data were processed and analyzed in Matlab. Because of the wide ranging kinetics for the seven different GBS sequences, the association time ranged from 250-700s and 175-250s for the WT and the A477T GR-DBDs, respectively; similarly, dissociation times ranged from 100-800s and 100-200s for the WT and the A477T GR-DBDs, respectively.

Gel Shift:

Gel shifts were performed using unlabeled GR-DBD WT and GR-DBD A477T expressed and purified as described for NMR experiments and stored at -20°C in 50% glycerol. Double-stranded oligos with an Alexa488 fluorophore conjugated to one the 3' ends (IDT) were generated for Pal and Sgk sequences as listed in Table 1.1. Protein and DNA were incubated for 30 min at 5nM final DNA concentration with GR-DBD titrations in Binding Buffer (20mM Tris pH 8, 50mM NaCl, 1mM EDTA, 10ug/mL dIdC, 5mM MgCl₂, 200ul/mL BSA, 5% glycerol, and 1mM DTT) on ice. Native 8% polyacrylamide gels were run at 200V in 0.5X TBE at 4°C. Alexa488 signal was imaged on a Typhoon scanner (GE Healthcare) and quantified using ImageQuant. Fraction GR-DBD bound was determined as $1 - \frac{[DNA_{free}]}{[DNA_{total}]}$. Binding curves were fit to the data using Kaleidograph.

Table 1.1 Binding sequences used in NMR studies

GBS name	Sequence (5' → 3')
Fkbp5	gtacAGAACAaggTGTTCTtcgac
Gha	gtacGGAACAtaaTGTTCCtcgac
Gilz	gtacAGAACATTGGGTTCCtcgac
Pal-F	gtacAGAACAaaaTGTTCTtcgac
Pal-R	gtacAGAACAAttTGTTCTtcgac
Pal-ttg	gtacAGAACATTGTGTTCTtcgac
Sgk	gtacAGAACAAttTGTCCTcgac
Sgk-ggg	gtacAGAACAaggTGTCCTcgac
Sgk-m1	gtacAGAACAAttTGTCCTcgac
Sgk-m2	gtacAGAACAAttTGTCCTcgac
Sgk-m3	gtacAGAACAAttTGTCCTcgac
Sgk-m4	gtacAGAACAAttTGACCTcgac
Sgk-m6	gtacAGAACAAttGGTCCTcgac
Sgk-m7	gtacAGAACAAttTGTCCTcgac
Itrip	gtacAGAACAaggAGTTACTcgac

Chapter 2

An allosteric pathway transmits sequence-specific DNA signals to modulate glucocorticoid receptor conformation and activity

2.1 Introduction

While one's genome sequence is invariant, gene expression must be tailored to the needs of specific tissues and in response to environmental and developmental changes. Transcriptional regulators coordinate this task, by integrating cellular, physiological and environmental input signals with gene-specific response elements [22], [23], to facilitate precise transcriptional outputs at target genes. This intricate process relies on combinatorial control, in which distinct combinations of factors assemble into transcriptional regulatory complexes at functional response elements. However, the determinants of specificity that define these transcriptional complexes are not understood.

The nuclear hormone receptor, glucocorticoid receptor (GR), utilizes combinatorial control to regulate hundreds of target genes in a tissue- and gene-specific manner. Fundamental to this process is the regulation of receptor activity

by multiple signals, such as hormonal ligands, coregulators, post-translational modifications, and DNA binding sequences. Each of these signals drives conformational changes in the receptor, and modulates its transcriptional regulatory activity[24-27].

Our lab previously demonstrated that DNA binding sequences are signals that direct GR structure and activity [6]. The GR binding sequence (GBS) varies loosely around a 15-base pair motif consisting of two imperfect palindromic hexameric half sites separated by a 3-base pair spacer[28]. GR makes direct contacts with 3 bases in each GBS half site. Crystallographic studies indicated that the precise sequence of the binding site modulates the conformation of GR at a loop region termed the lever arm, which does not itself contact the DNA. Moreover, GBSs that gave rise to different lever arm conformations were invariant at all nucleotide positions that make base-specific contacts with GR. Thus, direct base contacts cannot explain the GBS-specific lever arm conformations that were detected, indicating that non-contacted bases provide signals that modulate GR structure. Furthermore, GBS signals must be transmitted from the DNA interface to the lever arm, suggesting that these surfaces are linked by an allosteric path.

Our previous crystallography study left two important questions: (1) how does GR detect the specificity determinants within GBSs, and (2) how are DNA-dependent conformational changes transmitted to define GR activity? To answer these questions, we combined three experimental approaches: nuclear magnetic resonance (NMR), which is very sensitive to conformational changes in solution,

biophysical characterization of GR DNA binding and dimerization, and analysis of a GR mutant.

2.2 Results

GBS spacer affects GR occupancy, activity, and structure

We sought to determine the degree of sequence variability among endogenous GBSs to estimate the potential for DNA sequences to be unique signals that produce distinct GR activities. We identified GR binding regions in U2OS cells exogenously expressing full-length rGR, using GR chromatin immunoprecipitation (ChIP) followed by next-generation sequencing. An unbiased search for sequence motifs within the 1000 GR binding regions with the highest number of reads revealed a GBS motif composed of imperfect palindromic hexamers separated by a 3 bp spacer, similar to previously identified motifs based on smaller sample sets (*e.g.*, [29]) (**Fig. 2.1a**). Applying this sequence motif to 30,000 GR binding regions revealed that 90% of GBS sequences are unique, thus demonstrating that there is sufficient diversity for each to be a gene-specific signal. However, this would require an indirect readout mechanism, where GBS bases that are not directly contacted impart

sequence specificity. The GBS positions with the highest information content (>1 bit) correspond to the six bases that are directly contacted by the GR dimer [5], [6]. The remaining nine nucleotide positions each contain less than 1 bit of information and positions 3 and 13 lack sequence preference completely. Notably, GR displays significant base-preference at GBS positions that it does not contact directly: pyrimidines at spacer positions 7-9, as well as A and T at positions 6 and 10, respectively.

To investigate how varying the GBS at non-contacted bases affects GR activity, we monitored transcriptional induction in the presence of 100nM dexamethasone (dex) using a luciferase transcriptional reporter consisting of a single GBS upstream of a minimal promoter (**Fig. 2.1b**). We found that different GBSs differentially modulated GR activity. For example, transcriptional activation was similar for GBSs Pal-R and Sgk, which differ at GBS positions 13 and 15, whereas changing the spacer of Sgk from TTT to GGG resulted in nearly four-fold decreased induction. Changing the spacer only one base from T to G resulted in an intermediate two-fold decrease. Thus, bases that are not directly contacted by GR can modulate transcriptional induction, suggesting that indirect readout is a determinant of GR activity.

To investigate indirect readout of the GBS spacer, we aligned the crystal structures of GR-DBD: Pal and GR-DBD:Fkbp5 complexes [6], whose GBSs differ only in the spacer (**Fig. 2.1d**). These structures reveal that the minor groove of the Pal spacer is narrower than that of the Fkbp5 spacer, with average widths of 3.8 Å and 6.4Å, respectively, as measured by Curves+ [30]. As the Pal

and Fkbp5 GBSs have spacer sequences of AAA or GGG, respectively, the sequence-specific difference in minor groove width is consistent with previous studies showing that short A-tracts narrow the minor groove[31].

Examination of GR contacts to the DNA phosphate backbone near the GBS spacer indicated that the orientation of the side chain of lysine 490 (K490) is dependent on the spacer sequence (**Fig. 2.1e**). In the Pal complex, the K490 side chain reaches across the spacer minor groove to hydrogen bond with the phosphate backbone at the complement of position 7 of the spacer. In the Fkbp5 complex, which has a wider spacer minor groove, K490 does not reach across the spacer to contact the distal strand, but instead makes a phosphate backbone contact to the proximal strand at position 11. This suggests that GR may “measure” the spacer minor groove width as an indirect readout of spacer sequence. From analysis of crystal structures, as many as 10 GBS nucleotide positions participate in phosphate backbone contacts with GR, providing a potential mechanism for measuring DNA shape across multiple positions in the GBS. Because DNA groove width is dependent on nucleotide sequence, we speculate that GBS spacer groove width serves as a GBS-specific signal that modulates GR function.

Figure 2.1 Non-contacted GBS bases modulate GR structure and activity

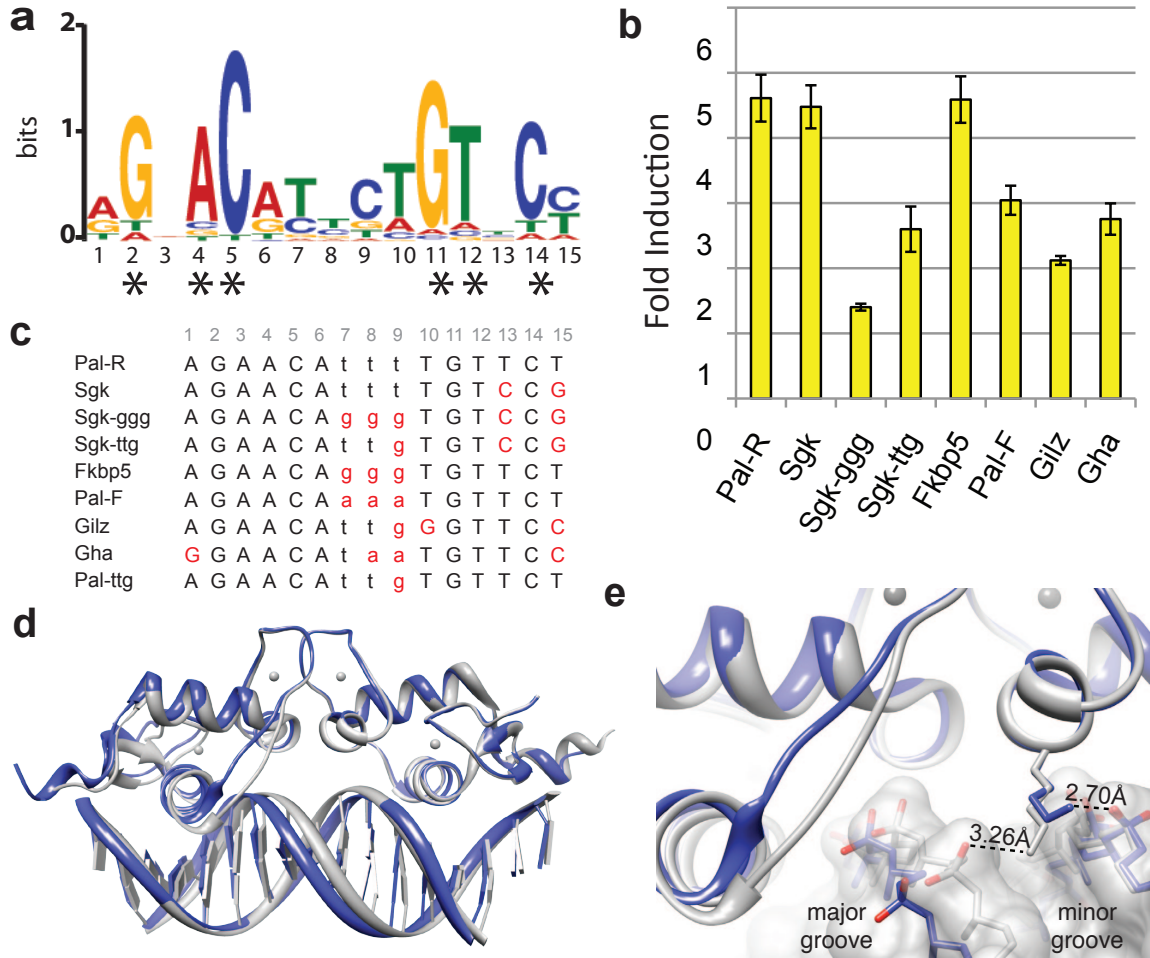


Figure 2.1: Non-contacted GBS bases modulate GR structure and activity.

(a) The GR binding motif identified by GR ChIP-sequencing in U2OS-GR cells using MEME in "zero or one motif per site" mode with a 2nd order background Markov Model based on the top 1000 peaks. (b) Luciferase induction of GBS reporters with 100 nM dexamethsone treatment compared to ethanol control in U2OS cells. Error bars are calculated as s.e.m. of four or more independent experiments (c) List of the GBS sequences used in this study. The 15-bp GBSs shown here were centered within identical flanking sequences resulting in a total dsDNA of 24-bp. Spacer regions are indicated in lowercase. (d) Alignment of crystal structures of GR-DBD:Pal (PDB ID: 3G99, grey) and GR-DBD:Fkbp5, (PDB ID: 3G6U, blue) shows sequence-specific lever-arm conformations and spacer minor groove widths. (e) Zoomed view of K490 side chain with a hydrogen bond to the phosphate backbone of the spacer minor groove of Pal GBS (grey) but not Fkbp5 (blue).

Non-contacted GBS bases modulate GR conformation

We hypothesized that the GBS affects GR activity by influencing GR conformation in a sequence-specific manner. We monitored GR-DBD conformation by ^{15}N -HSQC, which measures the chemical environment of the amide bond of individual amino acid residues (**Fig. 2.2**). For GR-DBD bound to a semi-palindromic GBS (Gha), we were able to assign over 90% of the peaks in the HSQC spectrum to their corresponding residues using standard 3D methods. Notably, we observed peak splitting for a subset of residues, where two peaks correspond to a single residue. This was the case for 10 of the 78 assigned residues in the GR-DBD:Gha spectrum. Peak splitting indicates two unique chemical environments, reflecting either exchange between two conformations of the GR dimer or conformational asymmetry between the GR dimer partners.

Next, we compared HSQC profiles for a panel of GBSs that differ in nucleotide sequence only at base positions that are not directly contacted by GR. The peak assignments for the GR-DBD:Gha spectrum were transferred to spectra of these GR-DBD:GBS complexes. The overlay of spectra for GR-DBD bound to Fkbp5 (red) and Sgk (green) or Gha (blue) revealed a unique chemical shift pattern for each GBS complex. For example, GR-DBD:Fkbp5 and GR-DBD:Sgk spectra showed significant chemical shift differences from GR-DBD:Gha for ~25% of assigned residues. This indicates that each GR-DBD

complex is structurally distinct and that the GBS-specific GR conformations must be dependent on GBS bases that are not directly contacted by GR.

Specific GBS base positions modulate discrete regions of GR-DBD

We compared spectra of the GR-DBD bound to GBSs that differ at specific nucleotide positions (**Fig. 2.3**). Pair wise comparison of GR-DBD:GBS complexes that differ only in the spacer revealed significant chemical shifts for residues A477 and G478, with distinct patterns dependent on spacer sequence (**Fig. 2.3a**, top). Specifically, GBSs with a TTT spacer (Pal-R and Sgk) share the same A477 and G478 conformation, whereas GBSs with a GGG spacer (Fkbp5 and Sgk-ggg) share a second conformation. The asymmetric spacer, TTG, results in peak splitting for A477 and G478, suggesting conformational asymmetry of GR dimer partners.

We used chemical shift difference analysis, which is sensitive to long-range conformational changes [32], [33], [34], to determine how differences in GBS base position affect specific regions of the GR-DBD. For example, changing the spacer from TTT to GGG produced conformational changes in the recognition helix (H1), lever arm, dimerization loop (D-loop) and a short helical stretch upstream of H2 (**Fig. 2.3b-c**, top). GBS variants that differ by only one nucleotide (TTT vs. TTG) affected many of the same regions of the GR-DBD as changing all three spacer positions (**Fig. 2.3c**, middle).

Changing the GBS from palindromic to asymmetric by varying positions 13 and 15 resulted in a different pattern of conformational shifts than changing the GBS spacer (**Fig. 2.3a**, bottom). In this case, residues G453, K461, and Y497 undergo peak splitting, with one of the doublet peaks significantly and consistently shifted. This suggests that introducing asymmetry at one GBS half site induces an alternate conformation for one of the GR-DBD dimer partners. Pair wise comparison of GBSs that differ only at positions 13 and 15 displayed chemical shift differences that mapped to zinc-finger 1 (upstream of and within H1) and H3 (**Fig. 2c**, bottom, and **Supplementary Fig. 2.10**).

Therefore, in addition to the lever arm identified by crystallography, NMR revealed several regions of GR-DBD whose conformations are influenced by the precise binding sequence. Furthermore, distinct GBS nucleotide positions affected specific regions of GR-DBD—notably, changes in GBS spacer induce conformational shifts in H1, the lever arm and D-loop, implying a path of conformational shifts between the DNA interface and the dimerization interface (**Fig. 2.3b**). Having previously demonstrated that the lever arm affects GBS-specific structure and activity [6], this NMR study suggests that the dimerization interface plays a similar role. Furthermore, the apparent pathway of conformational shifts suggests that variations in GBS affect GR structure at a second site.

Figure 2.2 Comparison of ^{15}N -HSQC spectra of three GR-DBD:GBS complexes.

a

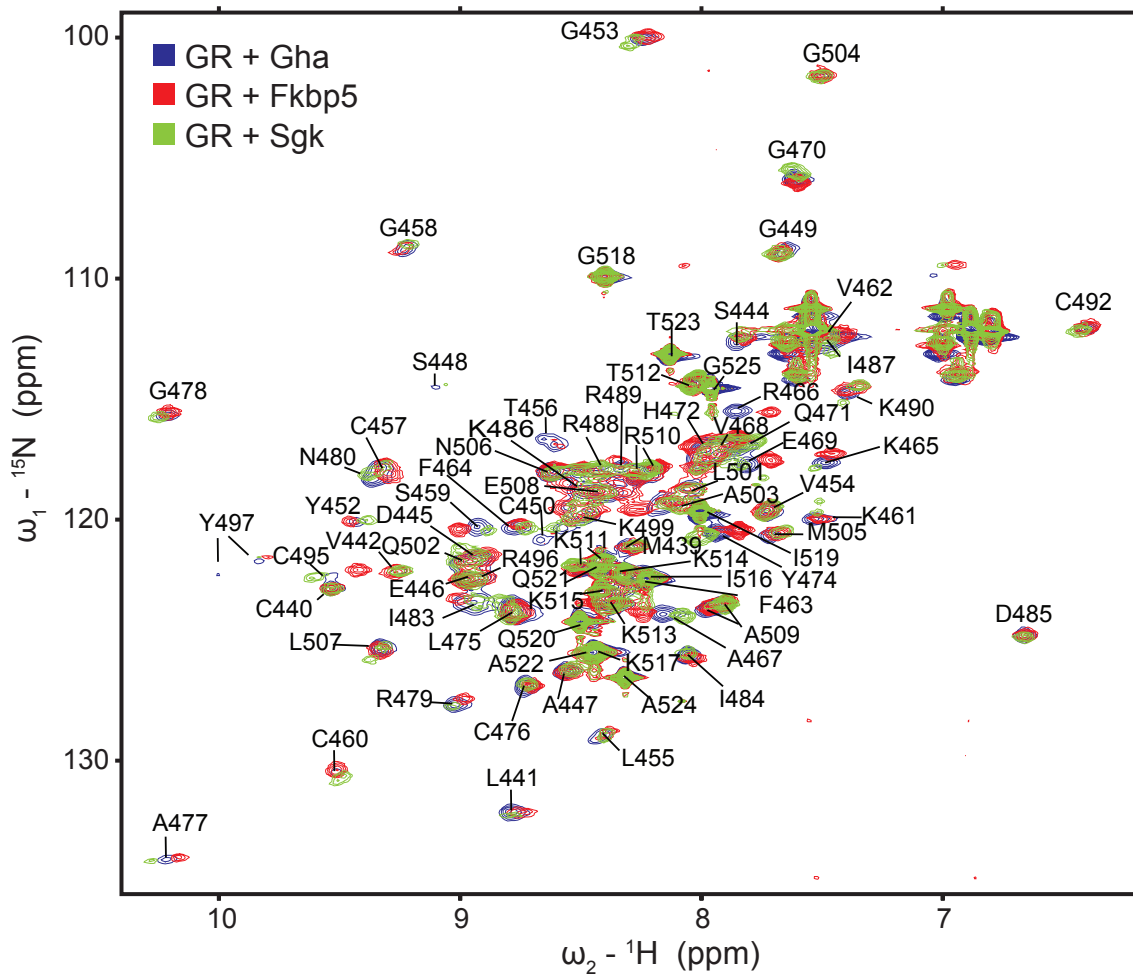


Figure 2.3 GBS affects GR-DBD conformation at distinct surfaces.

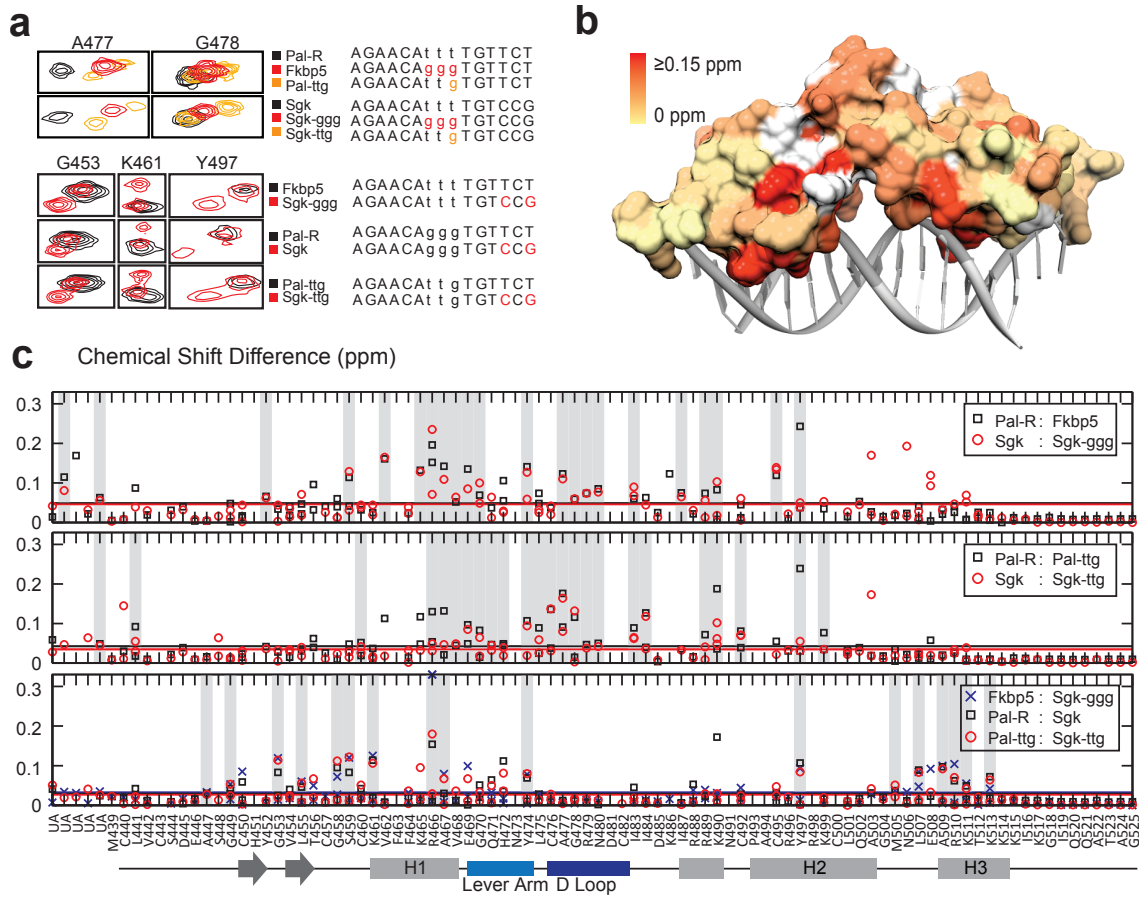


Figure 2.3: GBS affects GR-DBD conformation at distinct surfaces.

(a) Effect of specific base changes to GBS spacer (top) or half site (bottom) at selected residues that shared common shift patterns. (b) Magnitude of combined ^1H and ^{15}N chemical shift difference ($\delta\Delta$) between GR-DBD:Fkbp5 and GR-DBD:Pal spectra for each assigned residue colored onto the crystal structure of GR-DBD:DNA. Unassigned residues are colored white. (c) Chemical shift difference analysis for pair wise comparison of GR-DBD complexes with TTT spacer compared to GGG (top), TTT spacer compared to TTG (middle), or AGAACA half site compared to AGACCG (bottom). Peaks unambiguously arising from peak splitting were assigned to their corresponding residues and $\delta\Delta$ values for both peaks are plotted. Grey bars indicate residues where all comparisons show a $\Delta\delta$ greater or equal to the mean $\Delta\delta$ of all peaks in each pairwise comparison.

GR A477T affects GBS-specific transcriptional regulation

To investigate the functional significance of GBS-specific structural changes, we tested whether perturbing the dimer interface affected GR activity in a GBS-specific manner. Since the dimerization interface residue, A477, was significantly shifted by changes in spacer sequence, we focused on this residue. A477 makes one of the four dimerization contacts within the GR-DBD [5]—a backbone hydrogen bond between the carbonyl of A477 and the dimer partner amide of I483. A mutation in this residue, A477T, has been studied previously and has been suggested to alter GR activity at endogenous genes [35]. To determine how A477T affects transcription at the binding sequences that were investigated by NMR, we tested the impact of the A477T mutation in GBS reporter assays. GR A477T differed from GR WT in a GBS-specific manner: decreased (Pal-R, Sgk, Fkbp5), increased (Sgk-ggg, Sgk-ttg, Pal-F, Gha), or equivalent (Gilz) (**Fig. 2.4d**). Thus, a point mutation at the dimerization interface did not abolish GR activity, but instead resulted in reinterpretation of GBS signals by GR.

A477T mutation disrupts GR conformation at the dimer interface, recognition helix and lever arm

How the A477T mutation results in reinterpretation of GBSs by GR is not clear, as the structural and biophysical impact of this mutation has not been previously determined. We compared the chemical shift profile of GR WT to A477T bound to the Fkbp5 GBS (**Fig. 2.4a**). The GR-DBD A477T spectrum showed that many peaks overlaid well with GR WT, but that over 30% of residues were significantly shifted as a result of the A477T mutation. Importantly, these peaks did not overlay with those corresponding to the unbound GR A477T, indicating that the protein is completely bound to DNA (**Supplementary Fig. 2.12**). Transfer of peak assignments from the GR WT spectra to the GR A477T spectra was ambiguous because of the number and magnitude of shifted peaks. Instead, we quantified the chemical shift difference as the distance between each peak in the GR WT spectra to the nearest peak in the GR A477T spectra[36].

Comparison of GR WT and GR A477T for Gha, Fkbp5, and Sgk complexes (**Fig. 2.4b**) revealed A477T-specific shifts mapping to the D-loop and also to residues surrounding I483, suggesting that the A477T mutation disrupts the dimerization interface. Additionally, conformational shifts mapped to the lever arm and recognition helix of GR, despite their distance from the A477T mutation. Thus, for GR WT, conformational shifts associated with varying the DNA sequence map to the GR lever arm and the dimerization interface (**Fig. 2c**). Conversely, conformational shifts resulting from a mutation in the dimer interface affect the lever arm and DNA-binding interface. This further suggests that the dimerization and DNA interfaces are allosterically coupled.

Figure 2.4: Disrupting the dimerization interface alters GR-DBD conformation at the lever arm and DNA recognition helix.

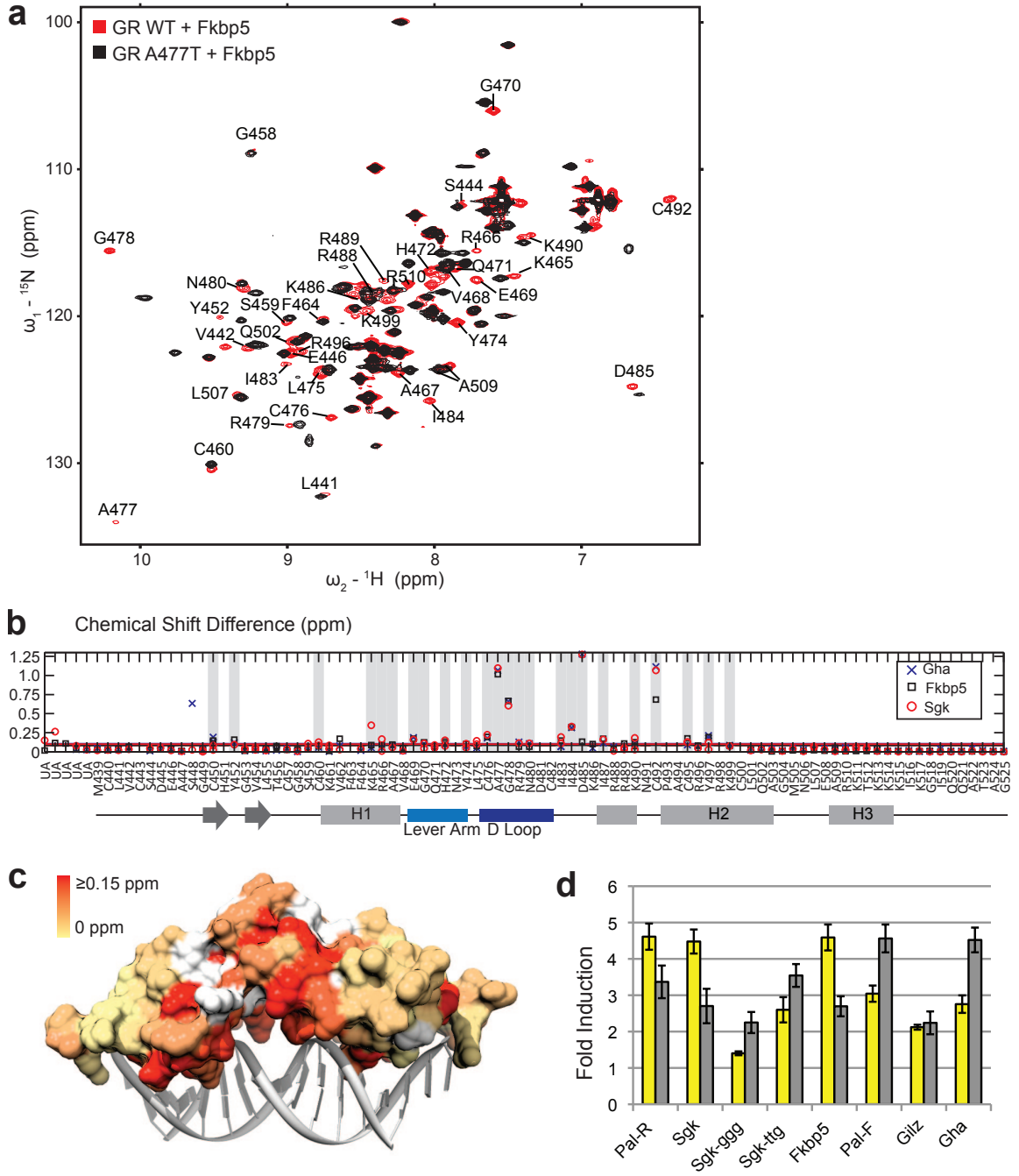


Figure 2.4: Disrupting the dimerization interface affects GR-DBD conformation at lever arm and DNA recognition helix.

(a) Comparison of ^{15}N -HSQC of GR WT (red) and A477T (black). (b) Chemical shift difference between GR WT and GR A477T spectra for three GBS complexes. Grey bars highlight residues with a chemical shift difference $\geq 0.05\text{ppm}$ between GR WT and GR A477T for all three GBSs. UA = unassigned. (c) Magnitude of combined proton and nitrogen chemical shift difference between for GR WT and GR A477T bound to Fkbp5 colored onto the crystal structure of GR-DBD:Fkbp5. Unassigned residues are colored white. (d) Comparison transcriptional induction for GBS luciferase reporters by GR WT (yellow) and GR A477T (grey) in U2OS cells treated with 100nM dex.

A477T disrupts GR cooperativity but not stoichiometry

To determine the mechanism by which the A477T mutation affects the GBS-specific activity of GR, we investigated DNA binding affinity by gel shift.

Comparison of GR WT and A477T binding to the Pal-R and Sgk GBSs showed reduced DNA-binding affinity of A477T (**Fig. 2.5a,c**). GR dimer complexes were formed at saturating concentrations for both GR WT and A477T, indicating that the mutant can indeed dimerize on DNA. As the WT GR binds cooperatively to DNA, we suspected that the decreased affinity of the A477T mutant resulted from reduced cooperativity. For the WT, the transition from free DNA to dimer complex occurs with only a minor population of monomer, clearly demonstrating strong positive cooperativity. In contrast, A477T displayed little cooperativity, nearly saturating DNA as a monomer prior to dimer formation (**Fig. 2.5a**). Also, the dimer species was substantially broadened for A477T relative to WT, likely reflecting enhanced dissociation. We further compared binding of GR WT and A477T to a GBS half site (**Fig. 2.5b**) to distinguish whether the reduced overall affinity of A477T was due to impaired DNA recognition resulting from this mutation. We found that monomer binding was equivalent for WT and A477T, indicating that the A477T mutation does not disrupt the DNA-binding ability of the monomer (**Fig. 2.5b and c**), suggesting instead that the reduced affinity is due to reduced cooperativity.

To quantitatively compare WT and A477T complexes, we used surface plasmon resonance (SPR) to monitor how binding sequence affects GR WT and A477T activity *in vitro* under similar conditions as used for NMR studies. We compared two GBSs whose transcriptional induction was reduced (PalR) or unaffected (Gilz) by the A477T mutation in reporter assays. The A477T mutation results in a 10-fold and 5-fold decreased binding affinity for PalR and Gilz, respectively (**Fig. 2.6a** and **d**). Notably, maximal binding was equivalent for GR WT and A477T, again indicating that the mutant binds to DNA at the same stoichiometry as WT (**Fig. 2.6b**). To analyze cooperativity, we fit SPR binding isotherms to Hill coefficients (n_H) and determined an n_H value of 2.1 and 1.8 for GR WT and 1.4 and 1.3 for A477T, for both Pal and Gilz GBSs, respectively (**Fig. 2.6d**). Thus, the A477T mutation results in reduced but not abolished cooperativity.

As the transcriptional activity of GR is likely dependent on the length of time the active dimer complex is bound at a given response element, we also quantified the impact of A477T on the kinetics of the GR-DBD:GBS complex. SPR binding traces revealed that GR WT dissociated from Pal and Gilz with a $t_{1/2}$ of 55 and 23 sec for PalR and Gilz, respectively. In contrast, GR A477T dissociated from both GBSs with a $t_{1/2}$ of 5 sec, reflecting 10-fold and 5-fold increased rates of dissociation, respectively. Intriguingly, the dissociation of GR WT is dependent on the GBS, whereas A477T kinetics appeared indiscriminating of sequence (**Fig. 2.6c**). This suggests that the A477T mutation disrupts GBS-specific signals that modulate GR dissociation.

To understand how dissociation kinetics impact GBS-specific activity, we extended our analysis to a larger panel of seven GBSs and determined $K_{1/2}$, $t_{1/2}$, and n_H for each GBS complex (**Supplemental Table 1**). For all GBSs, A477T had lower affinity, faster dissociation and reduced cooperativity compared to WT. We compared the relationship between transcriptional activity and $K_{1/2}$, $t_{1/2}$ and n_H to determine whether these DNA-binding properties could explain the GBS-specific transcriptional activity of WT and A477T. We found a surprising correlation between transcription and affinity ($R^2=0.7$) or dissociation ($R^2=0.9$) for A477T, but no relationship between transcription and affinity ($R^2=0.2$) or dissociation ($R^2=0.06$) for WT (**Fig. 2.7**). This indicates that disrupting the dimerization interface reduces GR transcriptional activity, to a simple product of affinity, and suggests that more sophisticated GBS-specific signaling by GR WT is dependent on the A477 residue.

Figure 2.5 A477T impairs dimerization but not monomer DNA-binding.

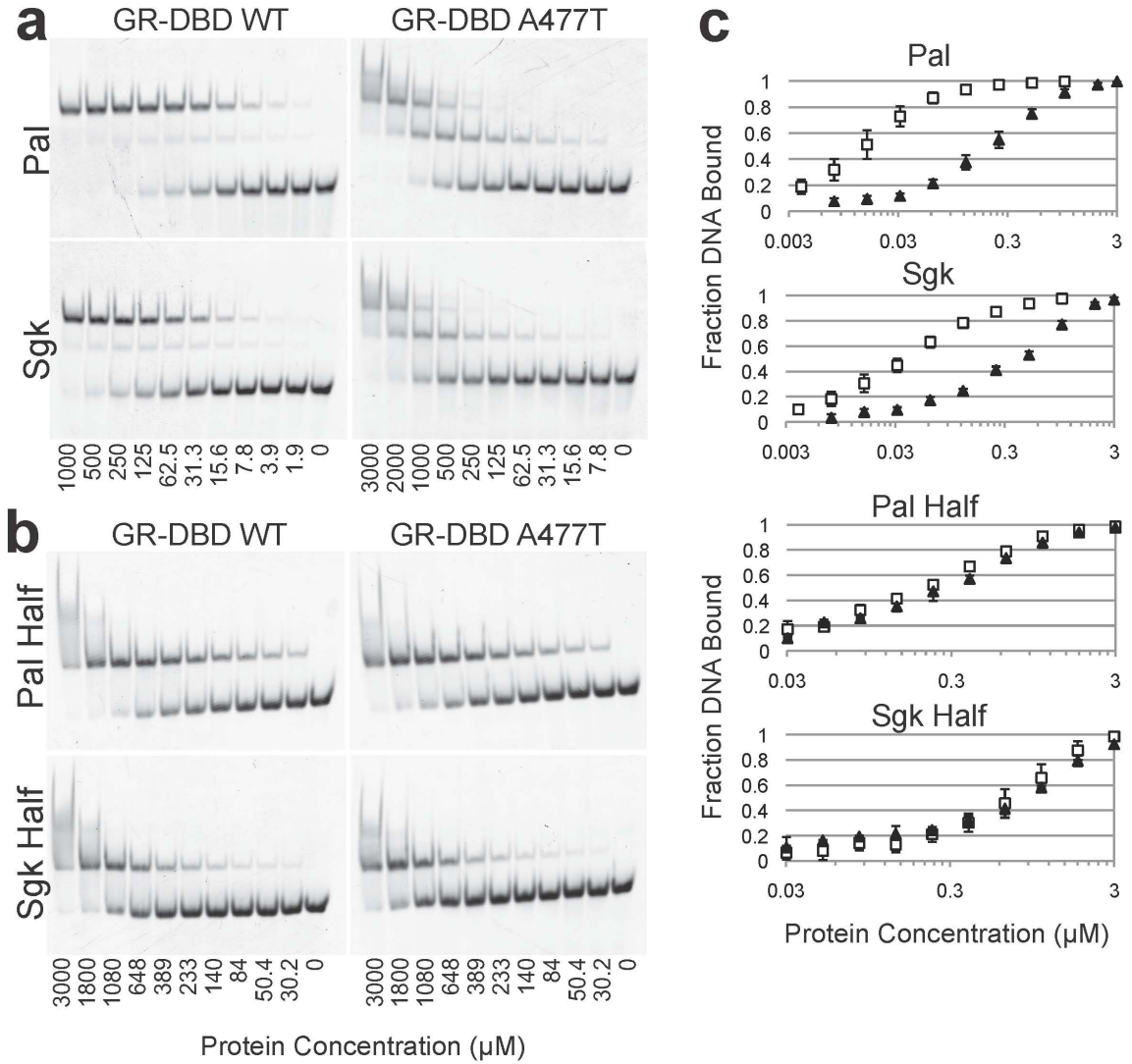


Figure 2.5: A477T impairs dimerization but not monomer DNA-binding.

Gel shift assay monitoring binding of GR-DBD WT and GR-DBD A477T to (a) 24bp Pal and Sgk GBSs conjugated with Alexa-488 fluorophore at a concentration of 5 nM. (b) Pal Half and Sgk Half GBSs, where one half-site is mutated to the least favorable nucleotide at each position based on the ChIP-seq binding motif. (c) Quantification of fraction DNA bound with increasing concentration GR WT (open squares) or GR A477T (filled triangles) for each binding site. Error bars=s.e.m, for n=2-4 replicates.

Figure 2.6 GR A477T disrupts cooperativity and GBS-specific dissociation.

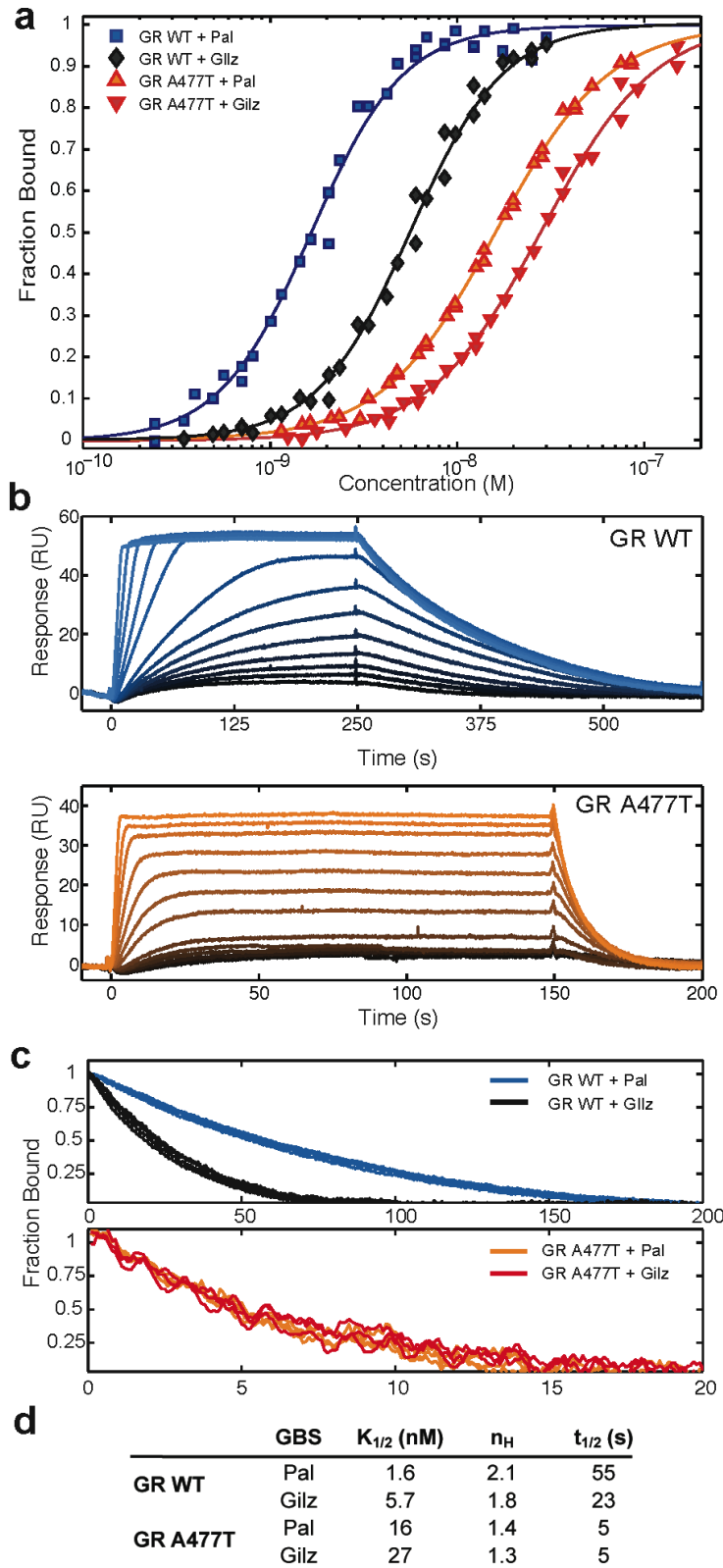
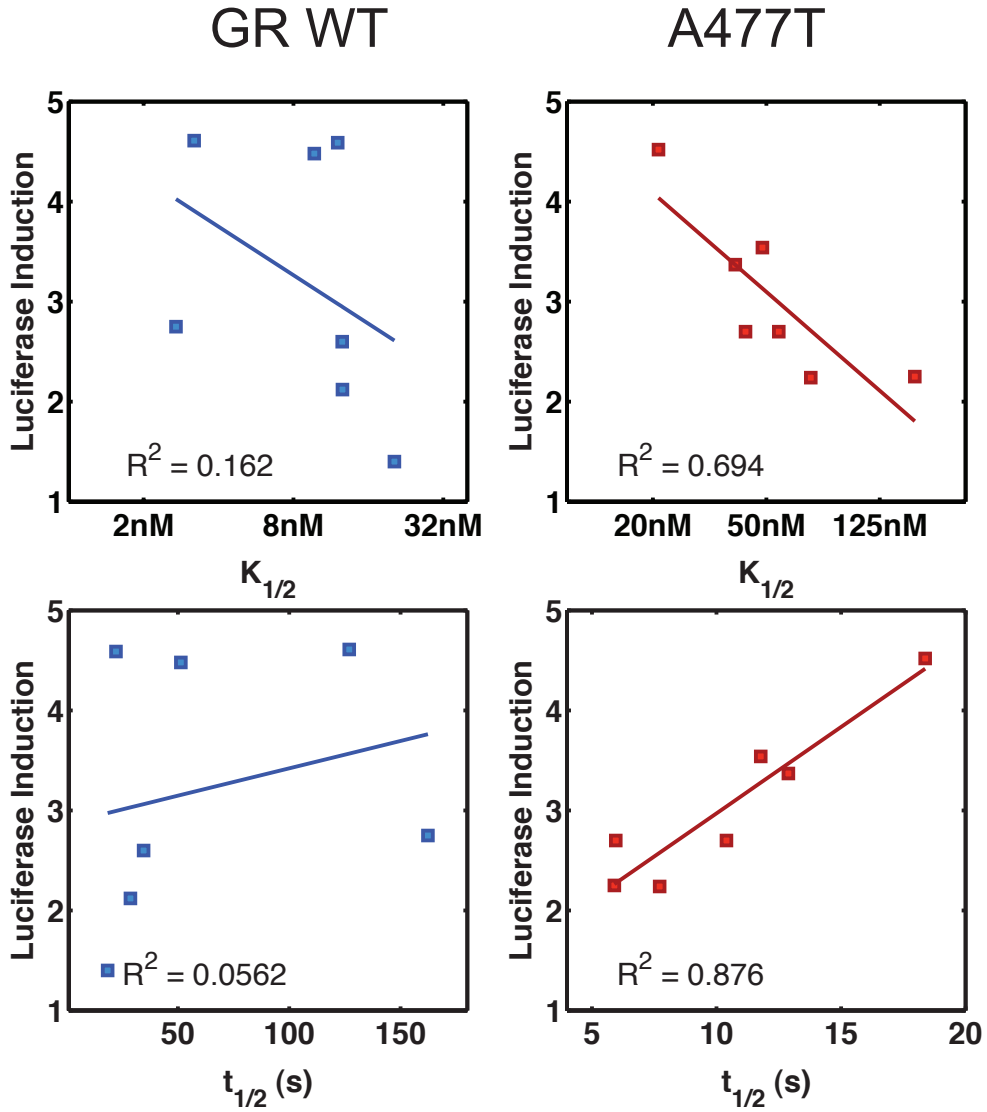


Figure 2.6: GR A477T disrupts cooperativity of dimerization and GBS-specific dissociation. (a) Binding isotherms for a concentration series of ~700pM to 200nM for GR-DBD WT and ~1.4nM to 400nM for A477T binding to immobilized biotin-GBS surfaces at 35°C from 3 separate titrations, normalized to fit B_{max} . (b) Binding traces from a single titration experiment for GR WT and GR A477T. (c) Dissociation curves for binding to Pal and Gilz GBSs for GR WT (top) and GR A477T (bottom). (d) Affinity ($K_{1/2}$), Hill coefficient (n_H) parameters from fitting isotherms to a Hill Equation. Parameters from titration experiments were normalized to B_{max} individually and fit globally, $n=3$.

Figure 2.7 GR A477T disrupts cooperativity and GBS-specific dissociation.

Correlation between transcriptional activity and binding affinity ($K_{1/2}$) or dissociation ($t_{1/2}$) determined for WT (blue) and A477T (red) binding to seven GBS surfaces at 8°C.



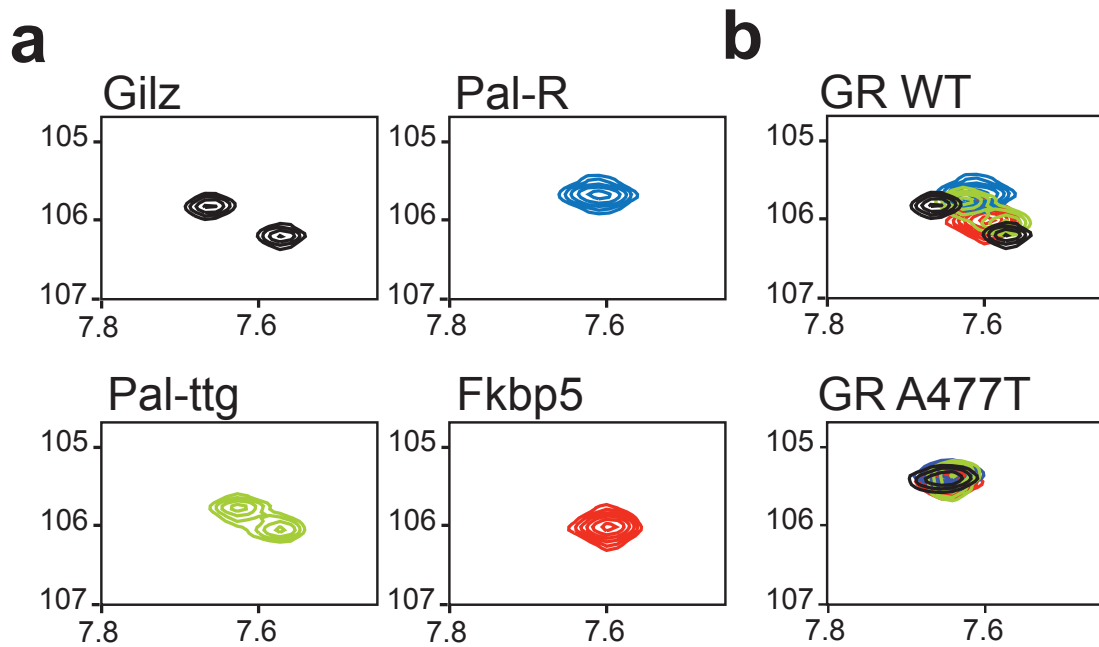
An allosteric path through the dimerization interface modulates lever arm conformation

To dissect the structural mechanism by which A477T results in reinterpretation of GBS signals, we monitored lever arm conformation, which is GBS-sensitive [6]. Using ^{15}N -HSQC as a read-out of conformation, the lever arm residue G470 displayed a single peak for symmetric GBSs, and doublet peaks for asymmetric GBSs (**Fig. 2.8a**). A simple interpretation of G470 peak splitting is that there is a unique lever arm conformation for each GR-DBD dimer partner, and that this conformation depends on the GBS half site to which it is bound. This predicts that GBSs that are identical at one half site, but different at the other will have one overlaid G470 peak and one non-overlaid peak. In contrast, G470 chemical shifts overlaid from GBS complexes that are identical at one half site showed that both singlet and doublet G470 peaks were unique in all four spectra. Thus, the lever arm conformation of each GR dimer partner depends on the sequence of both its directly contacted half site and the half site of its dimer partner (**Fig. 2.8c**). This suggests that lever arm conformation is determined by communication between dimer partners.

We hypothesized that the path connecting the recognition helix to the dimerization interface transmits GBS-signals between dimer partners. To test this, we compared the HSQC spectra of GR A477T bound to different GBSs (**Fig 2.8b**). In the GBS complexes tested, the G470 peaks collapsed to a single

overlaid peak, though other GR-DBD residues outside of the lever arm displayed GBS-specific conformations. Therefore, disrupting allosteric communication between dimer partners abolished the sequence-specific conformation of G470 within the lever arm. Building on the conclusions from the GBS reporter assays, this suggests that an allosteric path extending from the recognition helix to the dimerization interface integrates GBS signals between dimer partners. These signals are transmitted to the lever arm, and are likely further propagated to other domains of GR.

Figure 2.8 Sequence-specific lever-arm conformation is dependent on intact dimerization interface.



c Intact dimerization interface



Disrupted dimerization interface

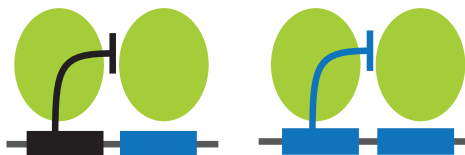


Figure 2.8: Sequence-specific lever-arm conformation is dependent on intact dimerization interface.

(a) ^{15}N -HSQC zoomed on chemical shift of residue G470 of lever arm for GR WT bound to two asymmetric GBSs (Gilz, Pal-ttg) and two palindromic GBSs (Pal, Fkbp5). (b) Overlay of G470 peaks from GR WT (top) and GR A477T (bottom) bound to Sgk, Pal, Gilz and Fkbp5 GBSs. (c) Model depicting how communication across the dimerization interface is necessary for GBS-specific conformations. Both half-sites of the GBS determine the conformation of each GR dimer partner by transmitting information from the adjacent GBS half-site across the dimerization interface through A477. (top). When the dimerization interface is disrupted, the sequence information from the adjacent half-site is lost, resulting in lever arm conformations that are insensitive to GBS.

2.3 Discussion

Genomic response elements are composed of sequence motifs that specify binding of distinct sets of transcriptional regulators to execute gene-specific control of transcription. While such gene specificity can certainly arise from the different combinations of motifs that reside at these composite response elements, our previous work suggested that even combinations of bases in a single binding motif could determine gene-specific activity. We showed here that 90% of 30,000 GBSs identified were unique, thus providing a great deal of signal diversity for potential gene-specificity. However, this would require that non-contacted bases of the GBS somehow impart a substantial amount of that specificity. Crystal structures comparing GR-DBD:GBS complexes suggested that sequence-specific differences in DNA shape might contribute to specificity. While other DNA-binding proteins utilize DNA shape in sequence recognition{Rohs:2009ky}, we suggest here that DNA shape may specify activity once GR is bound to DNA. To understand the effect of the isolated GBS sequence on GR structure and activity, we used a simplified system consisting of individual GBSs and the DBD of GR, in the absence of additional inputs. The quantitative NMR chemical shift differences highlighted by comparison of different GBS complexes revealed a potential allosteric path between the DNA-binding and dimerization interfaces that transmits signaling information embedded within GBSs.

Two results provided evidence that this pathway extends through the dimer interface and into the adjacent GR dimer partner. First, the lever arm conformation for each GR dimer partner is dependent not only on the sequence of the half site to which it is directly bound, but also on the sequence of the adjacent half site. Second, introducing a mutation in the dimerization interface diminished the effect of the half-site sequence on the adjacent dimer partner. Thus, GBS signals are not simply the sum of the information encoded in each half site. Instead, we propose that allosteric communication between GR dimer partners may enable integration of sequence-specific signals from both GBS half sites, exponentially increasing the informational complexity of the GBS. Moreover, we predict that this intermolecular allostery can be traced from the GR-DBD into other GR domains and even propagated into other factors of the transcriptional complex to determine gene-specific transcriptional outcomes.

Multidirectional signaling between several interaction surfaces of the receptor appears to be a critical feature of combinatorial control. For example, biological and biochemical studies with GR and other nuclear receptors have provided evidence that binding sequences can modulate receptor interactions with coregulators[16], that ligands can modulate interactions with DNA [37] and that both DNA and ligands can direct interactions with coregulators[19]. Additionally, we previously showed that co-recruitment of a coregulator with GR to the genome is gene-specific[38] and that different GBSs can confer differential cofactor requirements [6]. While these studies do not explain how all of these

signals are integrated, our structural analysis of the effects of GBS sequence on the A477T mutation provides a model where structural changes at the DNA-binding interface are coupled with changes at the GR dimerization surface, indicative of bidirectional allostery. It is likely that additional paths that detect other GR input signals act in tandem to form a regulated allosteric network. Indeed, evidence for allosteric paths that integrate ligand signals between dimer partners have been inferred from evolutionary conservation[20]. We speculate that in the cellular context, the particular combination of signals including GBS sequence, ligand structure, coregulator interactions and post-transcriptional modifications determine the composition and function of gene-specific transcriptional regulatory complexes. Therefore, this study sets the stage for a mechanistic understanding of signal integration in combinatorial control.

It remains to be determined whether each GBS-specific conformational profile represents a single conformation or an average of conformational states that are sampled by GR. Consistent with the latter, crystal structures of GR-DBD:GBS complexes suggest that the lever arm has alternate conformations that are dependent on the GBS. Here, our NMR spectra indicate multiple conformational states as evidenced by peak splitting for a subset of residues. Additional NMR experiments suggest that peak splitting arises from conformational exchange occurring within 200msec (**Figure 2.18**), thus two orders of magnitude faster than the half-life of the GR-DBD complex bound to DNA. Therefore, this peak splitting appears to be due to the GR-DBD dimer sampling at least two discrete conformations while bound to DNA. Extending this

view, we speculate that each GR-DBD:GBS complex may differentially access conformational states that preferentially interact with particular transcriptional coregulators. Future experiments investigating the interconversion between alternate conformations of different GR-DBD:GBS complexes will likely provide additional insight into mechanisms of specificity.

Our functional comparison of GR WT and GR A477T DNA-binding implied that the dissociation kinetics of the GR-DBD:GBS complex are affected by the binding sequence and accelerated by the A477T mutation. It is thus tempting to speculate that the GBSs may, in part, impact GR activity through altering the turnover of GR:DNA complexes. Previous studies indicated that interactions with response elements are highly dynamic, on the timescale of seconds [39], and that disassembly of regulatory complexes may be driven continuously by cellular factors such as chaperones or the proteasome [40]. How GR DNA-binding kinetics are regulated and how they impact transcriptional activity remains an open question. Our results suggest that binding sequences may differentially affect the association of transcriptionally active GR:DNA complexes, thus contributing to the specificity of gene regulation by GR.

2.4 Supplemental Figures

Figure 2.9 NMR assignment of DNA-bound GR-DBD.

The HSQC spectra of the ^2H , ^{13}C , ^{15}N -labeled GR-DBD dimer bound to the Gha binding site with stoichiometrically of 2:1 GR monomer to dsDNA (red). The GR-DBD:Gha spectra was measured on a 600MHz spectrometer at 35°C. Unlabeled peaks represent unassigned residues or side-chain H-N crosspeaks. These assignments were transferred to additional GR-DBD:GBS complexes.

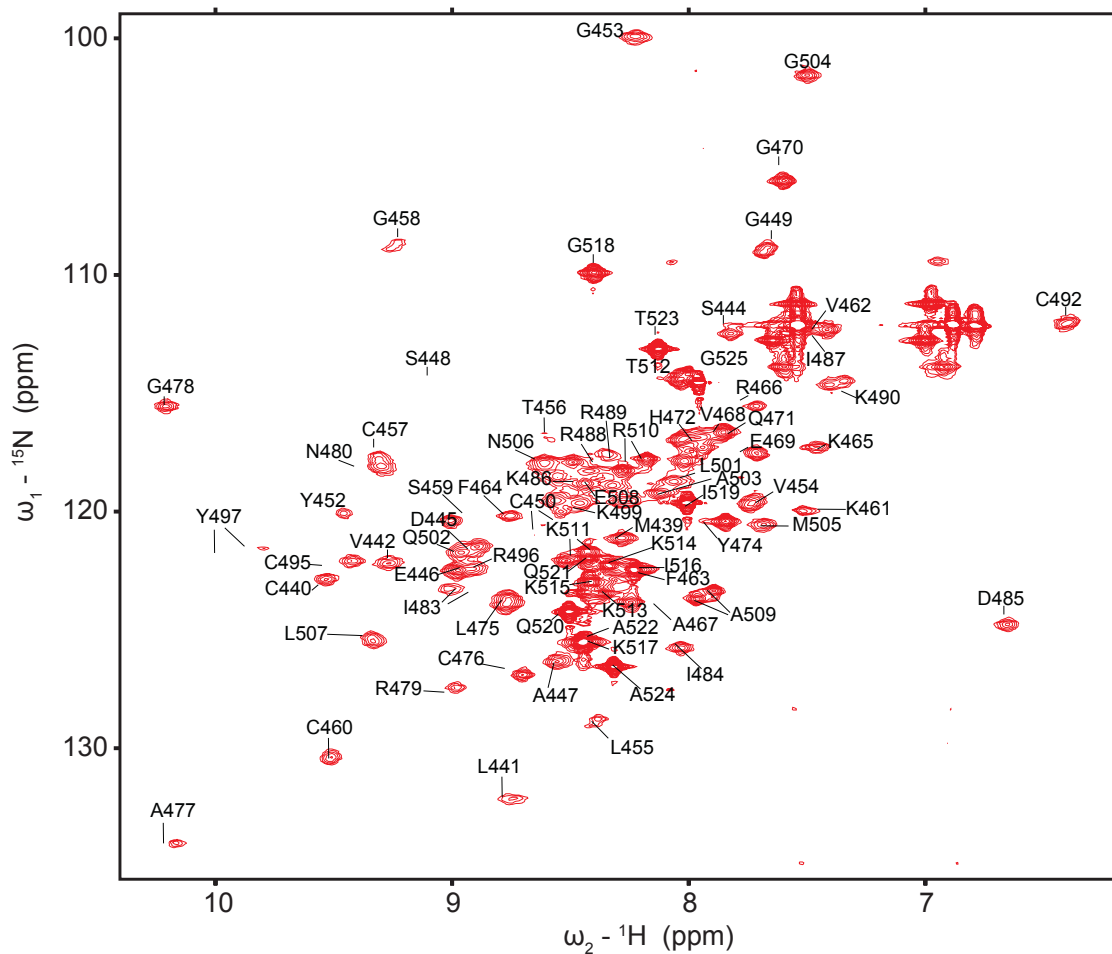


Figure 2.10 Heatmap of chemical shifts differences between GR-DBD WT complexes.

Chemical shift differences resulting from changing GBS positions 13 and 15 (left) or spacer positions 7-9 (right). Residues are colored as in figure 2.3.

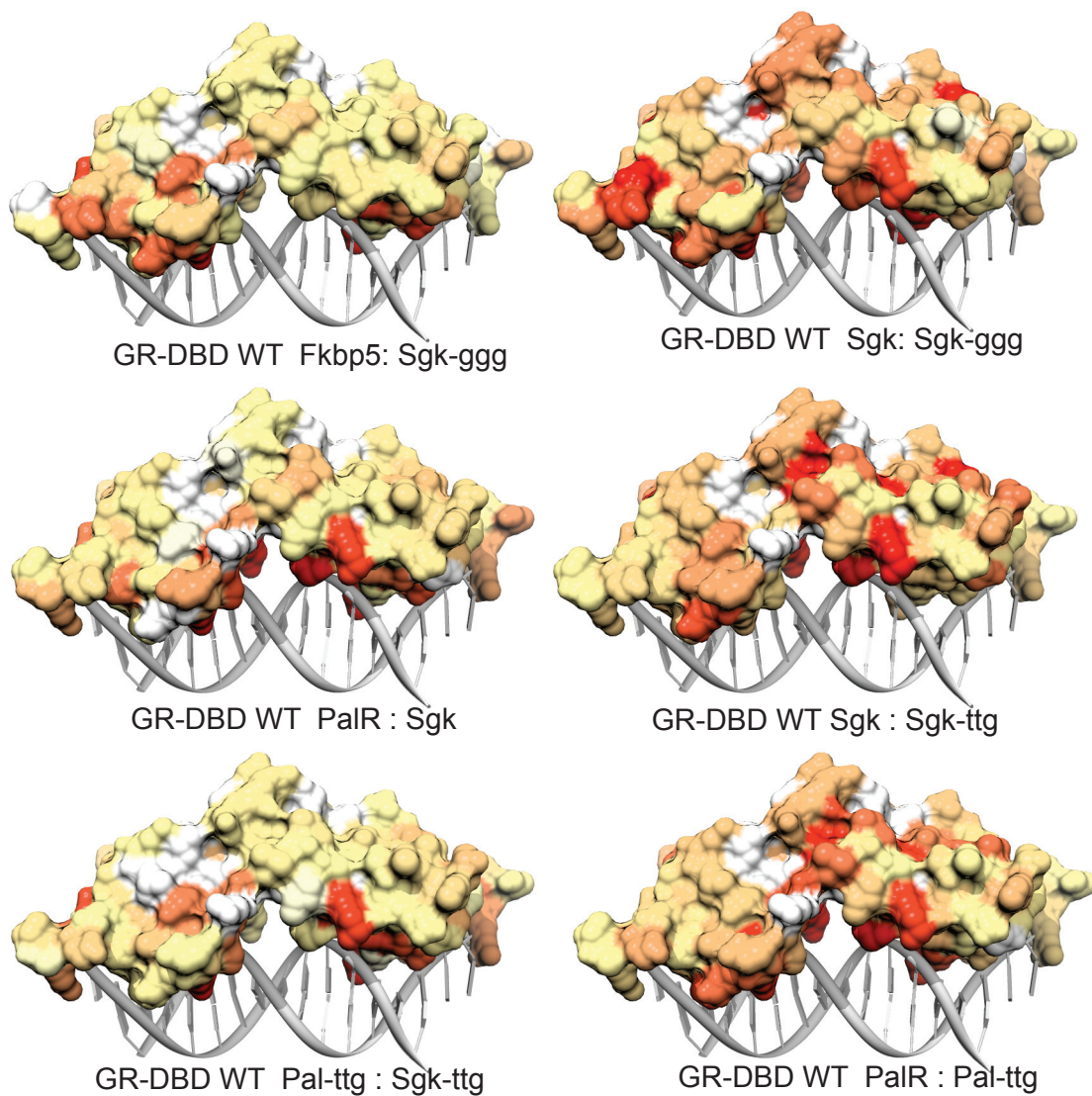


Figure 2.11 Heatmap of chemical shift differences between WT and A477T complexes.

Residues are colored as in figure 2.4.

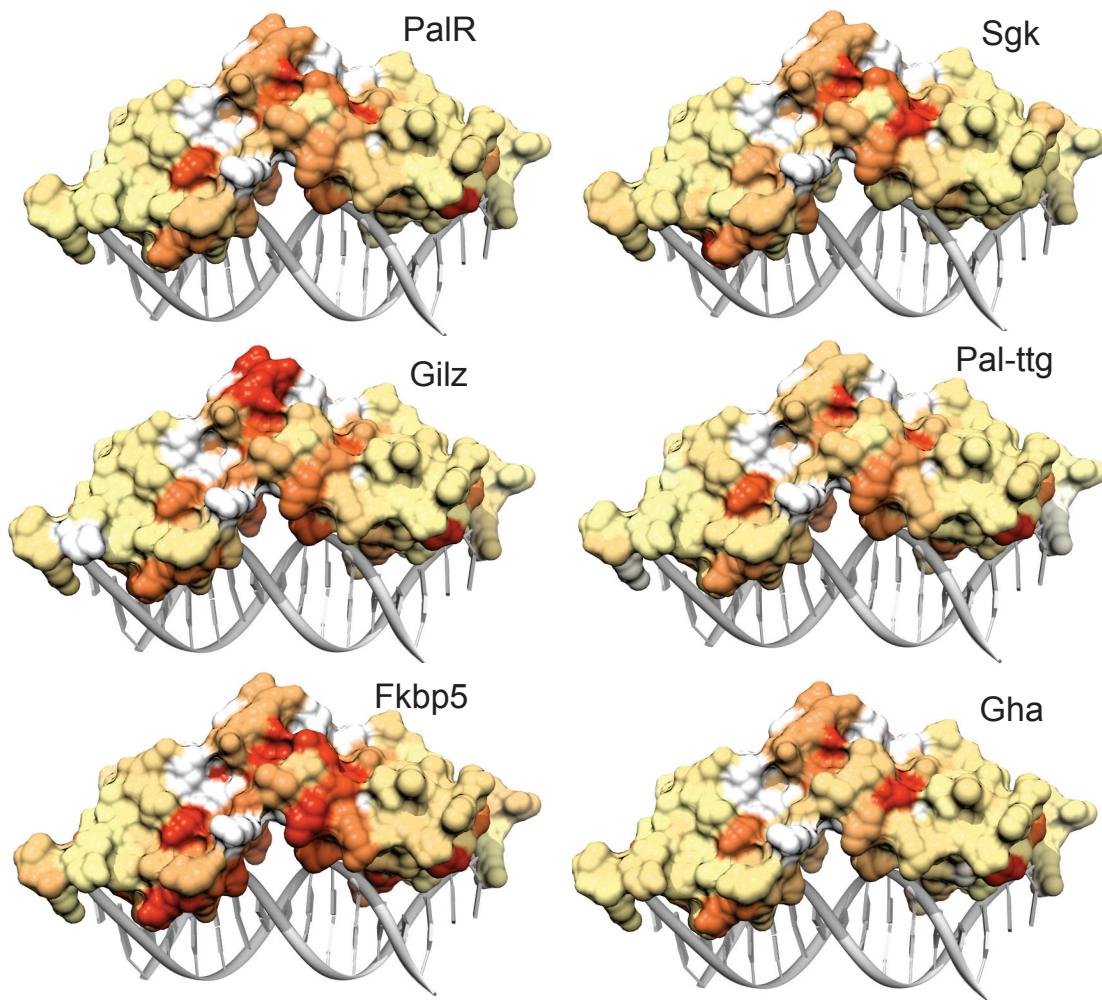


Figure 2.12 ^{15}N -HSQC comparison of the DNA-bound GR WT and GR A477T versus apo GR-DBD .

The peaks that differ between GR WT and A477T do not overlay with the apo GR peaks, suggesting that GR A477T is not a partially-DNA bound variant of GR WT. Peaks corresponding to residues in the recognition helix of GR are labeled to highlight that these residues in particular do not match the apo GR conformation.

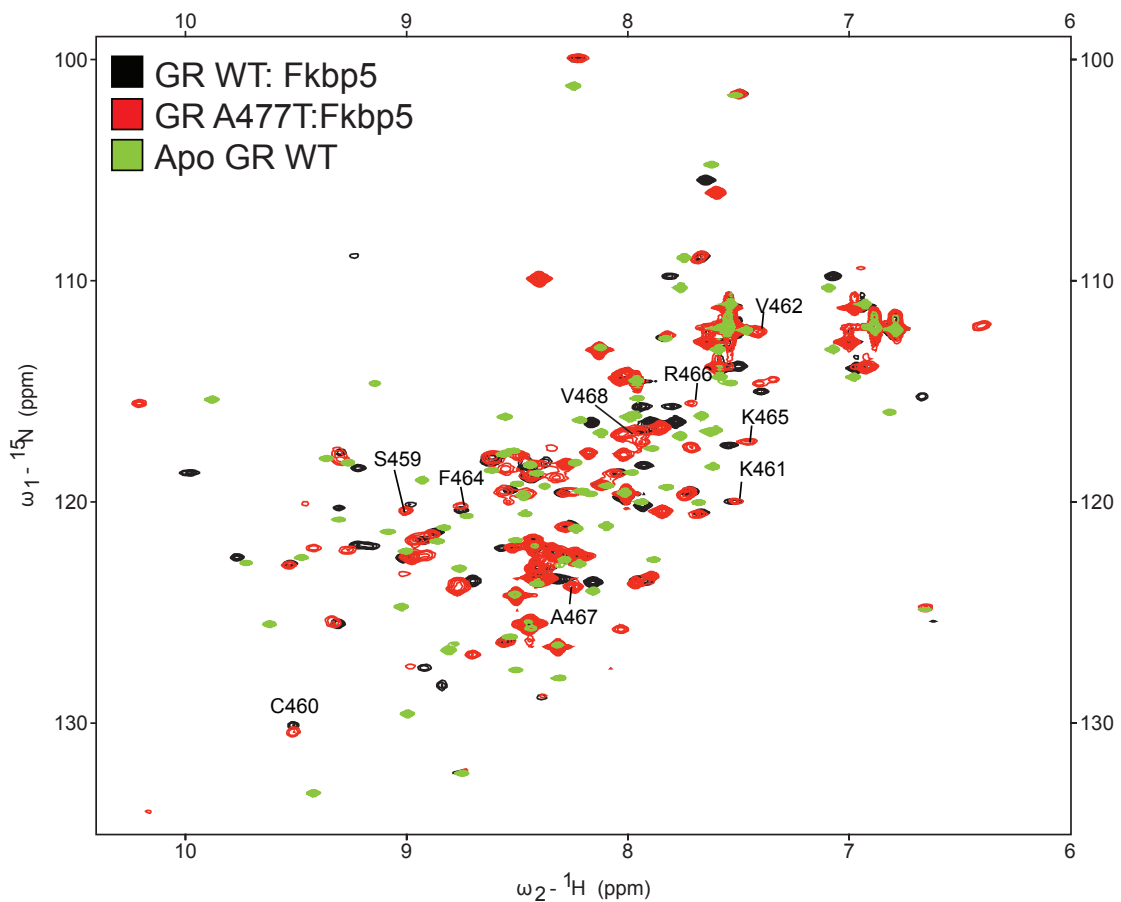


Table 2.1 Summary of DNA-binding parameters of GR-DBD across seven binding sites.

GR WT and A477T binding to seven GBS sequences detected by SPR. Data represents parameters extracted from fitting curves generated from globally averaged data from duplicate or triplicate experiments consisting of a 15-point dilution series of protein concentrations. These experiments were run at 8°C to avoid the dissociation of double-stranded DNA from immobilized surfaces occurring over time.

GBS	Wildtype		A477T	
	K 1/2	nH	K 1/2	nH
FKBP5	12.1 ± 0.2 nM	1.95 ± 0.06	55 ± 1 nM	1.42 ± 0.02
GHA	2.7 ± 0.2 nM	2.2 ± 0.2	21 ± 1 nM	1.17 ± 0.05
GILZ	12.6 ± 0.2 nM	1.87 ± 0.05	71 ± 5 nM	1.07 ± 0.03
PAL	3.1 ± 0.1 nM	2.1 ± 0.1	39 ± 1 nM	0.93 ± 0.03
SGK	9.7 ± 0.2 nM	1.84 ± 0.06	42 ± 1 nM	0.97 ± 0.02
SGKggg	20.4 ± 0.7 nM	1.92 ± 0.06	166 ± 23 nM	1.11 ± 0.05
SGKttg	12.6 ± 0.8nM	2.3 ± 0.2	48 ± 17 nM	1.4 ± 0.2

Figure 2.13 Effect of GBS Spacer on cooperativity and dissociation.

Cooperativity (n_H) and dissociation time ($t_{1/2}$) were determined by fitting GR binding to seven different binding sites as measured by SPR at 8°C. GBS spacer sequence can modulate GR cooperativity (compare SGK and SGKttg, top plot). Also, GBS spacer sequence can affect DNA-binding kinetics (compare Pal and Fkbp5, bottom plot).

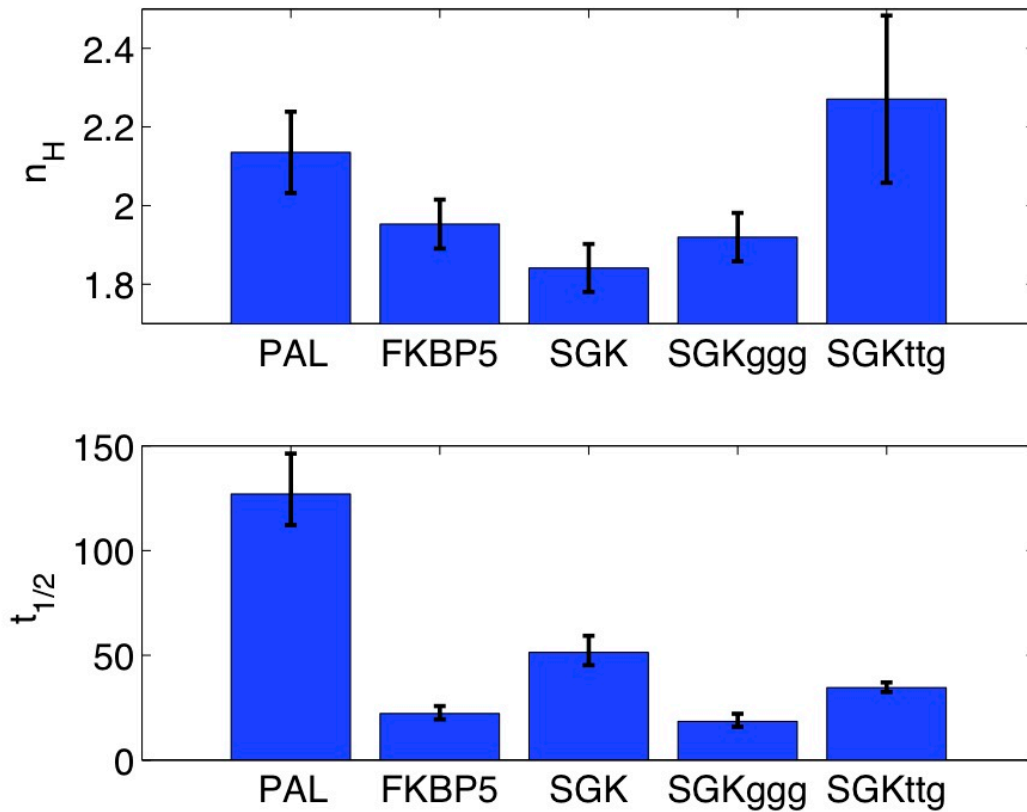


Figure 2.14 Comparison of affinity and dissociation of GR WT and A477T.

DNA-binding of GR-DBD WT and A477T was measured for seven GBS across 15 protein concentrations at 8°C. Binding isotherms were calculated from steady-state responses and fit to a 2-site model to generate $K_{1/2}$ measurements of affinity. Dissociation curves were fit to a single site model to determine apparent dissociation rates (k_{off}). Data points for each binding site are shown as closed circles for GR WT (blue), and A477T (red). Blue and red shading indicate the range of affinity and dissociation rates for each protein, respectively. GR WT has a broader range of dissociation rates across seven binding sites compared to A477T.

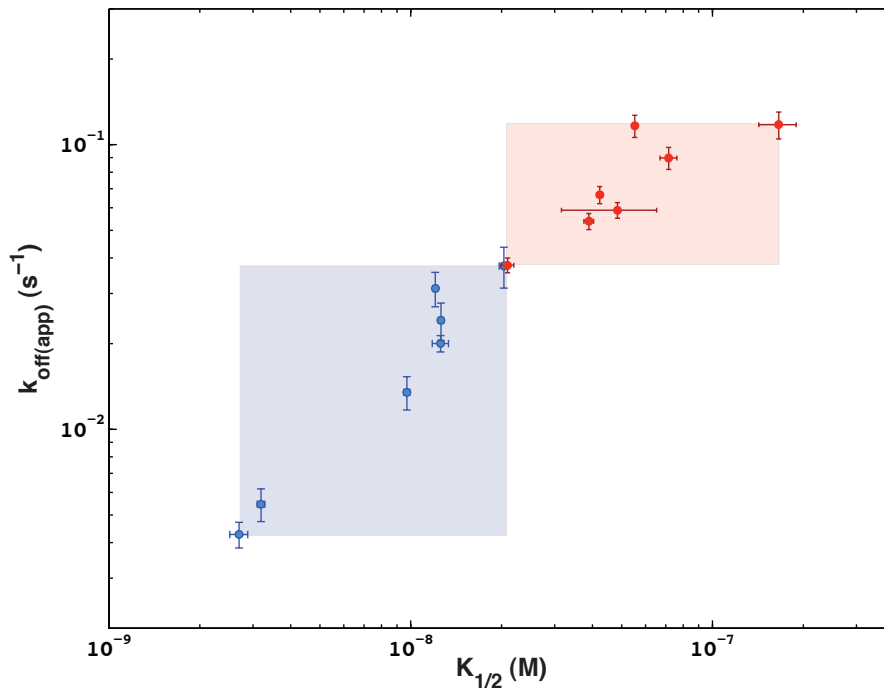


Figure 2.15 SPR comparison of GR WT and A477T across seven binding sites at 8°C.

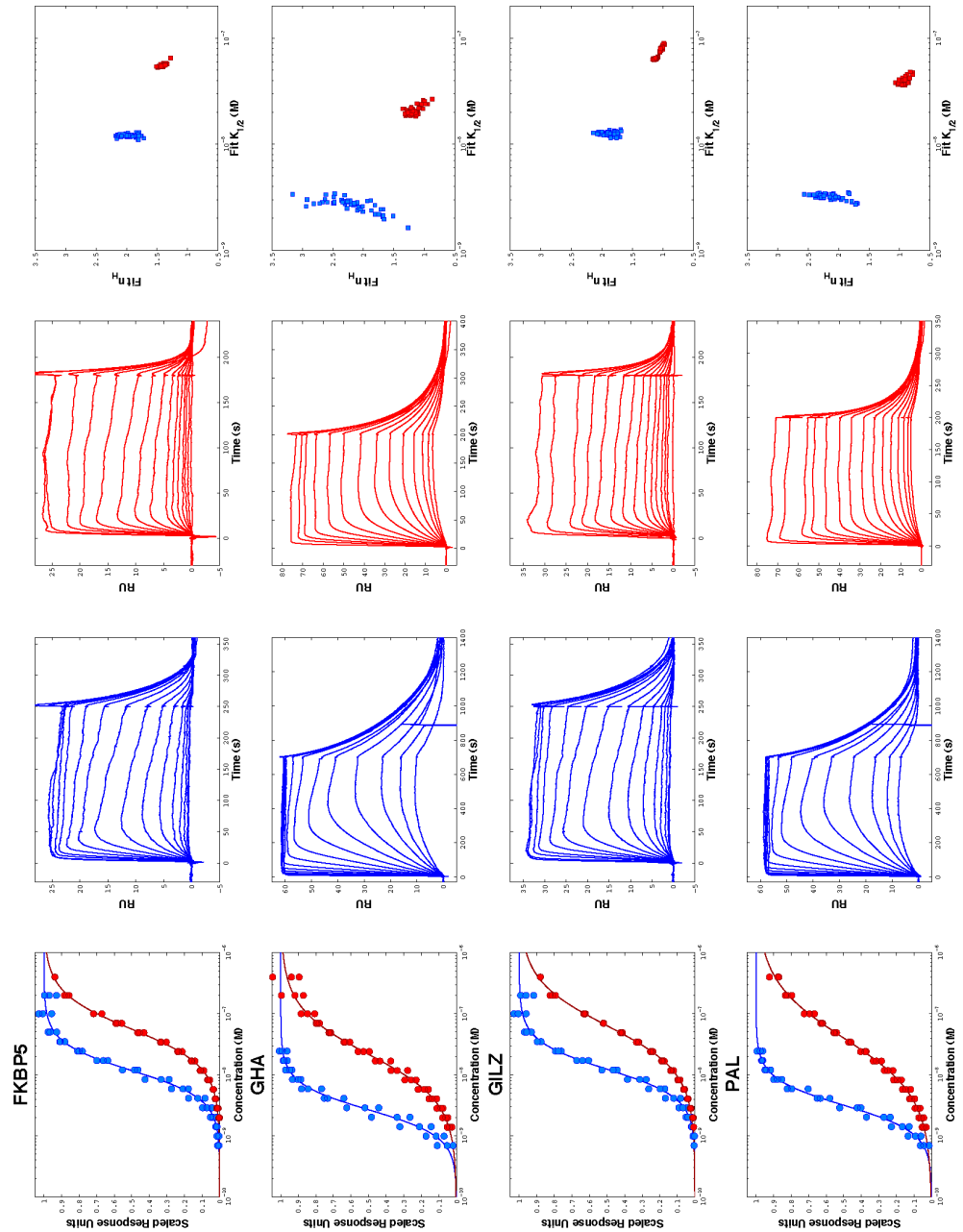


Figure 2.16 Assignment of ^{15}N -HSQC of GR-DBD at 25°C.

The ^{15}N -HSQC spectra of ^2H , ^{13}C , ^{15}N -labeled apo GR-DBD (aa 440-525) measured on a 500MHz spectrometer at 25°C. All 85 residues (except P493) were assigned to their corresponding H-N crosspeaks. Unlabeled peaks represent side-chain H-N crosspeaks.

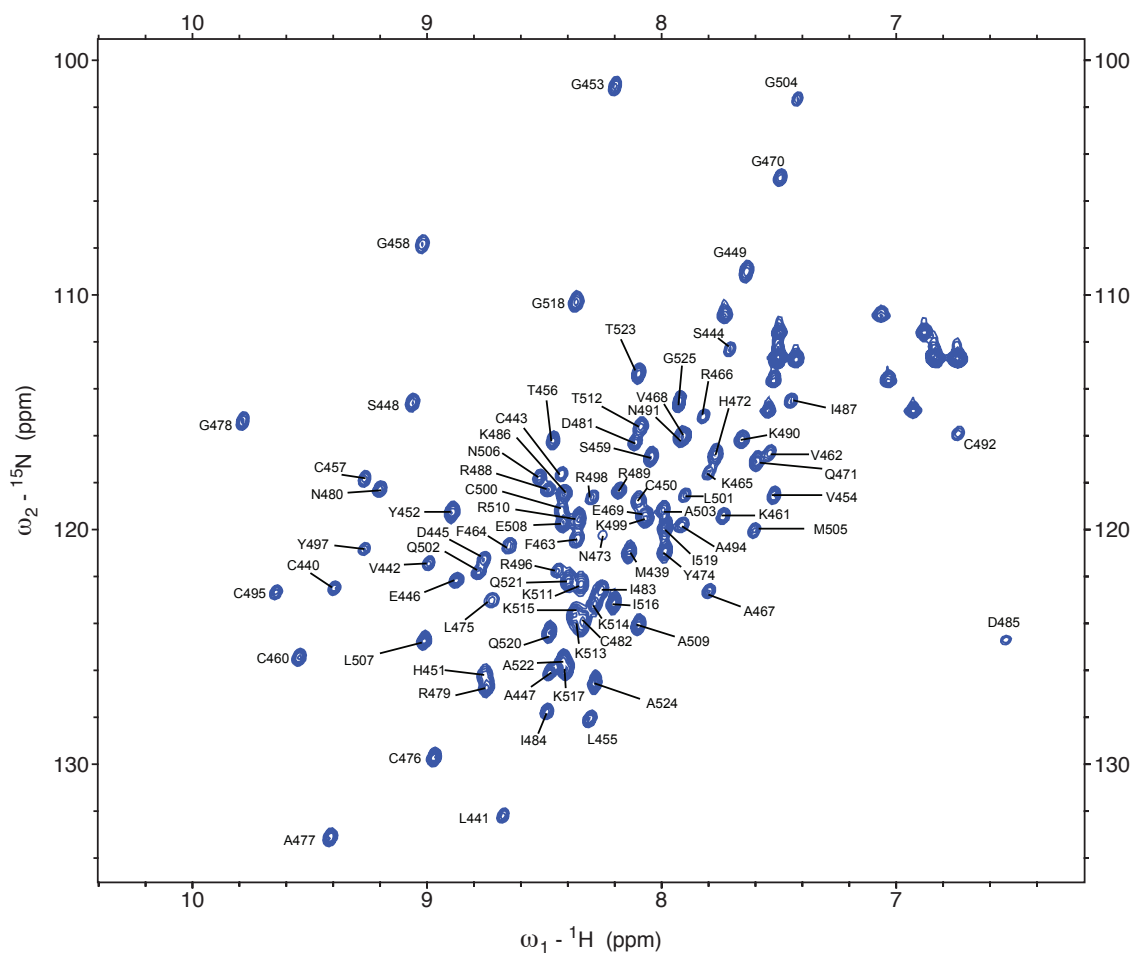


Figure 2.17 Comparison of apo and DNA-bound GR-DBD.

The ^{15}N -HSQC spectra of the apo ^2H , ^{13}C , ^{15}N -labeled GR-DBD (blue) overlaid onto the spectra of the ^2H , ^{13}C , ^{15}N -labeled GR-DBD dimer bound to the Gha binding site with stoichiometrically of 2:1 GR monomer to dsDNA (red).

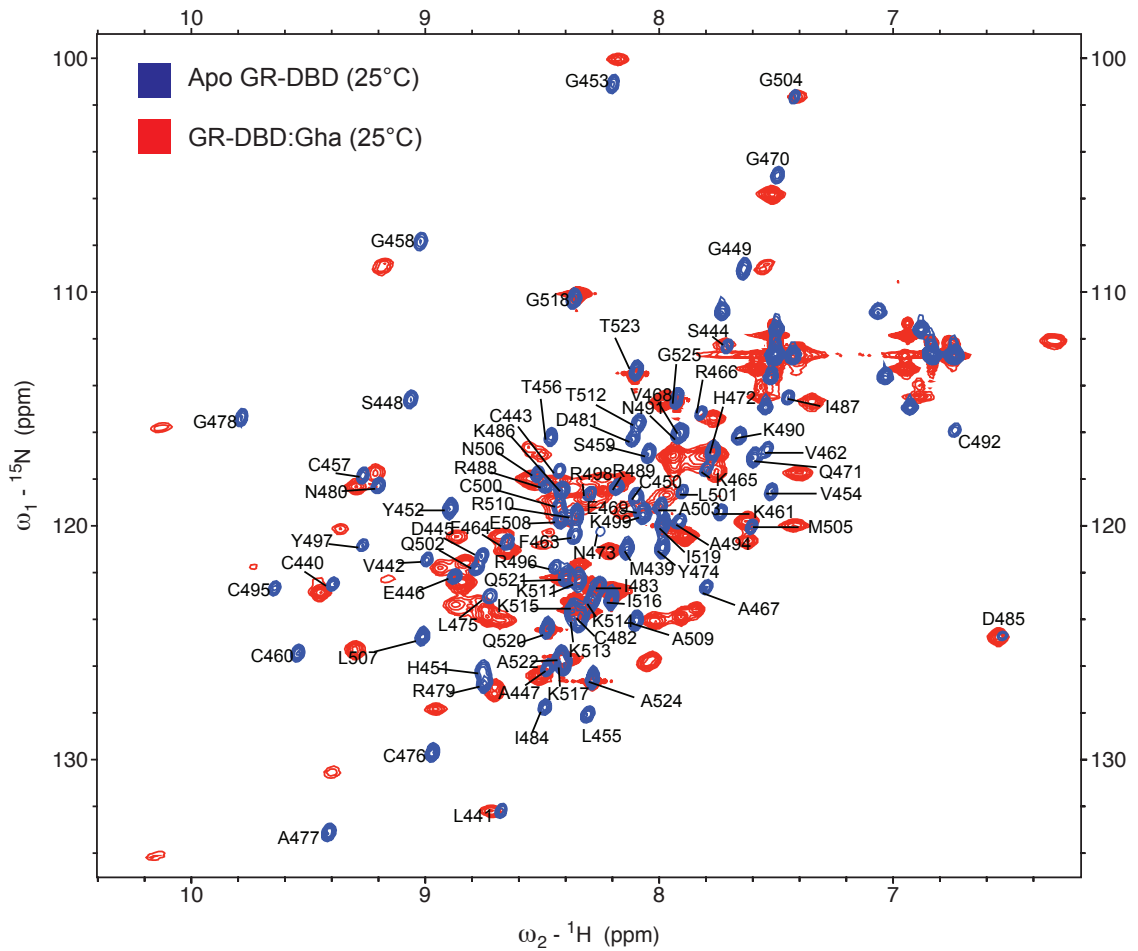


Figure 2.18 Analysis of GR-DBD conformational exchange.

NMR spectra showing chemical exchange of the GR-DBD:Sgk complex as measured using ^1H - ^{15}N zz-exchange[41]. Peak splitting is detected for the G453 residue peak by ^{15}N -HSQC and here by ^1H - ^{15}N zz-exchange with a delay of $T=0$, indicating 2 different conformational states (top left panel). At a 200msec mixing time ($T=200\text{msec}$), exchange peaks are visible for G453 as indicated by crosspeaks (top right and bottom left panel). Cartoon of expected crosspeaks for conformational exchange (bottom right). This suggests that conformational exchange occurs much faster than GR-DBD dissociation (< 200 msec versus 25-55 seconds).

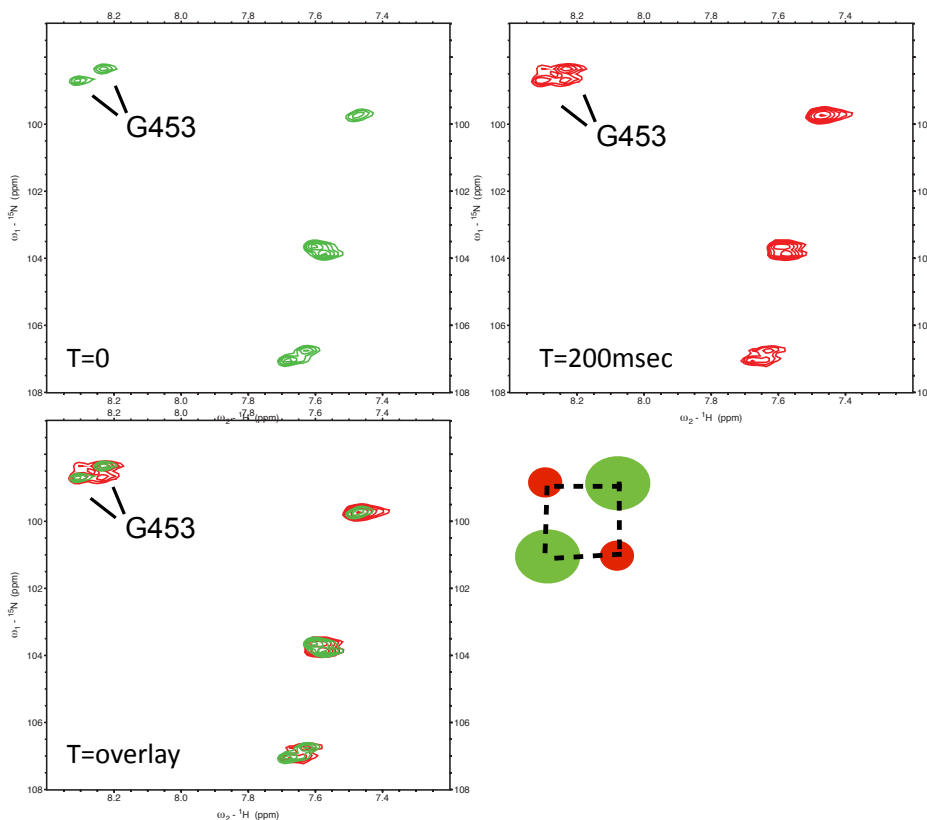
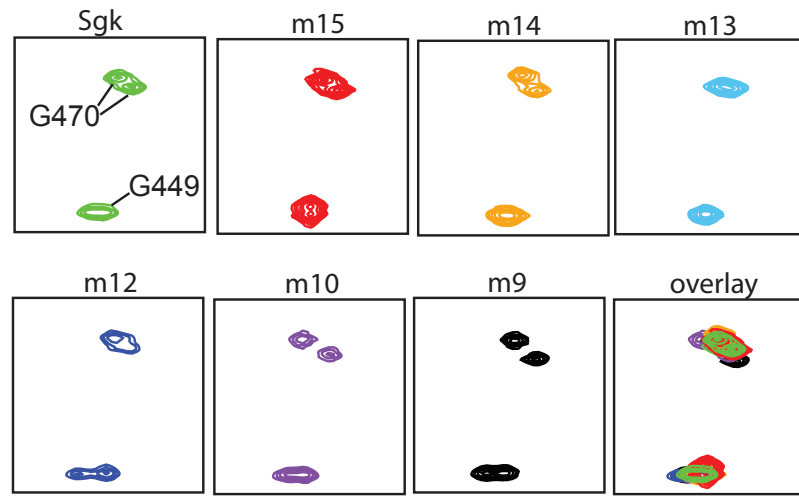


Figure 2.19 The effects of each GBS nucleotide position on the conformation of the lever-arm residue G470.

Comparison of the lever arm G470 residue in ^1H - ^{15}N HSQC of GR-DBD:WT bound to GBSs that differ at a single base position within the non-consensus halfsite. The broadening observed for mutation of the T12 GBS position, a base-specific contact, suggests that G470 may sample several conformations when this contact is absent (panel m12). This broadening is not observed when the base-specific contact to the C14 position is lost in the Sgk-m14 GBS. The largest chemical shift difference between the G470 doublet peaks is observed when the spacer or adjacent nucleotide is changed (positions 9 and 10).



	1	2	3	4	5	6	7	8	9	10	11	12	13	14	15
Sgk	A	G	A	A	C	A	t	t	T	G	T	C	C	G	
Sgk-m15	A	G	A	A	C	A	t	t	T	G	T	C	C	C	
Sgk-m14	A	G	A	A	C	A	t	t	T	G	T	C	T	G	
Sgk-m13	A	G	A	A	C	A	t	t	T	G	T	T	C	G	
Sgk-m12	A	G	A	A	C	A	t	t	T	G	A	C	C	G	
Sgk-m10	A	G	A	A	C	A	t	t	G	G	T	C	C	G	
Sgk-m9	A	G	A	A	C	A	t	g	T	G	T	C	C	G	

Chapter 3

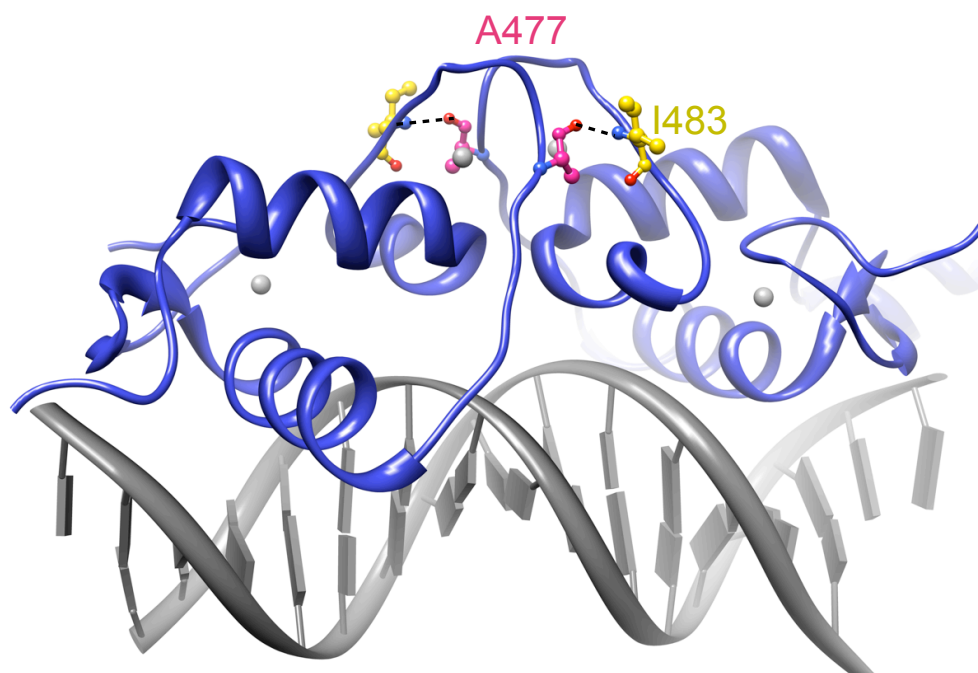
The role of the GR dimer interface in gene-specific transcriptional activation and DNA occupancy

3.1 Introduction

Previous work from the Yamamoto Lab showed that disruption of functional surfaces in each domain of GR (AF1, AF2 and DBD)—results in gene-specific effects on transcriptional regulation, indicating a differential role for each of these surfaces at GR target genes [42]. Taken together with studies demonstrating that particular GR coregulators are required or recruited in a gene-specific manner [38], [43], these results suggest that GR functional surfaces are differentially engaged at target promoters resulting in selective recruitment of transcriptional coregulators. Furthermore, DNA-binding sequence is sufficient to direct differential requirement of GR functional surfaces and coregulator usage [6]. In this study, we sought to categorize the function of a particular GR interaction surface in a single cell type by cross-examining two aspects of GR activity: regulation of endogenous gene-expression and occupancy at genomic response elements.

The structural, biophysical and cell-based studies described in Chapter 2 provide a model that the GR dimer interface plays a role in directing GR gene-specific transcriptional activity by relaying signals between the DNA-binding interface and other regions of the DBD. Comparison of GR WT and A477T by NMR indicated that this mutation induces conformational shifts in the DNA-binding interface (**Figure 2.4a**), consistent with the possibility that the DNA sequence specificity for A477T may be distinct from WT. Furthermore, transcriptional assays demonstrated that A477T is a more potent transcriptional activator than GR WT at selective GBSs (**Figure 2.4d**) and endogenous genes [42], despite its reduced affinity, suggesting that the A477T mutation can also impact GR signaling at a step downstream of DNA-binding [44]. Thus, a single mutation may impact gene-specific regulation through multiple mechanisms including (1) differential binding at genomic response elements and (2) different modes of GR activity mediated by structural changes in GR functional surfaces. Given our detailed understanding of the affect of the A477T mutation on GR-DBD structure and *in vitro* DNA binding (**Chapter 2**), this mutant serves as a precise tool to dissect the mechanism by which the A477 residue, and the dimer surface as a whole, contribute to GR gene-specific activity at endogenous genes.

Figure 3.1 GR-DBD:DNA highlighting the inter-subunit contact between A477 and I483



3.2 Results

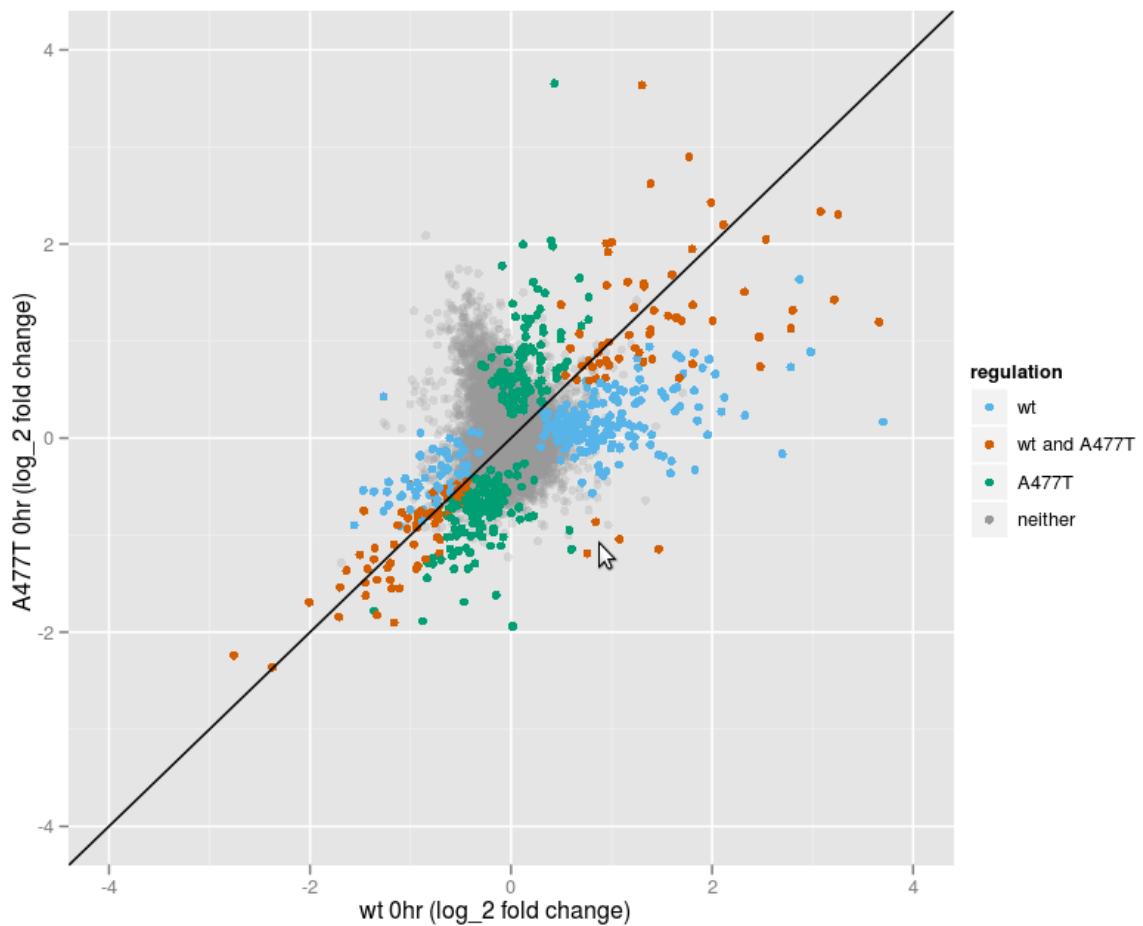
GR WT and A477T differentially regulate gene expression in U2OS cells

To investigate the affect of the A447T dimer interface mutation on GR transcriptional regulation, we identified GR-regulated genes in U2OS cell lines that stably over-expressing rGR WT or A477T [42] treated with 100 nM dexamethasone for 2, 4 and 24 hours by gene expression microarray (**Figure 3.2**). We found that the number of both up-regulated and down-regulated genes increased with longer dex-treatment, and therefore focused on the earliest (2 hour) time point in order to favor the identification of GR primary target genes, rather than downstream secondary targets.

We found 242 dex-regulated genes were specifically regulated only in GR WT and 256 genes were specifically regulated in A477T-expressing cells. In contrast to reports that A477T can only mediate transcriptional repression [45], the subsets of WT-specific and A477T-specific genes contained both GR-activated and GR-repressed genes. Additionally, 132 genes were similarly dex-regulated in both GR WT and A477T cell lines. Therefore, GR WT and A477T regulate a nearly equivalent number of target genes, despite that the A477T mutant has a lower DNA-binding affinity *in vitro* at all binding sites tested (**Figure 2.5** and **Table 2.1**). Furthermore, the A477T gain-of-function at 256 genes

indicates that the mutation modifies rather than impairs GR function. Taken together with the findings described in Chapter 2, the 132 genes that are regulated by both WT and A477T suggest that there is a subset of targets where GR activity is independent of the inter-subunit communication mediated by A477T.

Figure 3.2 Effect of GR A477T mutation on GR gene transcription



Scaterplot of dex-regulated genes in U2OS cell lines over-expressing GR WT or GR A477T as measured by gene expression microarray (Illumina Bead Arrays RefSeq8). Cells were treated for 2 hours with 100nM dexamethasone compared ethanol and dex-regulated genes for GR WT and A477T are compared by scatterplot as log₂ fold change.

We hypothesized that the affect of the A477T mutation on GR gene-specific regulation may in part be due to (1) differential DNA-binding and sequence recognition of A477T compared to WT and/or (2) different modes of transcriptional regulation. To address the first mechanism, we examined genomic binding of GR WT and A477T by chromatin immunoprecipitation followed by deep sequencing (ChIP-seq). We monitored GR occupancy after 90 minutes of dex treatment, in order to best capture GR binding events that are responsible for changes in gene expression detected at 2 hours of dex treatment by microarray. GR WT or A477T-bound chromatin was isolated by immunoprecipitation using an antibody against the N-terminal domain of GR, thus avoiding any affect that the DBD mutation (A477T) might have on antibody recognition. Enrichment of GR-bound regions was validated by quantitative PCR amplification of control endogenous GR binding sites in dex versus ethanol-treated samples (Rajas Chodankar, USC). ChIP-purified chromatin was amplified by PCR, ligated with sequencing adaptors and sequenced with paired-end reads using a Genome Analyzer II. Ten and seventeen million reads were sequenced for WT and A477T, respectively. Sequencing reads were mapped to the human genome and approximately 48,00 and 73,00 peaks were identified for the WT and A477T data set, respectively.

Gene expression and GR occupancy identify distinct classes of regulated genes

To identify GR-occupied regions responsible for GR WT or A477T-specific transcriptional regulation, we scanned for binding sites surrounding the transcription start sites (TSS) of genes that were differentially regulated in microarrays. Peaks identified near differentially-regulated genes were classified as candidate GR response elements (GREs) and selected for further study, giving preference to the following criteria including: (1) located <20 kB from the TSS, (2) associated with genes that are compact and with a low number of associated occupancy peaks (3) of physiological significance for GR regulation. Due to the scarcity of GR binding regions identified near GR-repressed genes, we focused on differential regulation of dex-induced gene targets.

From cross-comparison of genome-wide GR regulation and occupancy, we identified five distinct classes of GR activated genes, covering all possible combinations of binding and regulation: (1) bound and activated in WT but not A477T, (2) bound in both but regulated only in WT (3) bound and activated in A477T but not WT, (4) bound and regulated in both WT and A477T, (5) bound in both but regulated only in A477T (**Figure 3.2**). GR occupancy peaks for candidate GREs described in Table 5.1 are shown mapped to their associated genes for 3 of the 5 gene classes (**Figure 3.3-3.5**). Classes 1, 3, and 4 most likely represent genes where the effect of A477T on GR transcriptional induction is at the level of GR DNA-binding. In contrast, classes 2 and 5 represent GREs

where the A477T mutation affects GR-dependent transcriptional induction downstream of DNA binding.

Table 3.1: Identification of Distinct Classes of Activated Genes.

Gene Class		1	2	3	4	5
Occupancy	WT	+	+		+	+
	A477T		+	+	+	+
Gene Expression	WT	+	+		+	
	A477T			+	+	+
* = number of binding regions being studied		MSX2**	GPR153	CHST15	RGS2	RP1L1****
		S100P**	GRASP1	HOXD1**	ZNF189	KIF25***
		WNT5A**	IGFBP1	ATP4a****	CRYGC	FBXO32**
		KCNA5***	ITPKA		SDPR	

Table 3.2: Identification of Distinct Classes of Activated Genes

Genes identified by microarray as GR WT-specific, A477T-specific or non-differential were sub-classified by GR occupancy as detected by ChIP-sequencing. Candidate genes were selected that had at least one GR occupancy peak within close proximity to the regulated gene (typically <20 kb) that was either WT-specific, A477T-specific or present in both WT and A477T. Gene expression by dexamethasone was validated by Q-PCR for genes classified below. In many cases, multiple GR occupancy peaks were associated with a single gene, as indicated by the number or asterics after the gene name.

Figure 3.3: GR occupancy of WT- and A477T-specific genes detected by ChIP-sequencing.

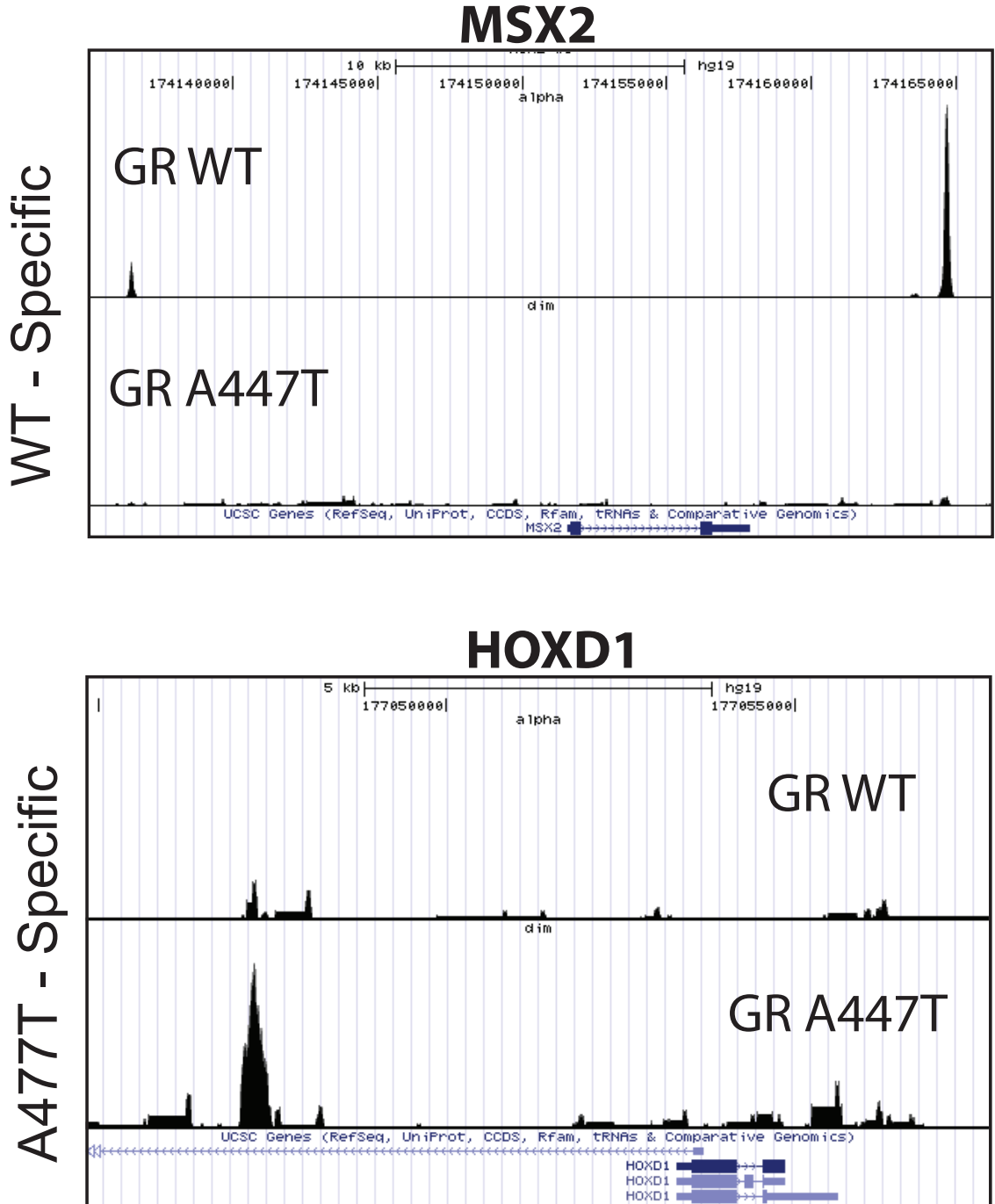


Figure 3.4 GR occupancy at WT and A477T non-differentially regulated genes by ChIP-sequencing.

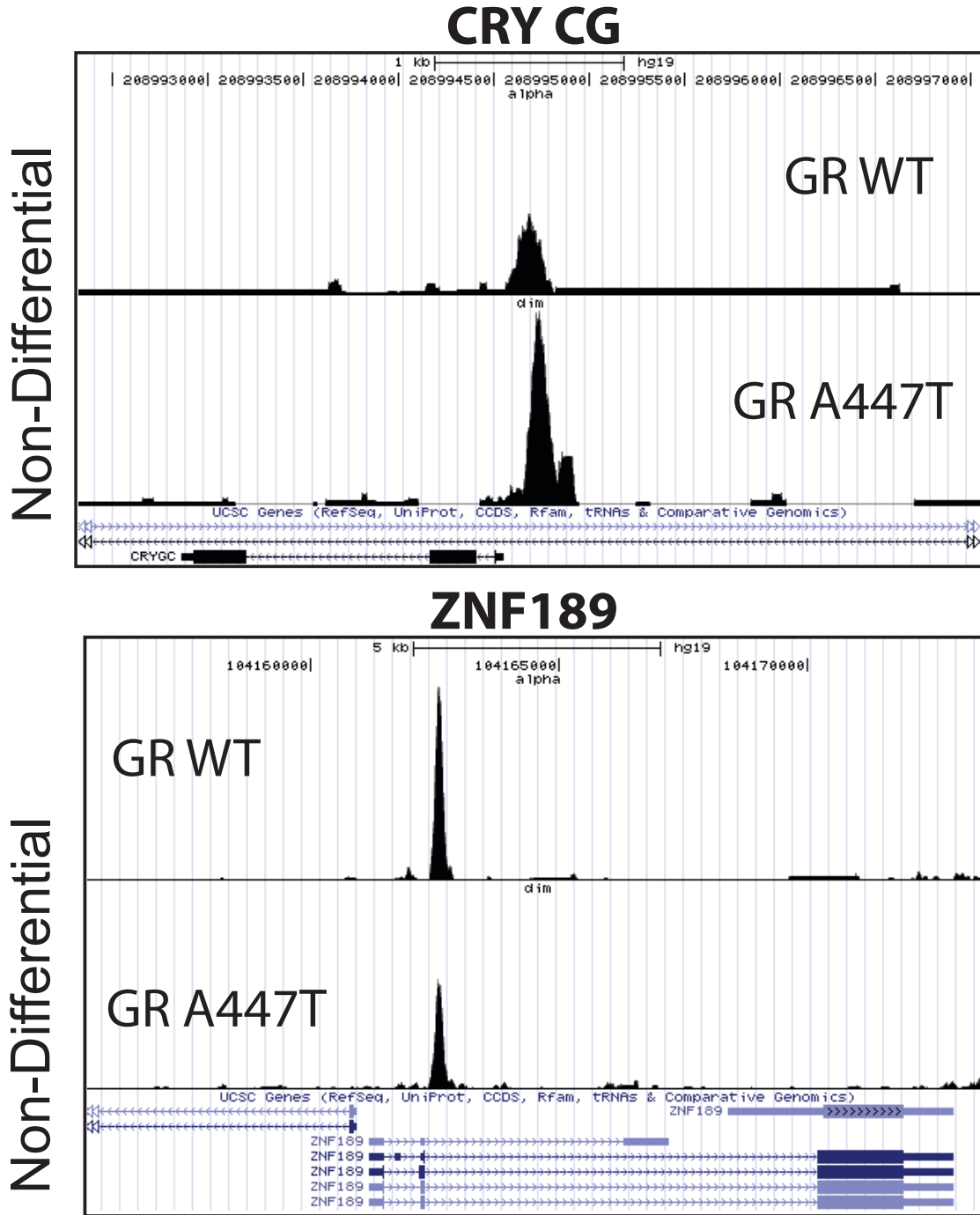


Figure 3.5 GR occupancy at WT and A477T occupied regions at A477T-specifically regulated genes.

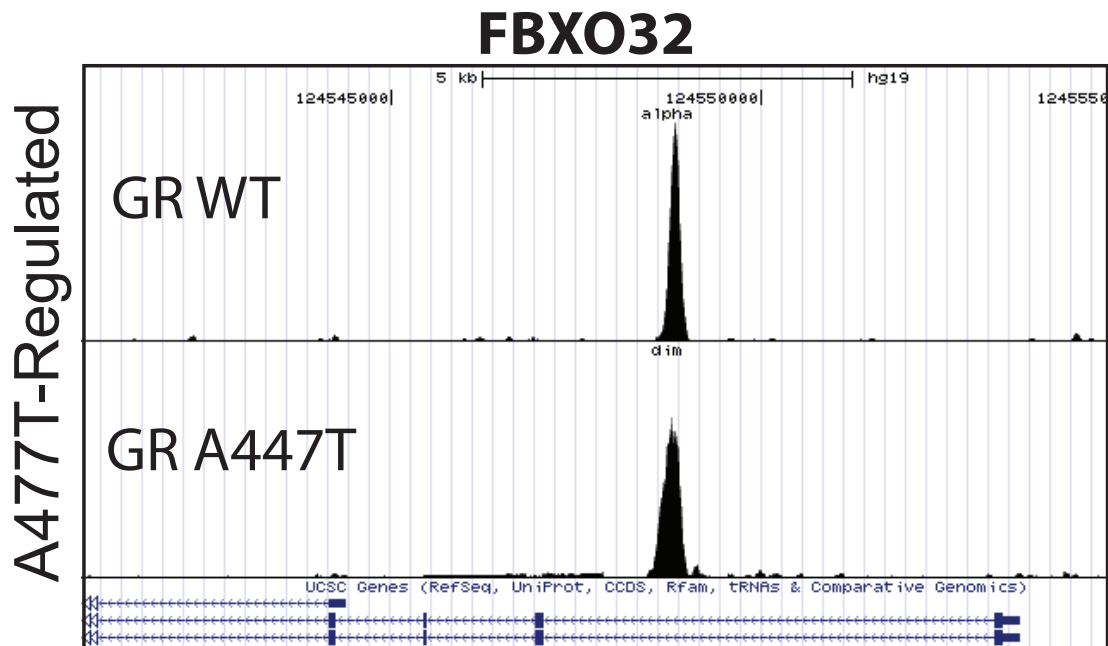


Figure 3.6 GR occupancy at WT and A477T non-differentially regulated regions with GBS half sites.

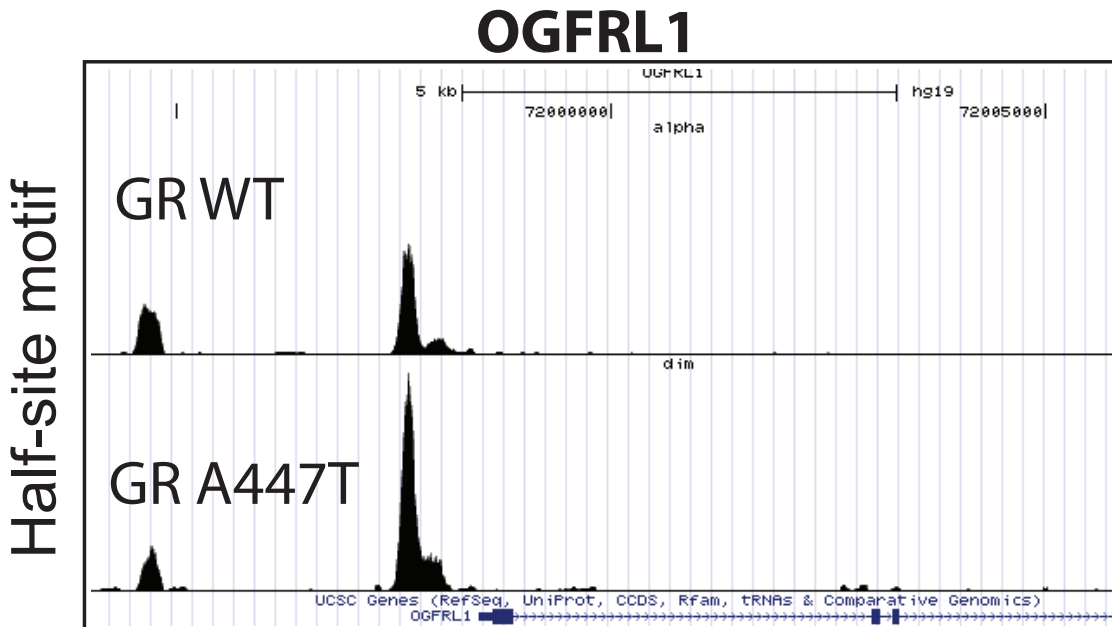
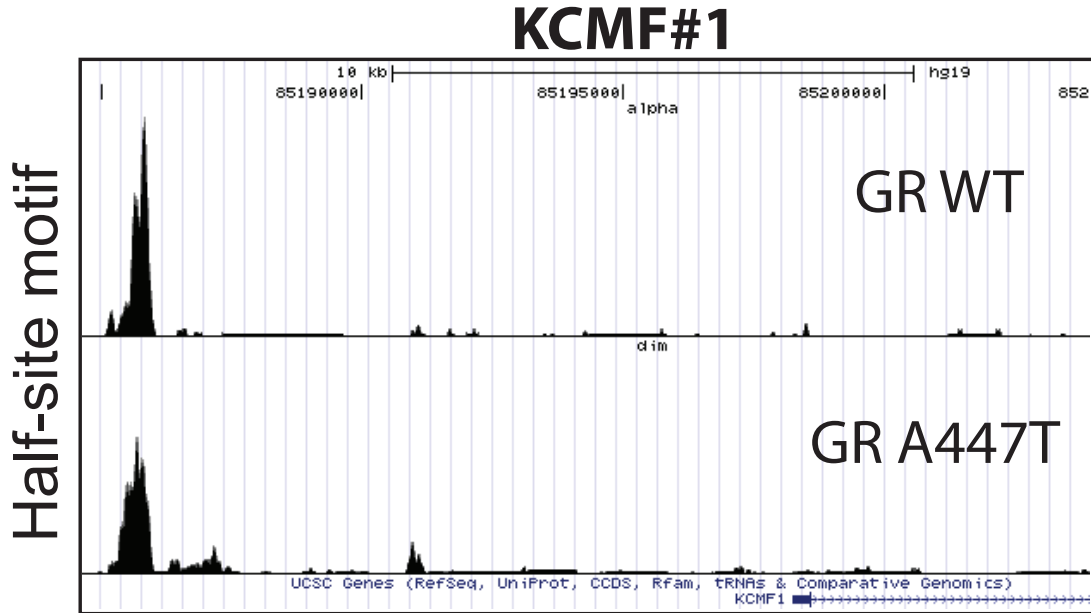
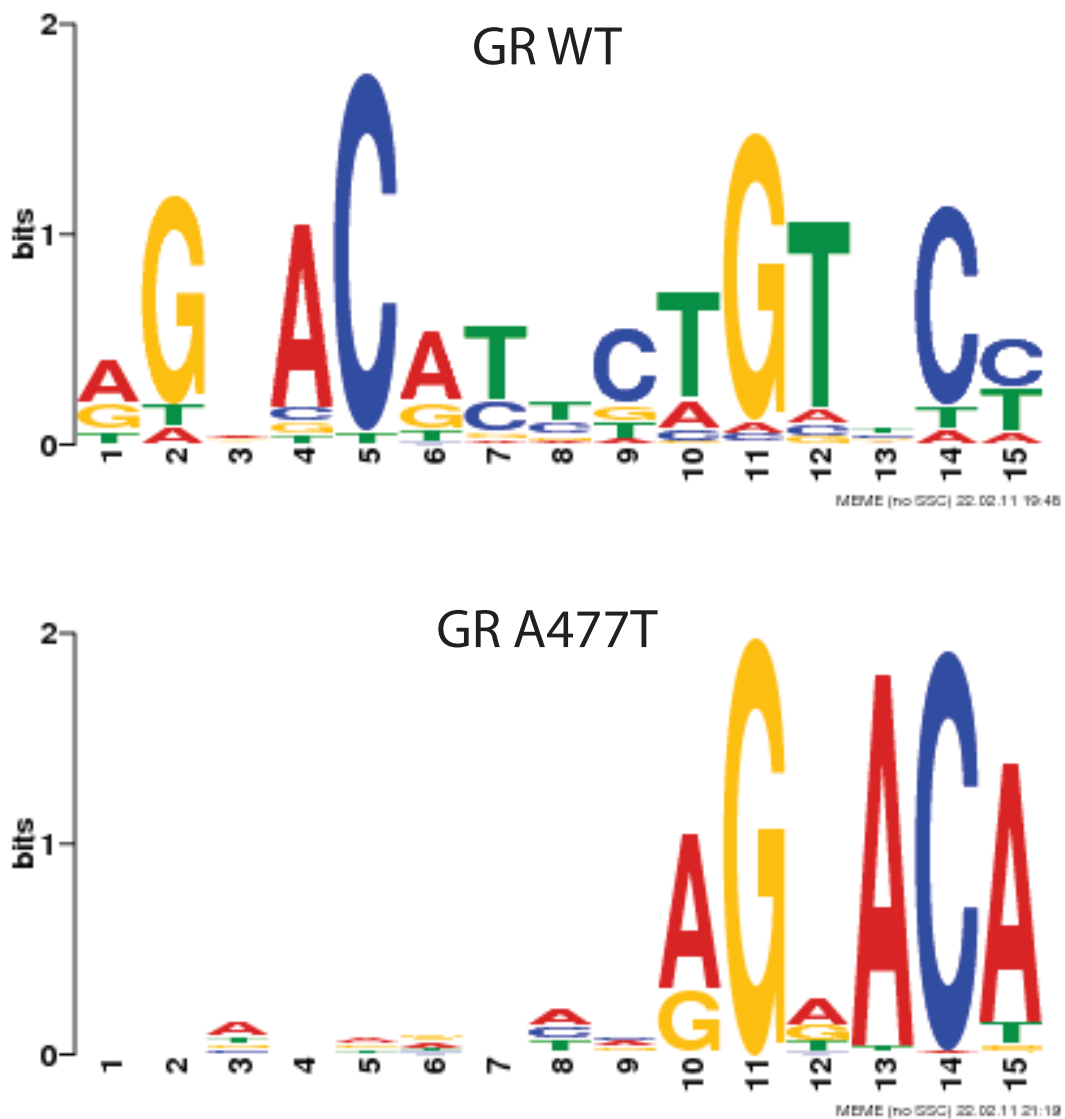


Figure 3.7 Comparison of WT and A477T binding motifs in U20S cells.

Motifs were generated from GR-bound peaks identified by GR ChIP-sequencing using MEME in “zero or one motif per site” mode with a 2nd order background Markov Model based on the top 1000 peaks. Motif searches were extended out to 18 base pairs, but with little gain in information value beyond 15 basepairs (for GR WT). 15 base pair motifs are shown.



To determine if binding regions identified by ChIP-sequencing were sufficient to direct GR WT or A477T-specific transcriptional regulation, approximately 500 bp genomic regions centered on identified peaks for genes listed in Table 5.1 were cloned into luciferase reporter plasmids and transfected into GR WT or A477T over-expressing U2OS cell lines. GR-dependent reporter induction with 100 nM dex was monitored by luciferase activity and normalized to treatment with ethanol control for a preliminary panel representing candidate GREs from 4 of the 5 gene classes (**Figure 3.8**). Intriguingly, both MSX2 binding regions were sufficient to recapitulate GR WT-specific luciferase induction and both HOXD1 binding regions were sufficient to recapitulate A477T-specific induction. Furthermore, ZNF189 was similarly induced by both GR WT and A477T, consistent with the pattern of transcriptional regulation of the endogenous gene. The FBXO32 gene, which was A477T-regulated but bound by both WT and mutant GR did not recapitulate endogenous gene expression patterns. Perhaps this mode of regulation requires interaction with additional DNA-bound factors outside of the 500 bp regions. The peak for RPL1, a negative control, had little effect on reporter activity. Encouraged by the reproducibility of GR WT and A477T-dependent regulation in a simple reporter system, future work will be done to expand this binding region reporter study to a comprehensive panel of all binding regions listed for the 5 classes of genes we identified in Table 3.1.

Motivated by the identification of the GR A477T binding motif corresponding to a GR half-site (**Figure 3.7**), we investigated an additional class of potential “monomeric GR” regulated genes consisting of OGFRL1 and

KCMF1. The candidate genes for this class were chosen because they were (1) regulated by both WT and A477T, (2) occupied by both WT and A477T, (3) have a peak overlapping a GR consensus half site, but not a full site, and (4) proximal to a gene TSS. For the OGFRL1 binding region #1, both WT and A477T activated transcription to a similar extent, mimicking endogenous regulation. In contrast, KCMF1 showed luciferase activation for both GR cell lines, whereas endogenous gene expression was repressed by GR.

Figure 3.8 Genomic response elements recapitulate WT and A477T-specific patterns of transcriptional regulation.

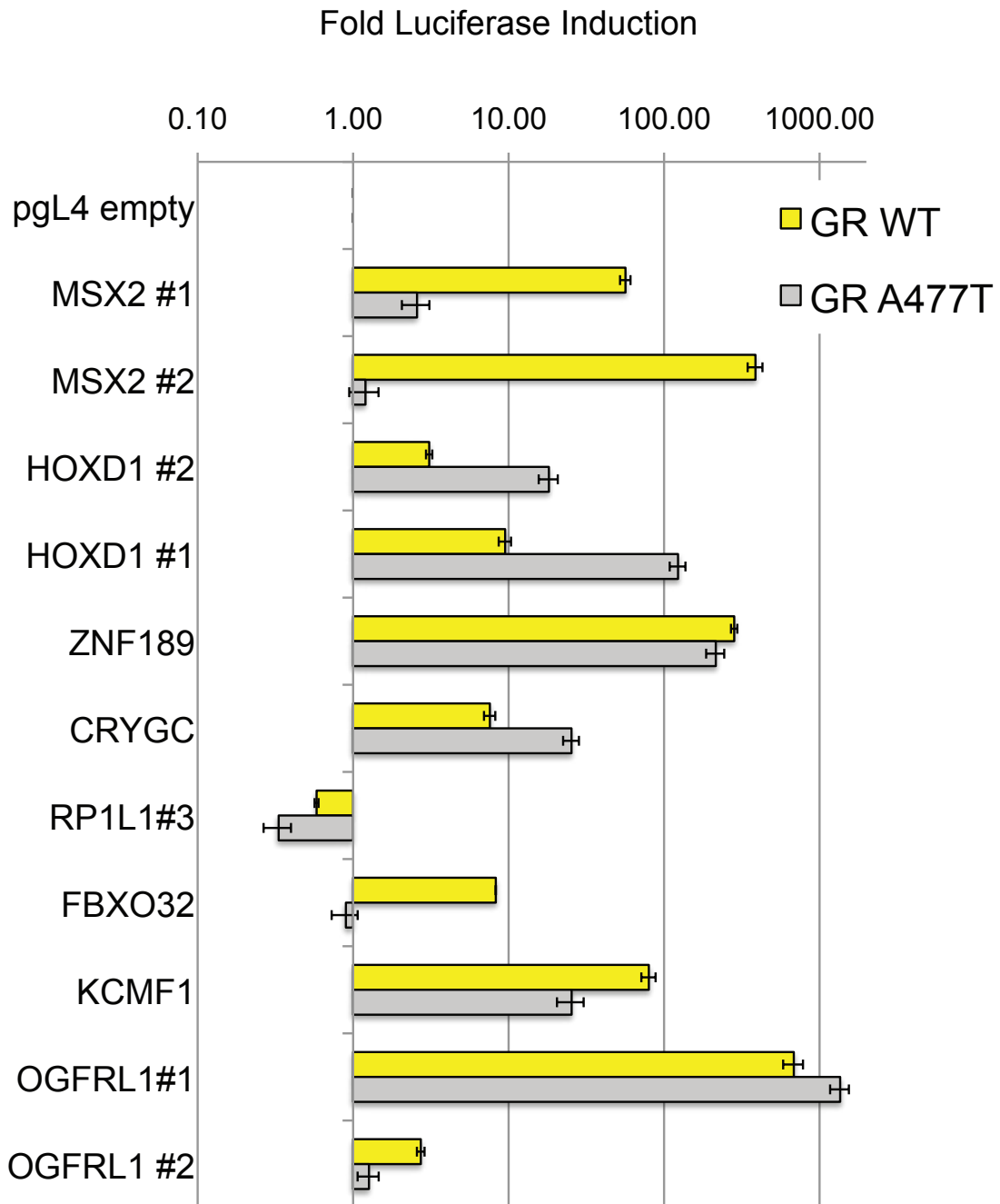


Figure 3.8: Genomic response elements recapitulate GR WT- and A477T-specific regulation.

Comparison of GR WT and A477T transcriptional induction for Class 1 (MSX2), Class 2 (HOXD), Class 4 (ZNF198, CRYCG), Class 5 (FBXO32) and potential GBS monomer-binding genes as described in Table 5.1. RPL1 is a negative control consisting of a peak present in both WT and A477T that is below the threshold for significant binding. Reporter plasmids contain 500 bp regions corresponding to GR binding regions identified by GR WT and A477T ChIP-sequencing for genes listed in Table 5.1. These regions were amplified from genomic DNA of parental U2OS cell lines (ATCC) and cloned into pGL4 vector with the luciferase gene under the control of a dex non-responsive E4 TATA promoter. Reporter plasmids were transiently transfected into U2OS cell lines stably over-expressing GR WT or A477T. GR-dependent luciferase induction with 100 nM dexamethasone treatment for 16 hours was normalized to Renilla control, then to ethanol induction and normalized to empty pGL4 vector. Error is S.E.M. of 3 biological replicates.

3.3 Discussion

We investigated the functional significance of the dimer interface and the intersubunit signaling pathway through the A477 residue by monitoring GR gene-specific activity according to two different parameters—GR transcriptional regulation and DNA response element occupancy. By comparing the effect of a single mutation on genome-wide gene expression and chromatin occupancy, we sought to identify classes of genes with similar modes of regulation, thus providing a handle to derive mechanisms of specificity. Our study revealed at least five classes of genes, suggesting that at least this many different mechanisms contribute to GR gene-specific regulation.

We found that the number of dex-regulated genes in U2OS cells overexpressing either GR WT and A477T was nearly identical. In particular, A477T regulated 256 novel genes that were unregulated by WT. Regulation of novel gene targets by the GR A477T mutant has been reported from genome-wide studies in liver cells[46] and, very recently, in U2OS cell lines [47]. This is surprising given the lower affinity of A477T for the canonical GR binding site *in vitro* (**Figure 2.5** and **2.6**). One possibility is that the structural changes induced by the A477T mutation modify GR sequence specificity, resulting in A477T binding DNA with high affinity at binding sequences that are distinct from those recognized by GR WT. Our *in vitro* binding study used only GR binding sequences adhering to the WT consensus sequence, and thus did not test this

possibility. Thus, there may be a binding motif that A477T recognizes with equivalent affinity as WT binds to a consensus GBS. However, the binding motif generated from A477T occupancy does not support this hypothesis, but instead suggests that A477T preferentially binds a sequence motif consistent with a GBS half site (**Figure 3.7**). Because the affinity of GR WT and A477T for a GBS half site is equivalent (**Figure 3.5**), it seems that the high-affinity DNA binding sequence recognized by A477T cannot explain the regulation of novel A477T target genes. Furthermore, half-site recognition is inconsistent with the sequence-specific transcriptional profiles of GR A477T at eight GBSs that all have the same strong half-site half and differ only in the sequence of the second halfsite (**Fig2.4d**).

It is not surprising that the *in vitro* DNA-binding affinity is insufficient in explaining the novel A477T targets identified by microarray, as DNA-binding affinities determined *in vitro* may not correlate with binding affinities in the cell. *In vivo* and cell-based studies of gene-specific regulation by the A447T mutant have led to the hypothesis that A477T transcriptional regulation is intact only at binding sites where GR interaction with response elements is mediated by protein-protein interactions with DNA-bound coregulators [48-50]. In this model, the A477T mutation would retain only a subset of WT function, suggesting that the mutation does not impair GR tethering to DNA through its interaction with other DNA-bound factors. This model would predict that only a subset of the GR target genes are regulated by A477T and thus also cannot account for the subset of 256 novel A477T-specific target genes.

Our data is consistent with a view that the A477T mutation has a more complex effect on GR gene-specific function. We suggest that each class of regulated genes in Table 3.1 invokes a different mechanism for generating specificity (**Figure 3.9**). One model to explain the gain-of-function A477T-specific regulation and binding at a given gene is that A477T disrupts an interaction with a factor that mediates GR turnover on DNA. Thus, at some genes, GR WT is actively dissociated rapidly from DNA, where GR A477T remains bound at response elements. While *in vitro* studies comparing the dissociation kinetics of WT and A477T (**Figure 2.6**) show that A477T dissociates more rapidly from DNA than WT ($t_{1/2}$ of 5 secs versus 55 secs, respectively), the fast dissociation rate of A477T is similar to that determined for GR WT in the cell (~4 secs) [51].

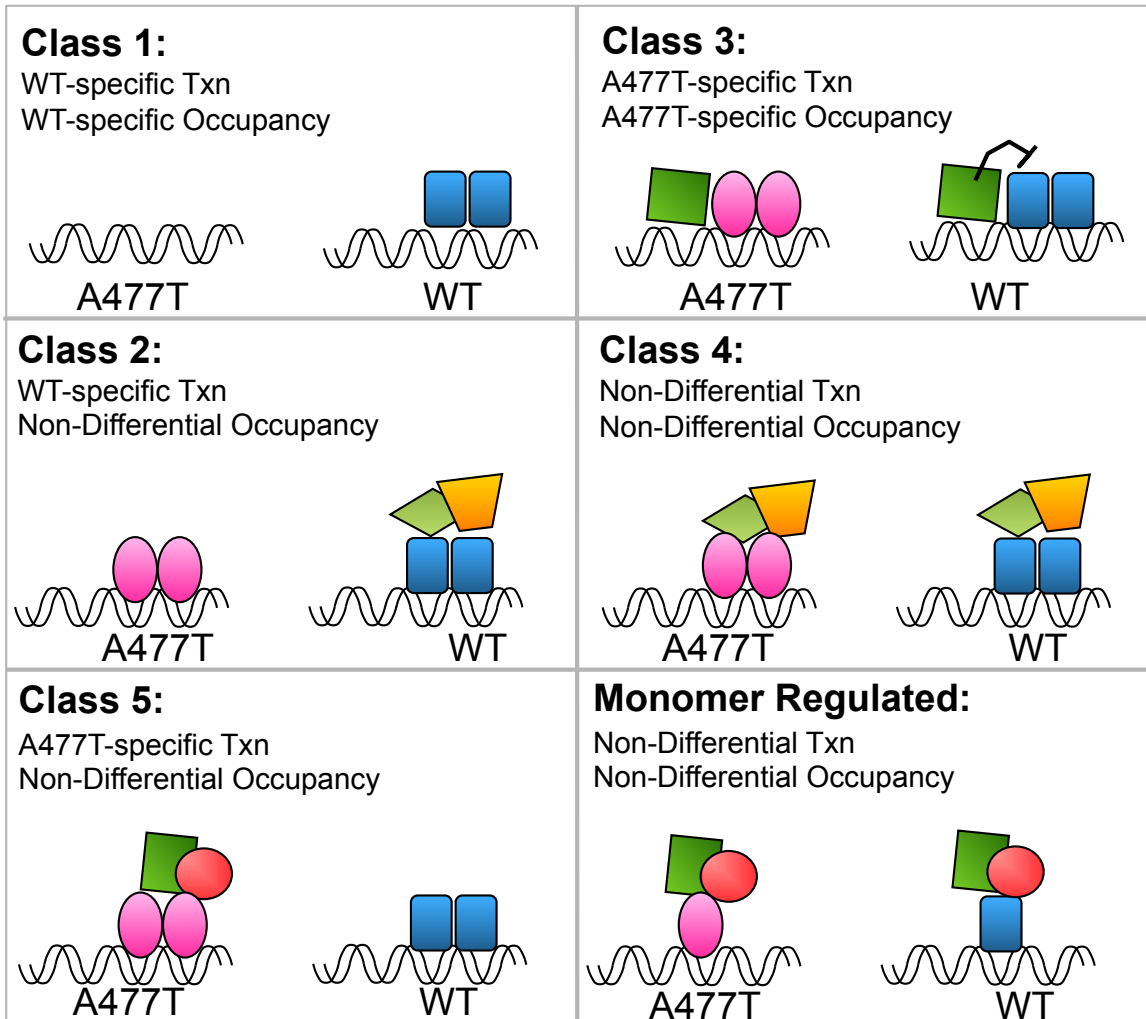
A second model to explain the large subset of GR A477T-specific genes is based on the differences in sequence specificity between WT and A477T. Because GR recognizes a consensus 15 bp sequence with ~10-fold higher affinity than GR A477T (based on *in vitro* binding), the majority of the WT receptor within the nucleus will be bound with high affinity to these selective sites. In contrast, the A477T recognizes a consensus half-site (**Figure 3.7**), which it binds with lower affinity (compared to the WT recognition of the 15 bp GBS). However, half sites are likely to be more commonly distributed throughout the genome than consensus 15 bp GBSs. Thus, while GR WT is predominantly bound at high affinity to specific 15bp GBSs, A477T has no preference for these sites over the numerous half-sites throughout the genome. However, A477T appears to have a more stringent requirement for an “ideal” GRE halfsite with the

sequence “AGAACA”, based on the higher information content of the A477T motif compared to the WT motif (**Figure 3.7**). Thus, response elements that are overlooked by GR WT, may be bound by A477T, due to lack of discrimination between half sites and full sites. A caveat of this model is that it assumes a limiting amount of GR in the nucleus, in order to explain why GR WT would not also associate with the lower affinity half-sites. Further analysis of the binding motifs identified within the WT and A477T non-differential genes may lend insight into this model, as one might predict that these are genes that contain at least one “ideal” halfsite within the consensus 15bp GBS, thus meeting the requirement for both the WT and the A477T binding motifs.

A third model, that can potentially explain multiple classes of WT and A477T regulation is that structural differences induced by the A477T mutation may impart differential interaction of WT and A477T with GR coregulators and other transcription factors, thus contributing to gene-specificity (**Figure 3.9**). Therefore, by grouping GR target genes according to these mechanistic classes, we believe that the coregulators responsible for each regulatory patterns may be revealed. To test this hypothesis, future studies will investigate the requirement of a panel of 30 known GR coregulators in the WT and A477T-dependent regulation of target genes listed in Table 3.1, by cofactor knockdown in U2OS-GR cells. These experiments will be done using luciferase reporters driven by ~500 bpGR binding regions associated with genes that recapitulate endogenous expression patterns (as in **Figure 3.8**). One limitation of this experiment is that it requires that the specificity determinants for a given cofactor are encoded within

the 500 bp response element. While this requirement is stringent, an advantage is that it will allow for further mechanistic characterization of cofactor interactions within GR WT and A477T complexes by further “promoter-bashing” of GR binding regions.

Figure 3.9 Model for mechanisms of regulation by WT and A477T.



Chapter 4 A naturally occurring insertion of a single amino acid rewires the transcriptional program induced by the glucocorticoid receptor

4.1 Introduction

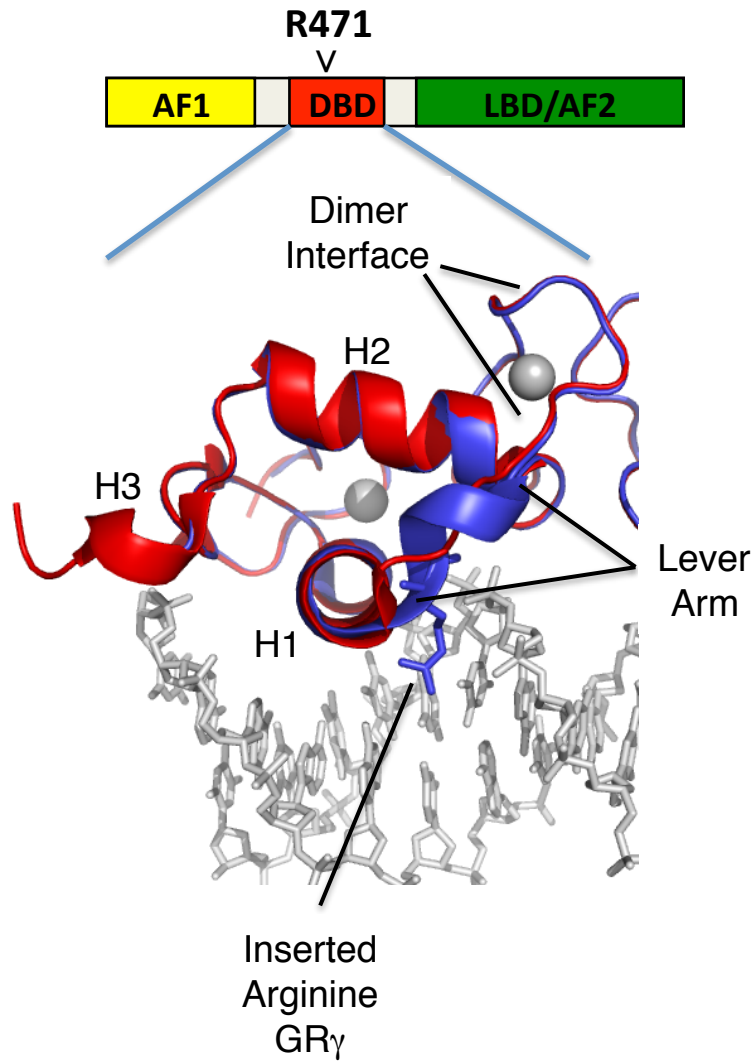
The functional experiments described by Meijssing, et al. and in Chapter 2 of this thesis provide evidence that the GR DNA binding sequence not only localizes GR to appropriate genomic response elements, but also encodes information for the regulation of a particular gene. Both NMR and crystallographic studies suggest that interactions at the protein:DNA interface are coupled with sequence-specific structural changes at the lever arm [6](and Chapter 2). Furthermore, NMR comparison of GR WT and A477T when bound to different GBSs suggests that the dimerization interface plays a role in integrating sequence-specific signals between GR dimer partners to modulate the lever arm conformation. This lead us to propose that allosteric communication between the GR DNA-binding interface and other GR-DBD surfaces, such as the lever arm in particular,

contribute to GR gene-specific activity. However, the functional significance of the sequence-specific conformations of the lever arm is not clear.

The position of the lever arm within the isolated GR-DBD structure suggests that it is accessible for protein-protein interactions, either with other domains of GR (AF1, LBD, hinge region) that are absent in our structural studies of the DBD, or with transcriptional coregulators that interact with the DBD. Cofactor interactions mediated specifically by the GR lever-arm have yet to be identified. While the interaction surfaces between domains of full-length GR are not known, crystallography studies with related receptors—a heterodimeric retinoid X receptor (RX) and peroxisome proliferator-activated receptor (PPAR) complex—indicate that the DBD region corresponding to the lever arm of GR are positioned to interact with the LBD of the heterodimer partner (RXR) or are highly accessible to bind other factors (PPAR) [52].

Interestingly, a natural isoform of GR (GR γ) differs from the predominant GR species (GR α , referred to as GR WT in previous chapters) by a single amino acid insertion in the lever arm. The additional amino acid is a consequence of alternative splicing resulting in the inclusion of an arginine in the lever arm. This isoform variant is widely conserved suggesting a functional role in GR signaling [53], [54]. The crystal structures of the GR α :DBD and GR γ :DBD show that the insertion does not alter base-specific contacts to DNA, but does alter the conformation of the lever arm [6]. Therefore, the GR γ variant serves as a specific tool to investigate the functional significance of lever arm conformation in GR gene-specific regulation.

Figure 4.1 Model for mechanisms of regulation by WT and A477T.



4.2 Results

Transcriptional regulation and genomic binding by GR α and GR γ

To determine how disrupting the lever arm affects GR gene-specific transcription, genes that were regulated by 3 hours of dex treatment were compared between U2OS cells expressing either GR α or GR γ (Sebastiaan Meijnsing, data not shown). While a large number of genes were regulated similarly by both GR isoforms, subsets of genes were regulated specifically by either GR α or GR γ . To test whether the observed set of differentially regulated GR α and GR γ genes were a consequence of isoform-specific binding, ChIP-seq experiments were performed in isoform-specific U2OS cell lines (Sebastiaan Meijnsing, data not shown). Interestingly, in most cases isoform-specific regulation was not explained by isoform-specific binding, suggesting that perturbing the lever arm affects GR activity at a step downstream of binding.

To further dissect the mechanism of by which the GR γ insertion results in differential gene-transcription, we focused on the Inositol 1,4,5-triphosphate receptor interacting protein gene (ITPRIP) that was upregulated selectively only in GR γ -expressing U2OS cells after 4 hours of dex-treatment and also bound selectively by GR γ but not GR α , as confirmed by Q-PCR (**Fig. 4.2a and b**). We measured the DNA-binding affinity for GBSs that were either GR γ -specific

(ITPRIP) or isoform non-differential (FKBP5) by gel shift (**Fig. 4.2e**). Surprisingly, the GR γ isoform has a higher affinity for both binding sites—10-fold and 2-fold for the FKBP5 and ITPRIP GBSs, respectively. Therefore, the increased affinity of GR γ compared to GR α for ITPRIP could likely account for the GR γ -specific binding, but cannot not explain the subset of GR α -specific regulated genes or GR α -specific binding regions.

To assess whether the determinants of isoform specificity were encoded in the GR-bound genomic sequences, ~500 bp regions surrounding the GR-bound peak found at the ITPRIP (GR γ -specific) gene was isolated and cloned into a luciferase transcriptional reporter (**Fig. 4.2c**). The ITPRIP reporter recapitulated the isoform-specific regulation (**Fig. 4.2d**). Deletion of the 15 bp GR γ -specific GBS associated with the ITPRIP gene (AGAACA n nnAGT n nn) rendered the plasmid unresponsive to GR γ (GBS Δ). Furthermore, swapping the GBS sequence to that of the isoform non-differential motif (AGAACA n nnTGTTCT) was sufficient to switch its specificity such that both GR α and GR γ activated transcription to a similar extent. This suggests that the GBS plays a role in defining isoform specific regulation at a given gene. Thus, isoform specific regulation by GR γ may be explained by differential binding of GR γ to specific sequence motifs for some genes (approx. 25%).

For genes that are not regulated by differential binding to genomic regulatory regions, we hypothesized that differences in the lever arm between GR α and GR γ might also affect other functional domains of GR that impact GR

activity. Previous studies of the effect of point mutations in three GR functional domains—the dimerization interface (A477T), AF1, and AF2—have shown that the requirement for each of these domains is gene-specific [42]. To investigate the effect of perturbation of the lever arm in the context of disruption of other GR function surfaces, clonal U2OS cell lines were established which stably express similar levels of GR bearing the GR γ insertion in tandem with point mutations for one of each of the three other domains.

Similar to the observations made for the domain mutations alone, we found that GR γ employed different patterns of functional domain requirements than GR α . This is shown for two GR α -specific target genes, pancreatic lipase (PNLIP) and serine protease inhibitor Kazal-type 5-like 3 (SPINK5L3) (**Fig. 4.3**). For example, the A477T mutation resulted in decreased transcriptional induction at the SPINK5L3 gene. However, combining the A477T and the GR γ insertion rescued the loss of function of A477T, increasing activation ~8-fold of that of the GR γ perturbation alone. Thus, this suggests that there is crosstalk between these two DBD surfaces (the dimerization interface and the lever arm), providing functional evidence for the structural changes in the lever arm as a consequence of the A477T dimer interface mutation (**Chapter 2**).

Figure 4.2 Isoform specific binding and regulation by GR γ

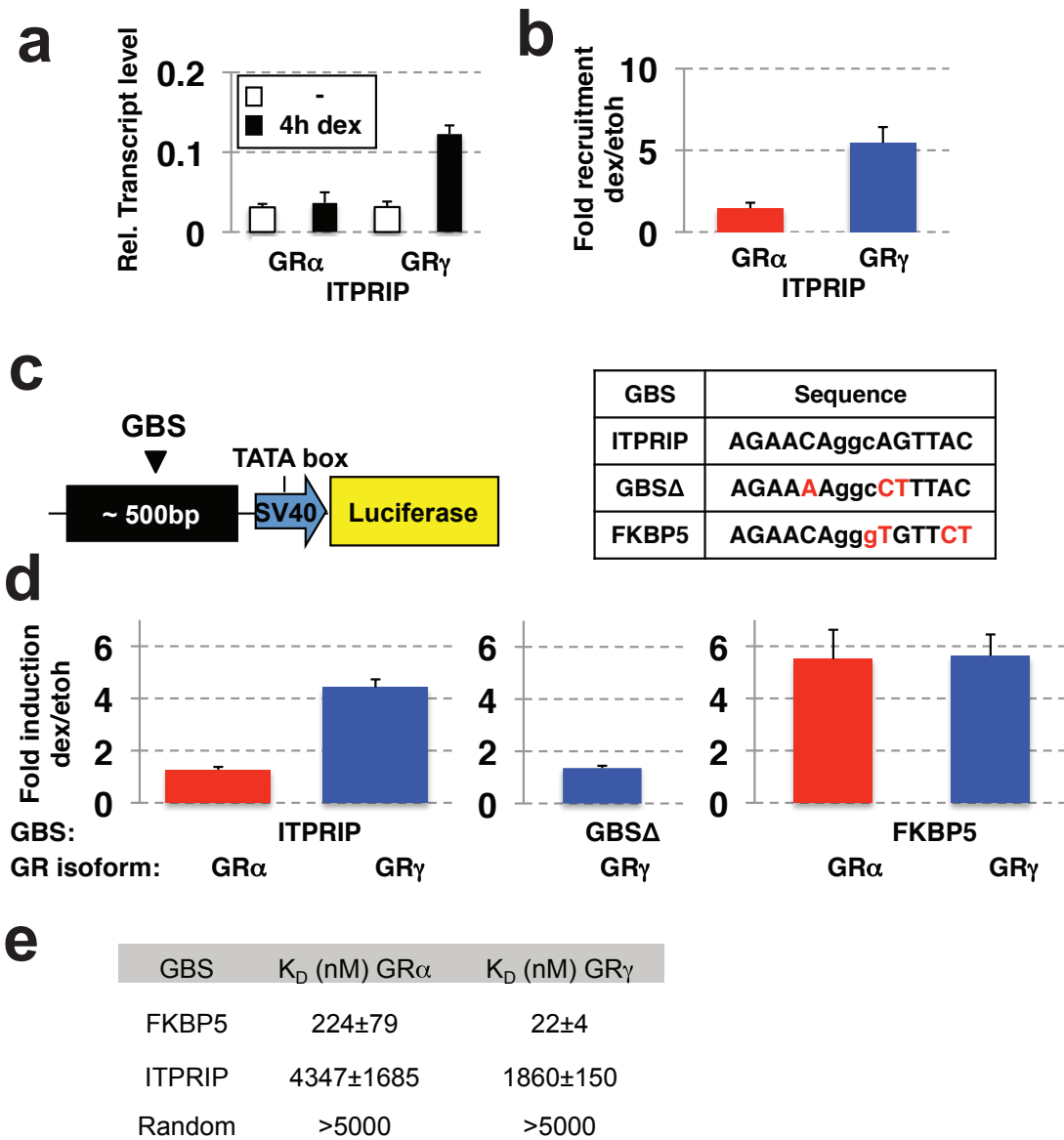


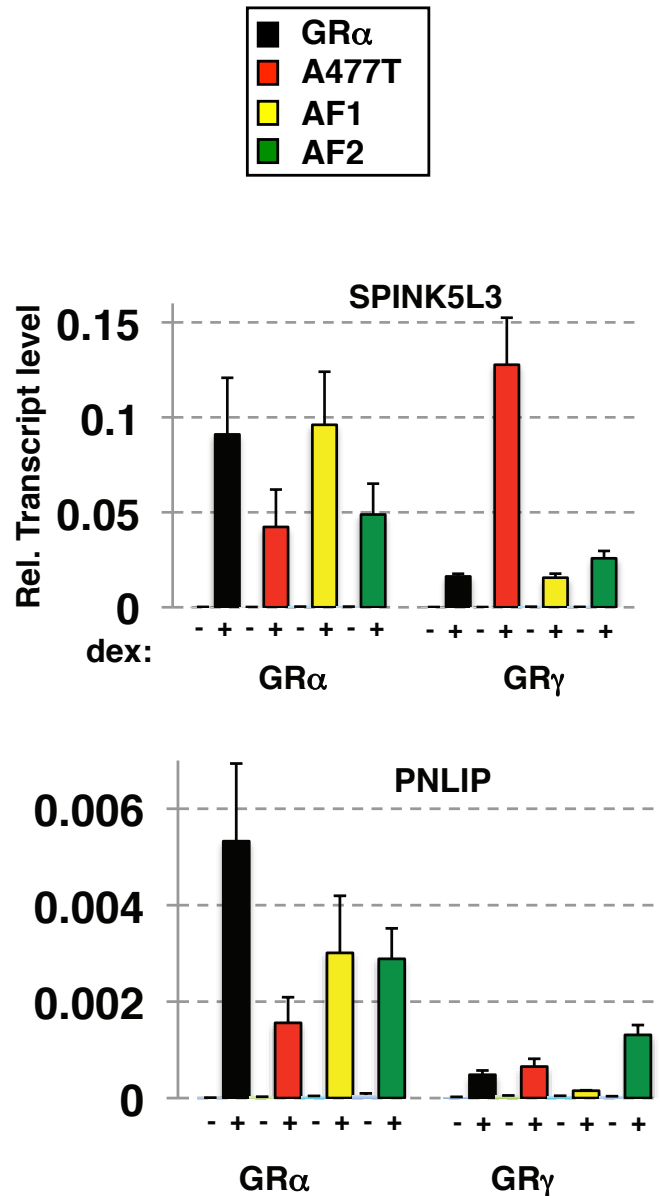
Figure 4.2 Isoform specific binding and regulation by GR γ .

(a) GR γ -specific transcriptional regulation of ITPRIP. Relative transcript levels of treated (4h, 100nM dex) or untreated cells expressing GR α or GR γ were analyzed by real-time quantitative PCR. Averages \pm Standard Error of Mean (S.E.M.) are shown (n=3). (b) GR γ -specific genomic binding to a region within +/- 10 kb of the transcription start site for ITPRIP by GR α and GR γ . U2OS cells stably expressing GR α or GR γ were treated with hormone for 90 minutes and chromosomal GR binding was quantified by Chromatin immunoprecipitation and real-time quantitative PCR. Fold enrichment relative to ethanol vehicle control \pm S.E.M. are shown (n=3). (c) Genomic fragment centered on ITPRIP binding site with GBS variants as indicated were cloned upstream of a minimal SV40 promoter driving luciferase. (d) Fold induction (dex treated vs non treated) by GR isoform as indicated for the ITPRIP reporters with GBS variant construct as indicated \pm S.E.M (n=3) are shown. (e) Affinity of GR α -DBD and GR γ -DBD for 5' cy-5 labeled 23-bp DNA duplexes containing the FKBP5 and ITPRIP GBS as measured by gel shift.

Figure 4.3 GR γ compensates for A477T mutation at SPINK5L3 gene.

The effect of point mutations in GR functional domains on the transcriptional regulation by GR α and GR γ . U2OS cells stably expressing GR variants were treated with 100nM dex for 4hrs and relative luciferase expression levels of treated and untreated cells were analyzed by real-time quantitative PCR.

Averages \pm S.E.M. for n=3.



Structural changes induced by single amino acid insertion in the lever arm

To understand how perturbation of the lever arm affects GR activity, we next examined how changes in GBS sequence and perturbation of the lever arm influence the conformation of the DNA binding domain (DBD). Previous comparison by x-ray crystallography of DNA-bound GR α or GR γ indicated that the structural changes induced by GBS sequence variants were restricted to the lever arm [6]. However, crystal structures can be limited by packing contacts and crystallography is not well suited to detect conformational changes that are sampled by protein complexes in solution [55].

We turned to nuclear magnetic resonance (NMR) to determine if changes in the lever arm influence the structure of other regions of the GR DBD. ^{15}N -labeled GR α -DBD and GR γ -DBD protein was purified and incubated with GBS sequences FKBP5, a binding site matching the non-differential GBS motif, or to ITPRIP, a GBS matching the GR γ -specific motif. ^1H - ^{15}N HSQC peaks were assigned to amino acid residues for DNA-bound GR α -DBD and assignments were transferred to GR α :FKBP5 and GR α :ITPRIP spectra (**Fig. 4.4a** and **Fig. 4.6**). Conformational shifts between GR α and GR γ were analyzed by chemical shift difference analysis by calculating the distance between each peak in the GR α spectrum and the nearest peak in the corresponding GR γ spectrum.

As expected, when we compared GR α and GR γ the most pronounced changes in chemical shift mapped to the lever arm, likely reflecting the nearby insertion at position 471 of an arginine residue (e.g. E469, G470). However, the

changes were not limited to the lever arm, but also occurred at residues that orient the dimerization interface (such as G478, N480, R488) indicating a structural interplay between these two subdomains, paralleling the functional interplay we observed between these subdomains in transcriptional regulation (**Fig. 4.3**). Additional changes were seen in the recognition helix (F464, R466, A467, V468) helix 2 (C495, R496, L501, C502) and near helix 3 (L507-R510) indicating that conformational shifts in the lever arm impact the structure of remote regions within the DBD (**Fig. 4.4**).

To investigate possible structural mechanisms contributing to context-specific differential activity of GR α and GR γ , we compared conformational shifts associated with the GR γ arginine insertion between the non-differential GBS (FKBP5) and the GR γ -specific GBS (ITPRIP) (**Fig. 4.5a**). The two GBS complexes have extensive overlap of significantly shifted residues (**Fig. 4.5c**). Interestingly, the few GBS-specific chemical shift differences for GR γ map to the dimerization interface (I483, I484, R488), suggesting that the ITPRIP GBS might induce a conformation in the dimerization interface that is limiting activation by GR α but is compensated for by the structural changes induced by GR γ .

Finally, we compared the chemical shifts induced by changing the GBS sequence with those induced by perturbing the lever arm and found extensive overlap between the residues in the DBD that shift in response to changes in GBS and those induced by GR γ (**Fig. 4.5**). Although the affected residues overlap, the conformational states induced by GBS variants differ from those

induced by perturbation of the lever arm, indicating that GR γ may rewire DNA sequence-specific signals. Additionally, the widespread conformational shifts induced by GR γ , together with the transcriptional reporter data, suggest that the lever arm is structurally and functionally linked to other GR surfaces.

4.3 Discussion

Previous studies comparing GBS variants showed that binding sequences differently utilize GR functional surfaces and particular cofactors, indicating that events at the DNA:protein interface influence the function of other GR domains [6]. Here we tested how disrupting the lever arm influences which domains of GR are required for receptor activity. Disrupting GR domains in combination with perturbation of the lever arm (either the GR α and GR γ) indicated that, similar to binding sequence, the lever arm influences the GR domain requirements at a given gene.

Interestingly, we found several examples where the dimer mutation rescued the change in activity induced by the GR γ insertion in the lever arm (**Fig. 4.3**). This suggests that the A477 residue and the lever arm are in the same pathway that mediates gene-specific transcriptional regulation by GR.

Furthermore, NMR experiments indicated that there is structural communication

between the dimer interface and the lever arm that parallels the interplay between these two surfaces in our functional studies. Specifically, we found that the conformation of the dimer interface changed when we altered the conformation of the lever arm. However, the changes induced by perturbing the lever arm were not restricted to the dimer interface and the additional conformational changes we observed showed extensive overlap with the residues in the DBD that shift in response to changes in GBS sequence (**Fig. 4.5a**). This suggests that these structural changes are part of an allosteric pathway that propagates signals from the lever arm to the dimer interface, or vice versa, to modulate the gene-specific structure and function of GR. Notably, the sequence-specific conformations of the lever arm (such as residue G470) are disrupted by the A477T mutation in the dimer interface, whereas the sequence-specific conformations of the lever arm and dimer interface are maintained when the lever arm is perturbed by the GR γ insertion (**Fig. 4.6, middle**). This provides insight about the directionality of this allosteric pathway, indicating that GBS-specific signals are transmitted from the dimerization interface to the lever arm, and that the lever arm extends these signals to other GR domains (**Fig. 4.5d**).

Figure 4.4 GR γ lever arm insertion results in widespread conformational shifts in the GR-DBD.

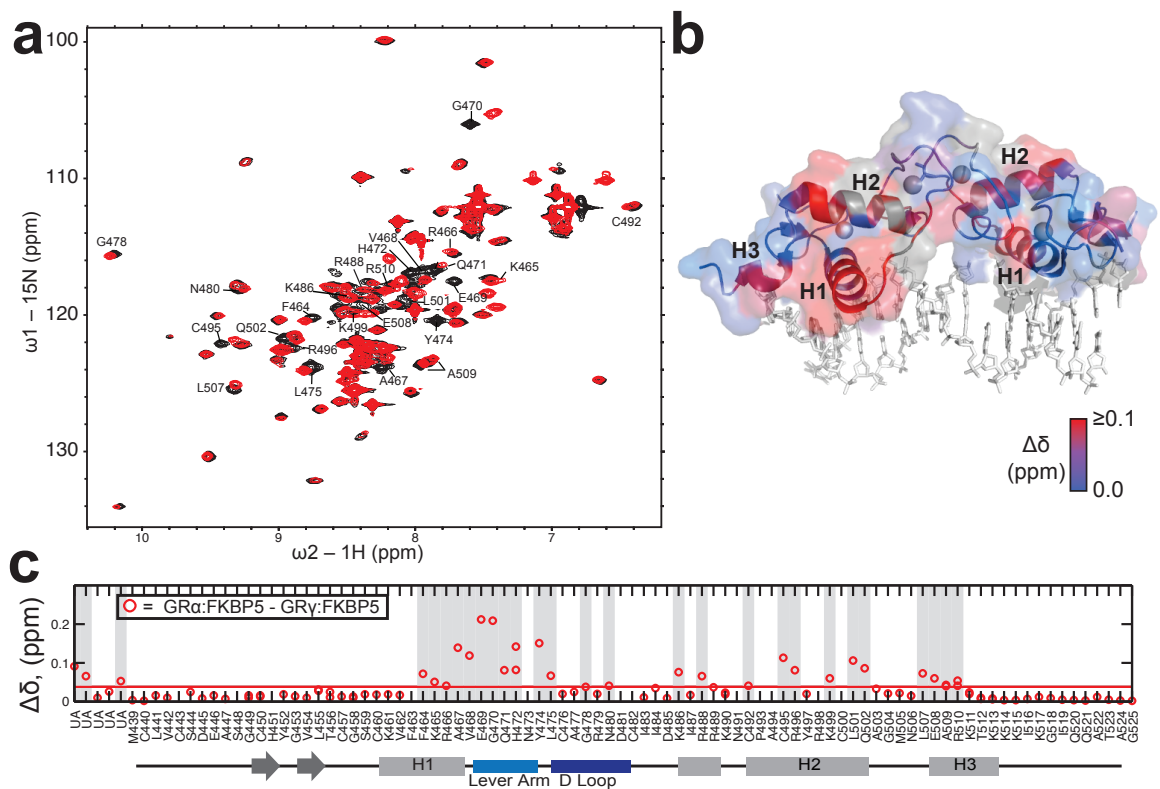


Figure 4.4 GR γ lever arm insertion results in widespread conformational shifts in the GR-DBD.

(a) Overlay of ^{15}N -HSQC spectra of GR α (black) and GR γ (red) bound to the FKBP5 GBS. Assigned peaks that were significantly shifted between the two spectra are labeled. (b) Combined proton and nitrogen chemical shift differences ($\Delta\delta$) between GR α :FKBP5 and GR γ :FKBP5 spectra for each assigned residue are colored onto the crystal structure of GR α : FKBP5 (PDB ID: 3G6U) according to the magnitude of $\Delta\delta$. Unassigned residues are in grey. (c) Chemical shift difference between GR α and GR γ 1H-15N HSQC spectra bound to FKBP5 (top) and ITRIP (bottom) for all assigned GR α residues. Chemical shift difference was measured as the minimal distance between each assigned peak in the GR α spectra and a peak in the GR γ (see Methods). Grey bars highlight residues with a shift difference greater than the mean (red line) of all peaks.

Figure 4.5 Comparison of conformational changes induced by GBS or arginine insertion in the lever arm.

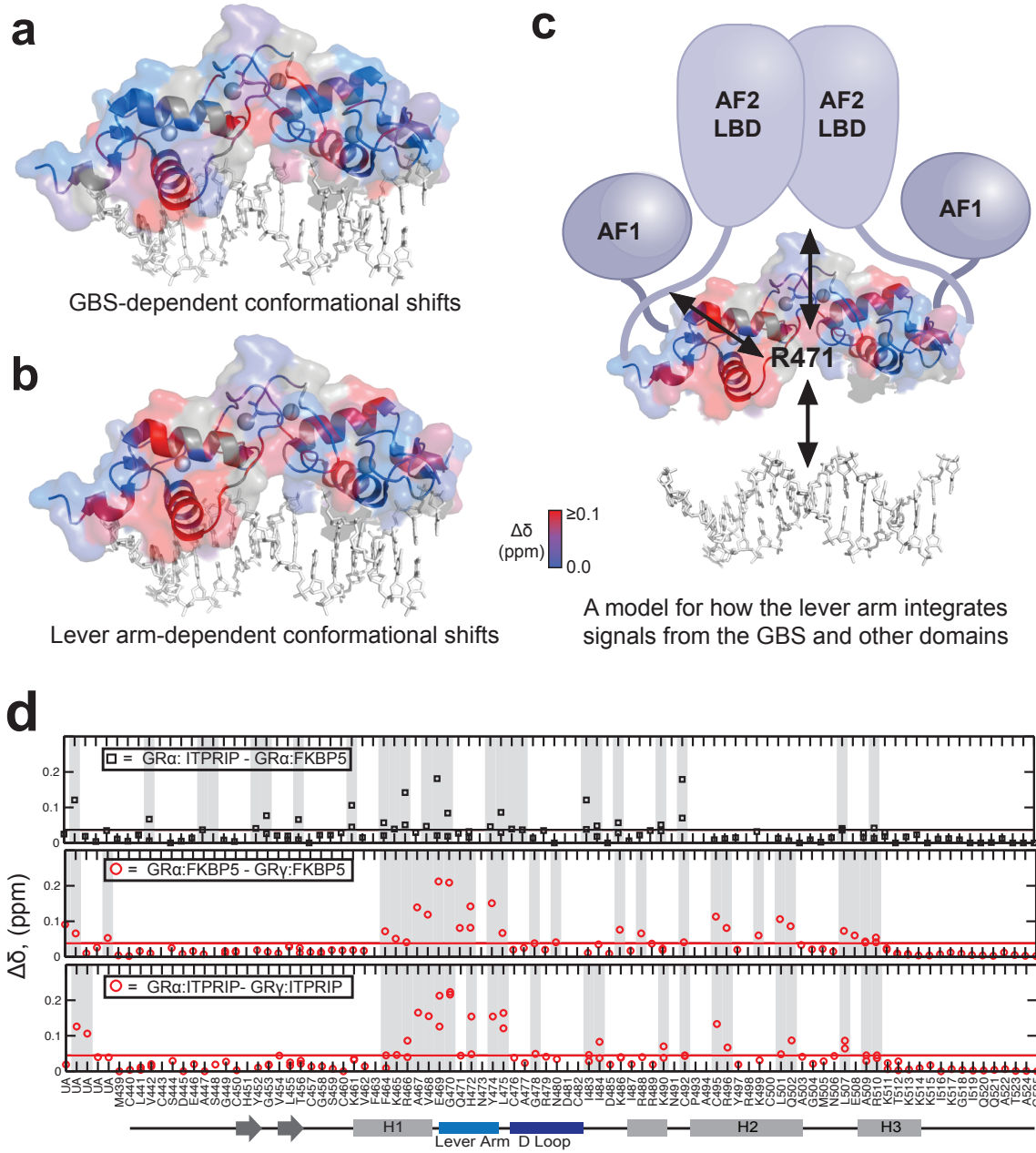
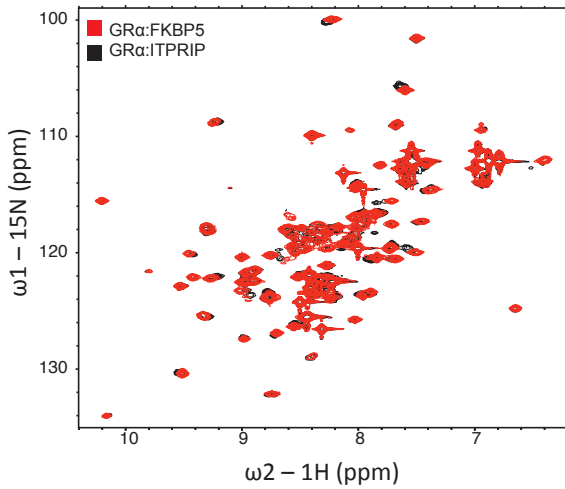


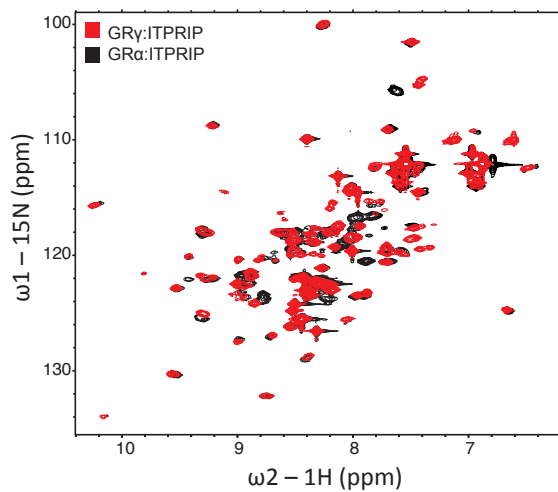
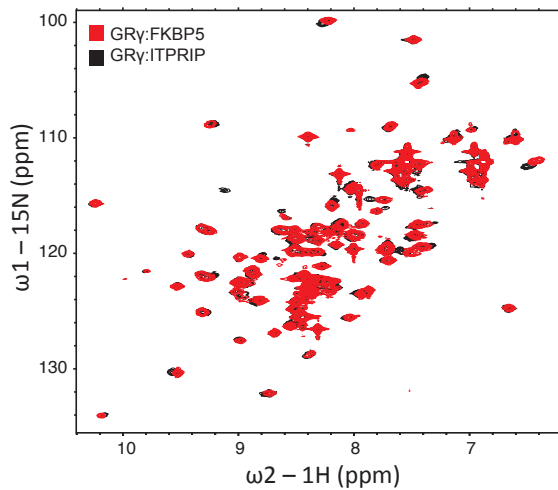
Figure 4.5 Comparison of conformational changes induced by GBS or arginine insertion in the lever arm.

(a) Combined proton and nitrogen chemical shift difference ($\Delta\delta$) between ^1H - ^{15}N HSQC spectra of GR α bound to ITPRIP versus FKBP5 (top), GR α and GR γ bound to FKBP5 (middle), and GR α and GR γ bound to ITPRIP (bottom) for all assigned GR α residues (x-axis). Residues with doublet peaks in the spectra are plotted as two data points. Grey bars highlight residues with a $\Delta\delta$ greater than the mean $\Delta\delta$ of all peaks in the comparison (black or red line). UA=unassigned peaks. (b) The GR α -DBD (PDB ID: 3G6U) colored according to chemical shift difference induced by either changing GBS sequence (ITPRIP versus FKBP5) or (c) arginine insertion in the lever arm (GR α versus GR γ bound to FKBP5). Unassigned residues are colored grey. (d) A model indicating how the lever arm integrates signals from GBS variants and other functional domains of GR to influence regulatory complex composition and activity.

Figure 4.6 Comparison of ^1H - ^{15}N HSQC for GR α -DBD and GR γ -DBD bound to FKBP5 and ITPRIP.



(a) GR α bound to FKBP5 (red) versus ITPRIP (black). (b) GR γ bound to FKBP5 (red) versus ITPRIP (black). (c) GR γ (red) and GR α (black) bound to ITPRIP.



References

- [1] R. K. Bledsoe et al., "Crystal structure of the glucocorticoid receptor ligand binding domain reveals a novel mode of receptor dimerization and coactivator recognition.," *Cell*, vol. 110, no. 1, pp. 93–105, Jul. 2002.
- [2] A. J. Copik, "Activation Function 1 of Glucocorticoid Receptor Binds TATA-Binding Protein in Vitro and in Vivo," *Molecular endocrinology (Baltimore, Md)*, vol. 20, no. 6, pp. 1218–1230, Dec. 2005.
- [3] Y. Tao, C. Williams-Skipp, and R. I. Scheinman, "Mapping of glucocorticoid receptor DNA binding domain surfaces contributing to transrepression of NF-kappa B and induction of apoptosis," *The Journal of biological chemistry*, vol. 276, no. 4, pp. 2329–2332, Jan. 2001.
- [4] Y. A. Bulynko and B. W. O'Malley, "Nuclear Receptor Coactivators: Structural and Functional Biochemistry," *Biochemistry*, vol. 50, no. 3, pp. 313–328, Jan. 2011.
- [5] B. F. Luisi, W. X. Xu, Z. Otwinowski, L. P. Freedman, K. R. Yamamoto, and P. B. Sigler, "Crystallographic analysis of the interaction of the glucocorticoid receptor with DNA.," *Nature*, vol. 352, no. 6335, pp. 497–505, Aug. 1991.
- [6] S. H. Meijnsing, M. A. Pufall, A. Y. So, D. L. Bates, L. Chen, and K. R. Yamamoto, "DNA Binding Site Sequence Directs Glucocorticoid Receptor Structure and Activity," *Science (New York, NY)*, vol. 324, no. 5925, pp.

407–410, Apr. 2009.

- [7] H. Baumann et al., “Refined solution structure of the glucocorticoid receptor DNA-binding domain,” *Biochemistry*, vol. 32, no. 49, pp. 13463–13471, Dec. 1993.
- [8] M. A. van Tilborg et al., “Structure refinement of the glucocorticoid receptor-DNA binding domain from NMR data by relaxation matrix calculations,” *Journal of molecular biology*, vol. 247, no. 4, pp. 689–700, Apr. 1995.
- [9] T. Härd et al., “Solution structure of the glucocorticoid receptor DNA-binding domain.,” *Science (New York, NY)*, vol. 249, no. 4965, pp. 157–160, Jul. 1990.
- [10] S. M. Holmbeck, H. J. Dyson, and P. E. Wright, “DNA-induced conformational changes are the basis for cooperative dimerization by the DNA binding domain of the retinoid X receptor.,” *Journal of molecular biology*, vol. 284, no. 3, pp. 533–539, Dec. 1998.
- [11] K. Dahlman-Wright, H. Siltala-Roos, J. Carlstedt-Duke, and J. A. Gustafsson, “Protein-protein interactions facilitate DNA binding by the glucocorticoid receptor DNA-binding domain.,” *The Journal of biological chemistry*, vol. 265, no. 23, pp. 14030–14035, Aug. 1990.
- [12] K. Dahlman-Wright, A. Wright, J. A. Gustafsson, and J. Carlstedt-Duke, “Interaction of the glucocorticoid receptor DNA-binding domain with DNA as a dimer is mediated by a short segment of five amino acids.,” *The Journal of biological chemistry*, vol. 266, no. 5, pp. 3107–3112, Feb.

1991.

- [13] H. Berglund, M. Wolf-Watz, T. Lundbäck, S. van den Berg, and T. Härd, “Structure and dynamics of the glucocorticoid receptor DNA-binding domain: comparison of wild type and a mutant with altered specificity.,” *Biochemistry*, vol. 36, no. 37, pp. 11188–11197, Sep. 1997.
- [14] T. Lundback and T. Hard, “Thermodynamics of Sequence-Specific Glucocorticoid Receptor-DNA Interactions,” *Biochemistry*, pp. 1–11, 1994.
- [15] J. Zhang et al., “DNA binding alters coactivator interaction surfaces of the intact VDR–RXR complex,” *Nature Structural & Molecular Biology*, vol. 18, no. 5, pp. 556–563, May. 2011.
- [16] J. M. Hall, D. P. McDonnell, and K. S. Korach, “Allosteric regulation of estrogen receptor structure, function, and coactivator recruitment by different estrogen response elements.,” *Molecular endocrinology (Baltimore, Md)*, vol. 16, no. 3, pp. 469–486, Mar. 2002.
- [17] R. Kumar, I. V. Baskakov, G. Srinivasan, D. W. Bolen, J. C. Lee, and E. B. Thompson, “Interdomain signaling in a two-domain fragment of the human glucocorticoid receptor,” *The Journal of biological chemistry*, vol. 274, no. 35, pp. 24737–24741, Aug. 1999.
- [18] S. J. Pfaff and R. J. Fletterick, “Hormone Binding and Co-regulator Binding to the Glucocorticoid Receptor are Allosterically Coupled,” *Journal of Biological Chemistry*, vol. 285, no. 20, pp. 15256–15267, May. 2010.

- [19] J. Zhang et al., "DNA binding alters coactivator interaction surfaces of the intact VDR–RXR complex," *Nature Structural & Molecular Biology*, vol. 18, no. 5, pp. 556–563, Apr. 2011.
- [20] A. I. Shulman, C. Larson, D. J. Mangelsdorf, and R. Ranganathan, "Structural determinants of allosteric ligand activation in RXR heterodimers.," *Cell*, vol. 116, no. 3, pp. 417–429, Feb. 2004.
- [21] S. N. Floor, B. N. Jones, G. A. Hernandez, and J. D. Gross, "A split active site couples cap recognition by Dcp2 to activation.," *Nature Structural & Molecular Biology*, vol. 17, no. 9, pp. 1096–1101, Sep. 2010.
- [22] K. Yamamoto, B. Darimont, R. Wagner, and J. Iniguez-Lluhi, "Building Transcriptional Regulatory Complexes: Signals and Surfaces," *Cold Spring Harbor Symposia on Quantitative Biology*, vol. 63, no. 1, pp. 587–598, 1998.
- [23] M. G. Rosenfeld, V. V. Lunyak, and C. K. Glass, "Sensors and signals: a coactivator/corepressor/epigenetic code for integrating signal-dependent programs of transcriptional response.," *Genes & Development*, vol. 20, no. 11, pp. 1405–1428, Jun. 2006.
- [24] I. Rogatsky, C. L. Waase, and M. J. Garabedian, "Phosphorylation and inhibition of rat glucocorticoid receptor transcriptional activation by glycogen synthase kinase-3 (GSK-3). Species-specific differences between human and rat glucocorticoid receptor signaling as revealed through GSK-3 phosphorylation," *The Journal of biological chemistry*, vol. 273, no. 23, pp. 14315–14321, Jun. 1998.

- [25] R. Kumar and W. J. Calhoun, "Differential regulation of the transcriptional activity of the glucocorticoid receptor through site-specific phosphorylation," *Biologics : targets & therapy*, vol. 2, no. 4, pp. 845–854, Dec. 2008.
- [26] K. W. Nettles et al., "Allosteric control of ligand selectivity between estrogen receptors alpha and beta: implications for other nuclear receptors.," *Molecular cell*, vol. 13, no. 3, pp. 317–327, Feb. 2004.
- [27] M. I. Diamond, J. N. Miner, S. K. Yoshinaga, and K. R. Yamamoto, "Transcription factor interactions: selectors of positive or negative regulation from a single DNA element.," *Science (New York, NY)*, vol. 249, no. 4974, pp. 1266–1272, Sep. 1990.
- [28] J. La Baer and K. R. Yamamoto, "Analysis of the DNA-binding affinity, sequence specificity and context dependence of the glucocorticoid receptor zinc finger region.," *Journal of molecular biology*, vol. 239, no. 5, pp. 664–688, Jun. 1994.
- [29] A. Y.-L. So, C. Chaivorapol, E. C. Bolton, H. Li, and K. R. Yamamoto, "Determinants of Cell- and Gene-Specific Transcriptional Regulation by the Glucocorticoid Receptor," *PLoS Genetics*, vol. 3, no. 6, p. e94, 2007.
- [30] R. Lavery, M. Moakher, J. H. Maddocks, D. Petkeviciute, and K. Zakrzewska, "Conformational analysis of nucleic acids revisited: Curves+," *Nucleic acids research*, vol. 37, no. 17, pp. 5917–5929, Sep. 2009.
- [31] R. Rohs, S. M. West, A. Sosinsky, P. Liu, R. S. Mann, and B. Honig, "The

- role of DNA shape in protein-DNA recognition.,” *Nature*, vol. 461, no. 7268, pp. 1248–1253, Oct. 2009.
- [32] A. Zhuravleva and L. M. Gierasch, “Allosteric signal transmission in the nucleotide-binding domain of 70-kDa heat shock protein (Hsp70) molecular chaperones.,” *Proceedings of the National Academy of Sciences of the United States of America*, vol. 108, no. 17, pp. 6987–6992, Apr. 2011.
- [33] R. Selvaratnam, S. Chowdhury, B. VanSchouwen, and G. Melacini, “Mapping allostery through the covariance analysis of NMR chemical shifts.,” *Proceedings of the National Academy of Sciences of the United States of America*, vol. 108, no. 15, pp. 6133–6138, Apr. 2011.
- [34] L. R. Masterson, A. Mascioni, N. J. Traaseth, S. S. Taylor, and G. Veglia, “Allosteric cooperativity in protein kinase A,” *Proceedings of the National Academy of Sciences of the United States of America*, vol. 105, no. 2, pp. 506–511, Jan. 2008.
- [35] S. Heck et al., “A distinct modulating domain in glucocorticoid receptor monomers in the repression of activity of the transcription factor AP-1.,” *EMBO*, vol. 13, no. 17, pp. 4087–4095, Sep. 1994.
- [36] S. N. Floor, M. S. Borja, and J. D. Gross, “Interdomain dynamics and coactivation of the mRNA decapping enzyme Dcp2 are mediated by a gatekeeper tryptophan.,” *Proceedings of the National Academy of Sciences of the United States of America*, vol. 109, no. 8, pp. 2872–2877, Feb. 2012.

- [37] J.-C. Wang et al., "Novel arylpyrazole compounds selectively modulate glucocorticoid receptor regulatory activity.," *Genes & Development*, vol. 20, no. 6, pp. 689–699, Mar. 2006.
- [38] K. B. Engel and K. R. Yamamoto, "The Glucocorticoid Receptor and the Coregulator Brm Selectively Modulate Each Other's Occupancy and Activity in a Gene-Specific Manner," *Molecular and cellular biology*, vol. 31, no. 16, pp. 3267–3276, Jul. 2011.
- [39] J. G. McNally, W. G. Müller, D. Walker, R. Wolford, and G. L. Hager, "The glucocorticoid receptor: rapid exchange with regulatory sites in living cells," *Science (New York, NY)*, vol. 287, no. 5456, pp. 1262–1265, Feb. 2000.
- [40] D. A. Stavreva, W. G. Muller, G. L. Hager, C. L. Smith, and J. G. McNally, "Rapid glucocorticoid receptor exchange at a promoter is coupled to transcription and regulated by chaperones and proteasomes," *Molecular and cellular biology*, vol. 24, no. 7, pp. 2682–2697.
- [41] N. A. Farrow, O. Zhang, J. D. Forman-Kay, and L. E. Kay, "A heteronuclear correlation experiment for simultaneous determination of ^{15}N longitudinal decay and chemical exchange rates of systems in slow equilibrium.," *Journal of biomolecular NMR*, vol. 4, no. 5, pp. 727–734, Sep. 1994.
- [42] I. Rogatsky, "Target-specific utilization of transcriptional regulatory surfaces by the glucocorticoid receptor," *Proceedings of the National Academy of Sciences of the United States of America*, vol. 100, no. 24,

- pp. 13845–13850, Nov. 2003.
- [43] H. F. Luecke, “The glucocorticoid receptor blocks P-TEFb recruitment by NF B to effect promoter-specific transcriptional repression,” *Genes & Development*, vol. 19, no. 9, pp. 1116–1127, May. 2005.
- [44] S. Robertson et al., “Abrogation of glucocorticoid receptor dimerization correlates with dissociated glucocorticoid behavior of compound a.,” *Journal of Biological Chemistry*, vol. 285, no. 11, pp. 8061–8075, Mar. 2010.
- [45] H. M. Reichardt and G. Schutz, “DNA Binding of the Glucocorticoid Receptor is Not Essential for Survival,” *Cell*, 1998.
- [46] R. Frijters et al., “Prednisolone-induced differential gene expression in mouse liver carrying wild type or a dimerization-defective glucocorticoid receptor,” *BMC genomics*, vol. 11, p. 359, 2010.
- [47] C. M. JEWELL, A. B. Scoltock, B. L. Hamel, M. R. Yudt, and J. A. CIDLOWSKI, “Complex human glucocorticoid receptor dim mutations define glucocorticoid induced apoptotic resistance in bone cells.,” *Molecular endocrinology (Baltimore, Md)*, vol. 26, no. 2, pp. 244–256, Feb. 2012.
- [48] J. Liden, F. Delaunay, I. Rafter, J. Gustafsson, and S. Okret, “A new function for the C-terminal zinc finger of the glucocorticoid receptor. Repression of RelA transactivation,” *The Journal of biological chemistry*, vol. 272, no. 34, pp. 21467–21472, Aug. 1997.
- [49] J. P. Tuckermann, H. M. Reichardt, R. Arribas, K. H. Richter, G. Schutz,

and P. Angel, "The DNA binding-independent function of the glucocorticoid receptor mediates repression of AP-1-dependent genes in skin.," *JCB*, vol. 147, no. 7, pp. 1365–1370, Dec. 1999.

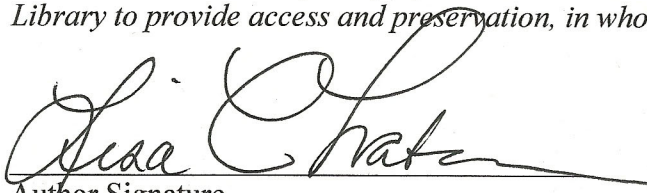
- [50] H. M. Reichardt et al., "DNA binding of the glucocorticoid receptor is not essential for survival.," *Cell*, vol. 93, no. 4, pp. 531–541, May. 1998.
- [51] T. C. Voss et al., "Dynamic Exchange at Regulatory Elements during Chromatin Remodeling Underlies Assisted Loading Mechanism," *Cell*, vol. 146, no. 4, pp. 544–554, Aug. 2011.
- [52] V. Chandra et al., "Structure of the intact PPAR-gamma-RXR-alpha nuclear receptor complex on DNA," *Nature*, pp. 350–356, Oct. 2008.
- [53] C. Rivers et al., "Characterization of conserved tandem donor sites and intronic motifs required for alternative splicing in corticosteroid receptor genes.," *Endocrinology*, vol. 150, no. 11, pp. 4958–4967, Nov. 2009.
- [54] C. Rivers, A. Levy, J. Hancock, S. Lightman, and M. Norman, "Insertion of an amino acid in the DNA-binding domain of the glucocorticoid receptor as a result of alternative splicing.," *The Journal of clinical endocrinology and metabolism*, vol. 84, no. 11, pp. 4283–4286, Nov. 1999.
- [55] J. S. Fraser, M. W. Clarkson, S. C. Degnan, R. Erion, D. Kern, and T. Alber, "Hidden alternative structures of proline isomerase essential for catalysis," *Nature*, vol. 462, no. 7273, pp. 669–673, Mar. 2009.

Publishing Agreement

It is the policy of the University to encourage the distribution of all theses, dissertations, and manuscripts. Copies of all UCSF theses, dissertations, and manuscripts will be routed to the library via the Graduate Division. The library will make all theses, dissertations, and manuscripts accessible to the public and will preserve these to the best of their abilities, in perpetuity.

Please sign the following statement:

I hereby grant permission to the Graduate Division of the University of California, San Francisco to release copies of my thesis, dissertation, or manuscript to the Campus Library to provide access and preservation, in whole or in part, in perpetuity.


Author Signature

04.03.12
Date